MARSHALL VICTOR CHAGAS SANTOS

USING A MULTI-LAYER LAGRANGIAN INVERSE ANALYSIS TO STUDY CO_2 ISOTOPE EXCHANGE IN PLANT CANOPIES

Thesis submitted to the Applied Meteorology Graduate Program of the Universidade Federal de Viçosa in partial fulfillment of the requirements for the degree of *Doctor Scientiae*.

VIÇOSA
MINAS GERAIS – BRAZIL
2019

Ficha catalográfica preparada pela Biblioteca Central da Universidade Federal de Viçosa - Câmpus Viçosa

T
S237u
2019

Santos, Marshall Victor Chagas, 1991-
Using a multi-layer Lagrangian inverse analysis to study CO2 isotope exchange in plant canopies / Marshall Victor Chagas Santos. – Viçosa, MG, 2019.
xx, 90 f. : il. (algumas color.) ; 29 cm.

Texto em inglês.
Inclui apêndice.
Orientador: Eduardo Alvarez Santos.
Tese (doutorado) - Universidade Federal de Viçosa.
Referências bibliográficas: f. 79-89.

1. Micrometeorologia. 2. Isótopos estáveis. 3. Dióxido de carbono - Concentração. 4. Difusão atmosférica - Modelos matemáticos. 5. Fotossíntese. I. Universidade Federal de Viçosa. Departamento de Engenharia Agrícola. Programa de Pós-Graduação em Meteorologia Aplicada. II. Título.

CDD 22 ed. 551.66

MARSHALL VICTOR CHAGAS SANTOS

USING A MULTI-LAYER LAGRANGIAN INVERSE ANALYSIS TO STUDY CO_2 ISOTOPE EXCHANGE IN PLANT CANOPIES

Thesis submitted to the Applied Meteorology Graduate Program of the Universidade Federal de Viçosa in partial fulfillment of the requirements for the degree of *Doctor Scientiae*.

APPROVED: May 10, 2019.

José Eduardo Macedo Pezzopane

Milton Edgar Pereira Flores

Hewlley Maria Acioli Imbuzeiro

Aristidés Ribeiro
(Co-adviser)

Eduardo Alvarez Santos
(Adviser)

This thesis is dedicated to God, my mother’s memory and family for always encouraging me and standing by me.

"*A statement closes the mind, a question opens the mind."*

— Robert Kiyosaki

ACKNOWLEDGEMENTS

Many people, agencies and institutions have provided support during the progression of this work. First and foremost, I would like to thank my advisor, Dr. Eduardo Alvarez Santos, for all your support, guidance and patience in answering my questions and giving me a hand with Matlab© functions. Thank you so much for always being an involved advisor, even working from distance during most of time in the course of this work.

Thanks to Dr. Aristides Ribeiro for having me in your lab over the first half of my doctorate. I would like to thank the late scientists Mike Raupach and Tom Denmead for suppling us with the LNF source code during the initial stages of this work. Thanks also to my committee members: Dr. Aristides Ribeiro, Drª Hewlley M. A. Imbuzeiro, Dr. José E. M. Pezzopane and Dr. Milton E. P. Flores for their comments and suggestion in improving my dissertation.

Special thanks for all who has involved in field experiments assistance and data collecting in Elora Research Station (ERS), Borden Forest Research Station (BFRS), and Konza Prairie Research Station (KPBS), especially to Dean Loutitt, Ralf Staebler and Kyle Stropes for their assistances at ERS, BFRS and KPBS, respectively. The institutions that have involved in this work, especially Federal University of Viçosa (UFV) and Kansas State University (KSU), also deserves a special mention for providing structure and human resource to make it all possible.

Thank you to Coordination for the Improvement of Higher Education Personnel (CAPES) for the stipend that was essential for the execution of this work. CAPES also provided my doctoral sandwich scholarship. This grant has allowed me to work as a Research Scholar during eight months in Laboratory of Micrometeorology

of Department of Agronomy at KSU under the supervision of lab head Dr. Eduardo Santos. I am grateful to Dr. Santos and to all faculty and people from Department of Agronomy of KSU for having me during my internship abroad. For sure, this was the greatest and valuable experience that I have ever had in my academic career so far.

Thanks to the Natural Science and Engineering Research Council, National Science Foundation (grant number EPS-0903806) and Agricultural Experiment Station (Contribution no. 19-206-J) for providing funding for research projects that make this work possible.

Thank you to my many office-mates that I had the opportunity to work with over the last four years, in special: Elias Pedroso, José Darlon, Hugo dos Santos and Mariana Reis. Thank you for mutual support and companionship, making this path enjoyable. I am also thankful to all colleagues from Applied Meteorology graduate program, in special those who shared good times with me even outside the work environment: Adolpho Rocha, Alex da Silva, Ana Beatriz, Emily Silva, Gabriel Abrahão, Marcel Abreu, Sandro Moreira and Raphael Pousa.

Thank you to Vinicius Perin and Prajaya Prajaprati, colleagues from Laboratory of Micrometeorology of Department of Agronomy in KSU that were friendly and fun to work with.

I wish to say a special thank you to Graça Freitas, our lovely secretary of the Applied Meteorology graduate program, who was always available to help us with any administrative issues, making the lives of all graduate students easier.

Thank you to my housemate who became a good friend, Reginal Filho, for all encouragement and for sharing many good times with me along the way.

Thanks to Cynthia Albuquerque for being a wonderful partner and the one who makes me a better and happier person every single day. Thank you so much for all your support and understanding over the last years.

Last but not least, I would like to thanks my parents Ana Maria (*in memoriam*) and Arnaldo Santos, for their unconditional encouragements and support in my academic pursuits; to my brother Marcell for his advices and partnership; and to my sister Marcelle and my nephew Raffael for their love.

BIOGRAPHY

Marshall V. C. Santos received his Bachelor of Science degree in Meteorology (2013) and also holds his Master's in Meteorology (Earth Surface Processes) from Federal University of Alagoas in 2015. Upon completing his Master's, Marshall came to the Federal University of Viçosa to pursue his doctorate in the Applied Meteorology graduate program, where he had the opportunity to develop part of his doctorate research abroad, working as Research Scholar at Kansas State University, Manhattan, KS, USA over 2017.

Marshall grew up in Maceió, capital of Alagoas State in Northeastern Brazil. Marshall's interest in the interaction between the land surface processes and the atmosphere started while undergraduate student, when he had the opportunity to join the former Laboratory of Agrometeorology and Solar Radiometry at Federal University of Alagoas. At this lab, he was first exposed to environmental physics and instrumentation as well as on applying this information on crop simulation models. Since then, Marshall's interest in understanding how environmental drivers affects crops and ecosystems production was substantially increased, so that his Ms thesis focused on a modelling assessment of the corn crop production in different edaphoclimatic conditions over Alagoas State regions. Currently, Marshall's is completing his doctorate. Marshall's doctoral research is focused on the use of a Lagrangian analysis to study CO_2 isotope exchange and for partitioning net CO_2 fluxes in plant canopies. Marshall's findings may contribute to improve our comprehension on processes governing isotope exchange at ecosystems.

SUMMARY

LIST OF FIGURES

LIST OF TABLES

LIST OF SYMBOLS

A	carbon gain during CO_2 assimilation, μmol m^2 s^{-1}.
a	diffusional discrimination factor, ‰.
c_a	atmospheric CO_2 concentration, μmol mol^{-1}.
c_i	leaf intercellular air spaces CO_2 concentration, μmol mol^{-1}.
C_i	scalar concentration at a given level i, μmol mol^{-1}.
C_R	scalar concentration at a reference level, μmol mol^{-1}.
C_n	concentration in the near-field region.
C_f	concentration in the far-field region.
CV	coefficient of variation, %.
D_{eq}	isotopic disequilibrium, ‰.
$\mathbf{D}_{ij}$	dispersion matrix.
$\mathbf{D}_{ij}^{(N)}$	dispersion matrix in the near-field region.
$\mathbf{D}_{ij}^{(F)}$	dispersion matrix in the far-field region.
d_r	refined index of agreement.
E	water loss during transpiration, mmol m^2 s^{-1}.
F_A	canopy net photosynthetic flux density, μmol m^2 s^{-1}.
F_R	non-foliar respiratory flux density, μmol m^2 s^{-1}.
F_N	net flux, μmol m^2 s^{-1}.
F_j	scalar flux for a given source layer j, μmol m^2 s^{-1}.
F_c	CO_2 flux, μmol m^2 s^{-1}.
g_s	stomatal conductance, mol m^2 s^{-1}.

GEP	gross ecosystem production, μmol m^2 s^{-1}.
HDO	deuterium composition of water vapour, ‰.
h	canopy height, m.
$I_N(\zeta)$	integral of $k_N(\zeta)$ from 0 to ζ.
I_F	ecosystem-scale ^{13}C isoforcing, m s^{-1} ‰.
i	index corresponding to concentration measurement level.
j	index corresponding to source layer.
L	Obukhov length, m.
m	number of source layers.
n	number of concentration measurement levels.
$k_N(\zeta)$	near-field kernel function.
NEE	net CO_2 ecosystem exchange, μmol m^2 s^{-1}.
P	atmospheric pressure, Pa.
R_{eco}	ecosystem respiratory flux density, μmol m^2 s^{-1}.
R^2	coefficient of determination.
R	molar gas constant, J mol^{-1} K^{-1}.
R	molar ratio of heavy to light isotope ($^{13}C/^{12}C$).
R_{std}	molar ratio of the heavy to light isotope for a known standard.
R_{VPDB}	standard molar ratio of the Vienna Pee Dee Belemnite.
R_g	incoming solar radiation, W m^{-2}.
S_j	scalar source strength for a given source layer j, μmol m^{-3} s^{-1}.
S_c	CO_2 source strength, μmol m^{-3} s^{-1}.
SD	standard deviation.
T_L	Lagrangian time-scale, s.

T_{air}	air temperature, ºC.
u_*	friction velocity, m s^{-1}.
v	leaf-to-air vapour pressure difference, mmol mol^{-1}.
WUE	water use efficiency, denoted as the ratio of A to E, mmol mol^{-1}.
z	concentration measurement height, m.
z_R	reference level of concentration measurement, m.
Z	height in the center of the source layer, m.
$\delta^{13}C$	carbon isotopic composition of an arbitrary component, ‰.
δ_a	isotopic composition of atmospheric CO_2, ‰.
δ_N	isotopic composition associated with net ecosystem CO_2 exchange (NEE), ‰.
δ_P	isotopic composition of CO_2 assimilated via photosynthesis, ‰.
δ_R	isotopic composition of non-foliar respired CO_2, ‰.
δ_F	isotopic composition of CO_2 flux, ‰.
$\Delta^{13}C$	discrimination against ^{13}C during photosynthesis, ‰.
Δ_3	$\Delta^{13}C$ of C_3 plants, ‰.
Δ_4	$\Delta^{13}C$ of C_4 plants, ‰.
Δ_{canopy}	canopy-scale discrimination, ‰.
Δz_j	thickness of source layer j, m.
$[CO_2]$	CO_2 mixing ratio, µmol mol^{-1}.
φ	leakage of CO_2 out of the bundle-sheath cells back to the mesophyll.
σ	standard deviation
σ_w	standard deviation of the wind vertical velocity.

LIST OF ACRONYMS

BFRS	Borden Forest Research Station.
DOY	Day Of Year.
EC	Eddy Covariance technique.
ERS	Elora Research Station.
FLUXNET	Global network of micrometeorological flux measurement sites.
FVS	Flux Variance Similarity method.
KPBS	Konza Prairie Biological Station.
LNF	Localized Near-Field theory.
QCLS	Quantum Cascade Laser Spectrometer.
IFR	Isotope Flux Ratio method.
IFP	Isotope Flux Partitioning method.

ABSTRACT

SANTOS, Marshall Victor Chagas, D.Sc., Universidade Federal de Viçosa, May, 2019. **Using a multi-layer Lagrangian inverse analysis to study CO_2 isotope exchange in plant canopies**. Advisor: Eduardo Alvarez Santos. Co-advisor: Aristides Ribeiro.

Stable isotopes of CO_2 are useful to study biosphere-atmosphere exchange processes. Recent advances in optical based isotope techniques has provided high-temporal resolution and accurate isotope measurements suitable for ecosystem scale studies. These novel measuring techniques can be combined with micrometeorological approaches, such as multi-layer Lagrangian models, to study CO_2 isotope exchange in plant canopies. The main objectives of this study were: 1) to evaluate the feasibility of the localized near-field theory (LNF) to study $^{13}CO_2$ and $C^{18}OO$ isotope exchange in different plant canopies; 2) to examine the LNF theory as an independent non-isotopic method to estimate separately the net-photosynthesis (F_A) and non-foliar respiration (F_R) in a corn canopy; and 3) to evaluate whether direct half-hourly estimates of isotope compositions of net CO_2 (δ_N), canopy (δ_P) and below-canopy (δ_R) fluxes from LNF could be used in a isotope based partitioning approach (IFP method) to partition NEE measurements. Concentration of stable isotopes of CO_2 were measured within and above a temperate deciduous forest, tallgrass prairie and corn field using a multi-port sampling system and the tunable diode laser spectroscopy (TDLAS) technique. An EC system was also used to measure the wind velocity and the net CO_2 fluxes (NEE) above the canopies. The performance assessment of LNF on estimating isotope exchange within different plant canopies and to partitioning NEE in a corn canopy included direct comparisons with the traditional isotope flux ratio (IFR) method and a night-time based flux partitioning (RP) approach, respectively. Changes in CO_2 storage were used to investigate the degree of decoupling between below and above-canopy airflows. Results showed that the LNF estimates of NEE and isotope CO_2 exchange for the forest canopy were greatly affected by the flux decoupling. However, the LNF theory was shown to be suitable within well-mixed short canopies, where changes in CO_2 storage were small. The magnitude of CO_2 concentration gradients

had great impact on both IFR and LNF δ_N estimates. Nevertheless, the LNF theory reduced roughly 74% the uncertainties of IFR method. For the non-isotope partitioning, The LNF F_A estimates captured the expected seasonal canopy physiological variation better than RP. Large uncertainties in LNF F_R estimates were observed when the canopy was fully developed under low turbulent mixing periods. For the isotope-derived partitioning, the IFP method was highly sensitive to the D_{eq}, where large uncertainties were found when D_{eq} < 3.2 ‰. However, a considerable reduction in the uncertainties and more realistic flux estimates were observed when weak D_{eq} (< 3.2 ‰) periods was filtered out from IFP predictions. Overall, these results suggests that LNF theory can be successfully used to study isotope exchange and partitioning NEE in well-mixed plant canopies. However, further studies are still needed to quantify the random and systematic errors associated with LNF predictions.

RESUMO

SANTOS, Marshall Victor Chagas, D.Sc., Universidade Federal de Viçosa, maio de 2019. **Usando uma análise Lagrangeana inversa de multicamadas para estudar fluxos isotópicos de CO_2 em dosséis vegetativos**. Orientador: Eduardo Alvarez Santos. Coorientador: Aristides Ribeiro.

Isótopos estáveis de CO_2 são ferramentas úteis para o estudo de processos de trocas gasosas na interação biosfera-atmosfera. Os avanços recentes nas técnicas de isótopos baseados em espectroscopia óptica, permitem que as razões de isótopos sejam medidas em ecossistemas com alta frequência e acurácia. Essas novas tecnologias para medição de isótopos podem ser combinadas com métodos micrometeorológicos, tais como modelos Lagrangeanos de multicamadas, para o estudo de fluxos isotópicos em dosséis vegetativos. Os principais objetivos desse estudo foram: 1) avaliar a viabilidade da teoria Lagrangeana de campo-próximo localizado (LNF) para estudar fluxos isotópicos de $^{13}CO_2$ e $C^{18}OO$ em dosséis vegetativos; 2) examinar a teoria LNF como um método independente para estimar a fotossíntese (F_A) e respiração não-foliar (F_R) em um dossel de milho; e 3) avaliar se as estimativas da composição isotópica da troca líquida de CO_2 (NEE) acima do dossel (δ_N), da F_A (δ_P) e da F_R (δ_R) fornecidas pelo método LNF podem ser utilizadas para separar as medições do NEE através de uma abordagem de particionamento isotópico (método IFP). Nesse estudo, as razões de mistura de isótopos de CO_2 foram medidas em diferentes níveis dentro e acima do dossel em floresta temperada, pradaria e milharal usando um sistema de amostragem multiporta e um sistema analisador de gases a laser de diodo ajustável (TDLAS). Além disso, os dados de velocidade do vento e do NEE foram coletados através de um sistema de covariância dos vórtices turbulentos (EC), instalado acima dos dosséis. A avaliação do desempenho do método LNF para a estimativa de fluxos isotópicos dentro de diferentes tipos de dosséis e para o particionamento do NEE em um dossel de milho foi realizada por comparações diretas com o método da razão de fluxo isotópico (IFR) e um método estatístico de particionamento de fluxo baseado na extrapolação de dados noturnos (RP), respectivamente. As variações no armazenamento de fluxo de CO_2 foram utilizadas para investigar o grau de desacoplamento entre os fluxos abaixo e

acima do dossel. Os resultados mostraram que as estimativas do NEE e dos fluxos isotópicos para o dossel de floresta foram fortemente afetados pelo desacoplamento de fluxo. No entanto, o método LNF se mostrou adequado quando utilizado em dosséis mais baixos com maior mistura turbulenta, onde as variações no armazenamento de fluxo foram pequenas. Ambos os métodos LNF e IFR foram afetados pela magnitude dos gradientes de concentração de CO_2. Apesar disso, o método LNF foi capaz de reduzir, em média, 74% das incertezas mostradas pelo método IFR. Para o particionamento de fluxo, o método LNF foi capaz de capturar as variações sazonais fisiológicas da F_A com maior eficiência do que o método RP. Por outro lado, grandes incertezas foram observadas para as estimativas da LNF F_R durante períodos de baixa mistura turbulenta quando o dossel estava completamente desenvolvido. Para o particionamento isotópico, o método IFP se mostrou altamente sensível ao desequilíbrio isotópico (D_{eq}), onde grandes incertezas foram observadas quando D_{eq} < 3.2 ‰. No entanto, uma considerável redução das incertezas e estimativas de fluxos mais realistas foram obtidas quando os períodos com baixo D_{eq} (< 3.2 ‰) foram excluídos das estimativas do IFP. Por fim, tais resultados sugerem que a teoria LNF pode ser utilizada eficazmente para estudar fluxos isotópicos e para partição do NEE em dosséis baixos com alta mistura turbulenta. No entanto, estudos adicionais ainda são necessários para quantificar os erros aleatórios e sistemáticos associados às estimativas do LNF.

CHAPTER 1 - A LITERATURE REVIEW ON THE USE OF STABLE ISOTOPES TECHNIQUES AND MICROMETEOROLOGICAL APPROACHES TO STUDY BIOPHYSICAL PROCESS AT ECOSYSTEMS

1.1 Stable isotopes in ecological and atmospheric studies

Isotopes of carbon (C), hydrogen (H), oxygen (O) and nitrogen (N) naturally occur in the atmosphere and biosphere. The term isotope comes from the Greek words "*iso*" and "*topos*", meaning equal and place, respectively, referring to the fact that isotopes occupy the same place in the periodic table of the elements. The isotopes are essentially different forms of atoms of the same element. For different isotopes of an element, the number of protons remains constant in their nuclei, but the number of the neutrons is different resulting in a distinct atomic mass. There are two types of isotopes: radioactive isotopes and stable isotopes. Radioactive isotopes of a given element show a nuclear decay, which consist in the loss of energy from an unstable nuclei by emitting ionizing radiation, forming different elements with time. On the other hand, the nuclei of stables isotopes remain constant and unchanged over the time. Taking as an example the carbon isotopes, it possess two stable isotopes (^{12}C and ^{13}C) and one radioactive isotope (^{14}C) with the same number of protons (i.e., 6 protons), but differing in the composition of nuclei only by the one additional neutron in ^{13}C and two additional neutrons in ^{14}C (Fry, 2006; Peterson and Fry, 1987).

Most chemical elements have stable isotopes, showing one dominant (more abundant) light stable isotope, for example: carbon-12 (^{12}C), hydrogen-1 (^{1}H), oxigen-16 (^{16}O) and nitrogen-14 (^{14}N), and one or two heavy stable isotope (less abundant): carbon-13 (^{13}C), hydrogen-2 (^{2}H), oxygen-17 (^{17}O), oxygen-18 (^{18}O) e nitrogen-15 (^{15}N), with natural abundance expressed in atoms % (Table 1.1).

Table 1.1. Natural abundance of stable isotopes, isotopic ratios and the standard molar ratios for the main stable isotopes used for ecological studies. Adapted from Dawson and Brooks (2001).

Element	Light isotope	Abundance (%)	Heavy isotope	Abundance (%)	Ratio	Standard
Hydrogen	^{1}H	99.985	^{2}H	0.015	$^{1}H/^{2}H$	SMOW[a]
Carbon	^{12}C	98.98	^{13}C	1.11	$^{13}C/^{12}C$	PDB[b]
Nitrogen	^{14}N	99.63	^{15}N	0.37	$^{15}N/^{14}N$	N_2atm[c]
Oxygen	^{16}O	99.759	^{17}O	0.037	$^{18}O/^{16}O$	SMOW, PDB
Sulphur	^{32}S	95.00	^{34}S	4.22	$^{34}S/^{32S}$	CDT[d]

[a] The standard for the hydrogen with molar mass equal to two (^{2}H), known as deuterium (D), is the Standard Mean Ocean Water (SMOW); [b] for the carbon the standard is the calcium carbonate stemming from a Belemnitella americana of the Pee-Dee (PDB) formation of South Carolina, EUA; [c] the nitrogen has as standard the atmospheric N_2; [d] for the sulphur the standard is the Canyon Diablo meteorite found in Arizona (EUA), known as "Canyon Diablo Troilite"(CDT).

The less abundant stables isotopes can be used as tracers in biochemical, biological and environmental studies (Dawson and Brooks, 2001). The isotope composition of substances in ecological studies was often measured by using a mass spectrometer, which provides the mass differences among stable isotopes or isotopologues, expressed in delta notation (δ):

$$\delta = \frac{R}{R_{\text{std}}} - 1 \tag{1.1}$$

where R and R_{std} are the ratio of the heavier to lighter isotopes (e.g., $^{13}C/^{12}C$; $^{18}O/^{16}O$) in the measured sample and standard sample (Table 1.1), respectively.

An increase in δ indicates an increment of the amount of heavy isotopes in the sample (Peterson and Fry, 1987). A positive δ indicate that the isotope ratio in the sample is larger than that of the standard, i.e. the sample is more enriched in heavy isotopes than the standard. On the other hand, negatives δ values mean that the sample is more depleted in heavier isotopes than its standard. For instance, considering an unknown sample with $\delta^{13}C$ of -23‰, this means that this sample has isotopic ratio

($^{13}C/^{12}C$), 23 parts per mil (‰) or 2.3 % smaller than the standard isotope ratio for carbon (PDB).

Since the 1980s, there has been an increase in the use of stable isotopes in ecological and atmospheric studies (Bowling et al., 2008; Dawson and Brooks, 2001; Deleens et al., 1983; Ehleringer et al., 1997; Farquhar et al., 1989; Marshall and Zhang, 1994; O'leary, 1988; Yakir and Sternberg, 2000). Such an increase was driven certainly by the need to quantify and study the biosphere–atmosphere exchange processes to diagnosing changes in the climate system. Advances on optical technologies for mass spectroscopy over the last several years have allowed the high-frequency and near-continuous isotope measurements (Bowling et al., 2003). These new technologies opens new insights to biosphere-atmosphere exchange studies (Griffis, 2013).

Nowadays, stable isotopes techniques are important tools to help physiologists, ecologists and others researchers to study biogeochemical interactions in the environment. The natural abundance of stable isotopes can be used, for example, to trace patterns and to verify physiological mechanisms in organisms as well as in the establishment of nutrient cycling pathways in terrestrial and aquatic ecosystems (Cernusak et al., 2013; Farquhar et al., 1989; O'leary, 1988; Victoria et al., 1992; Yakir and Sternberg, 2000). In addition, stable isotopes are useful to other applications regarding to examine biosphere-atmosphere exchange, including: flux partitioning of net ecosystem CO_2 exchange and evapotranspiration; and environmental controls on temporal variations in isotope composition of respiratory fluxes, among other several applications (Bowling et al., 2001; Griffis, 2013; Zobitz et al., 2008).

1.2 Isotope discrimination against ^{13}C during photosynthesis

The primary source of carbon for terrestrial ecosystems is the atmospheric CO_2, which has a current $\delta^{13}C$ value of approximately -8.5 ‰ (Graven et al., 2017). Most of plants can be classified in two main groups based on their photosynthetic pathway: C_3 and C_4 plants. The C_3 photosynthetic pathway includes most trees, shrubs, soybean, rice, wheat, barley and others. The C_4 pathway is the carbon fixation mechanism used by plants such as corn, sorghum, sugarcane and other tropical grasses. The process of isotopic discrimination, which leads to isotopic fractionation, consists of an enrichment or depletion of heavy isotope in the sample studied (product) to its respective source, in this case the atmospheric CO_2. The carbon isotope discrimination ($\Delta^{13}C$) is denoted as follows (Farquhar et al., 1989).

$$\Delta^{13}\mathrm{C} = \left[\frac{(\delta_\mathrm{a} - \delta_\mathrm{p})}{(1 + \delta_\mathrm{p})}\right] \tag{1.2}$$

where δ_p is the isotope composition ($\delta^{13}C$) of plant material and δ_a is the $\delta^{13}C$ of atmospheric (source) air.

As showed in the Figure 1.1, C_3 and C_4 plants has a lower ^{13}C composition than the atmospheric CO_2, and that means that plants discriminate against ^{13}C during photosynthesis (Farquhar et al., 1989; Farquhar and Sharkey, 1982). Studies on the isotope composition between different photosynthetic pathways showed that C_3 plant tissues have an average $\delta^{13}C$ of -26.7‰, which is about 18‰ more negative than the atmospheric CO_2. On the other hand, C_4 plant tissues have an average $\delta^{13}C$ value of -12.6 ‰, about 4‰ more negative than $\delta^{13}C$ of the atmospheric CO_2 (Cerling et al., 1997; Farquhar et al., 1989).

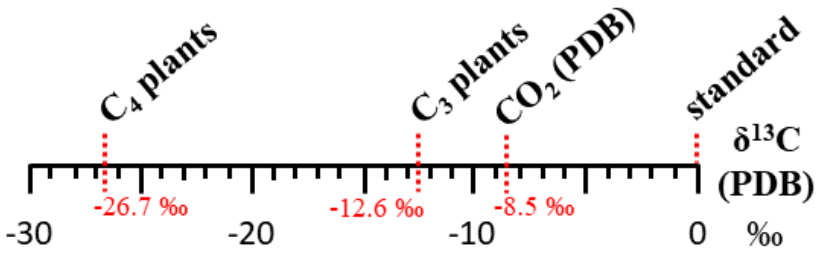

Figure 1.1. Isotope delta values ($\delta^{13}C$) of photosynthetic pathways and source (atmospheric) CO_2, PDB.

Cerling et al. (1997) studied the $\delta^{13}C$ composition of 825 modern grasses from different regions in the world and found averaged $\delta^{13}C$ (±SD) values of -26.7 ± 2.3‰ and -12.7 ± 1.1‰ for C_3 and C_4 plants, respectively. In practice, variations in $\delta^{13}C$ reflects the consequences of minor physiological variations associated to changes in stomatal conductance under different environmental conditions. Hence, the $\delta^{13}C$ also can be useful to distinguish the C_3 and C_4 plants, as well as to study stomatal conductance responses under different environmental conditions (Cerling et al., 1997; Farquhar and Sharkey, 1982; Shimoda et al., 2009).

In C_3 and C_4 species, the CO_2 diffuses from the atmospheric air to the carboxylation sites within leaves through the stomatal pores. The $^{12}CO_2$ diffuses slightly faster to the carboxylation sites than $^{13}CO_2$ due to its lighter atomic mass. This difference in diffusion rates between isotopologues can be represented by a diffusional discrimination factor (a) of 4.4‰ (Farquhar et al., 1989). Therefore, leaves have a more negative $\delta^{13}C$ than the one for atmospheric air simply due to diffusion effect. However, a alone is not sufficient to explain the $\delta^{13}C$ values of C_3 plants (Figure 1.1). CO_2 uptake by C_3 plants is limited more by the rate of carboxylation of Rubisco enzyme than by diffusion, so the most of the discrimination of C_3 plants is that connected with carboxylation (29.0 ‰) (Estep et al., 1978; O'leary, 1988). On the other hand, the PEP-carboxylase, the principal CO_2 fixation enzyme in C_4 plants, has

a discrimination factor of approximately 2.2‰ (Deleens et al., 1983). Hence, the major contributor for $\delta^{13}C$ differences between C_3 and C_4 plants are a result of distinctions in carboxylation enzymes (Ehleringer et al., 1997; Farquhar et al., 1989).

1.3 Use of stable isotopes to identify physiological responses to environmental changes

Carbon stable isotopes have been applied to study plant carbon-water relation (Farquhar et al., 1989; Farquhar and Cernusak, 2005; Ponton et al., 2006; Seibt et al., 2008; Werner et al., 2012). A characteristic of such studies is the use of carbon stable isotopes as a means to determine the water use efficiency (WUE), which in turn is useful to evaluate plant physiological responses to environmental changes such as seasonal variations and prolonged drought events. WUE is defined as the ratio of biomass produced to the rate of transpiration, and represents, in general terms, how effective is the use of water by plants (Stanhill, 1986). The $\Delta^{13}C$ integrates biophysical parameters, such as WUE, over time which biomass was formed. Therefore, the variations in $\Delta^{13}C$ can also be interpreted as variations in WUE by plants (Ehleringer et al., 1992).

The $\Delta^{13}C$ by plants is increased or reduced as the partial pressure of CO_2 in the intercellular spaces (c_i) of leaves varies with respect to the partial pressure of CO_2 in ambient air (c_a). The c_i/c_a ratio is defined as the equilibrium between the supply of CO_2, that penetrates the plant through the stomatal pores and the CO_2 demand by the mesophyll inside the leaf. The c_i/c_a ratio is directly proportional to the A/g_s or A/E ratios. Therefore, as suggested above, when $\Delta^{13}C$ is combined with v estimative it provide a measurement of plant WUE. Hence, stable isotopes of CO_2 can become an important tool to evaluate physiological responses to the variations in the ambient

(Marshall and Zhang, 1994; Ponton et al., 2006). This makes it possible, for example, the selection of species more tolerant to droughts (Monneveux et al., 2006; Smedley et al., 1991; Stewart et al., 1995).

The supply of CO_2 to the intercellular spaces of leaves is controlled by the ambient CO_2 concentration (c_a) and by the stomatal conductance (g_s) (Farquhar et al., 1989; Farquhar and Sharkey, 1982). The stomata allow CO_2 to diffuse into the leaves when conditions are favourable to the photosynthesis, while preventing the excessive loss of water by plants. However, the stomata are not simply opened or closed; its degree of openness is a continuous variable that seriously limits the diffusion of CO_2 in leaves when the supply of water from soil is relatively low as well as when the evaporative demand on the atmosphere is relatively high (Marshall and Waring, 1984). Hence, the $\Delta^{13}C$ variation in C_3 plants (Δ_3) can be expected in response to the soil water availability and the vapour pressure deficit on the atmosphere. These responses can be manifested through precipitation gradients (Stewart et al., 1995) or, more precisely, along soil water availability gradients that account for both the local availability of soil water and potential evapotranspiration (Cernusak et al., 2013).

For C_4 plants, the knowledge about genetic mechanisms and physiological process underlying $\Delta^{13}C$ has been much more limited, due to C_4 plant more complex mechanisms for CO_2 fixation. Variation in $\Delta^{13}C$ of C_4 plants (Δ_4) in response to environmental factors (e.g. soil water limitation) are much lower than C_3 plants but significant, which can vary between 1-3‰ (Cernusak et al., 2013; Farquhar et al., 1989). The interpretation of Δ_4 is challenging because its variability is not related to a unique factor, as generally occurs in C_3 plants. In this case, Δ_4 depends on both c_i/c_a ratio and the leakage of CO_2 out of the bundle-sheath cells back to the mesophyll (φ) (Buchmann et al., 1996). The factor φ play an important role on determining variations

in Δ_4, because it reduces the opportunity of Rubisco to discriminate against ^{13}C. In addition, the c_i/c_a ratio can be positive or negative depending on whether the φ is larger or smaller than 0.37 (Cernusak et al., 2013; Farquhar et al., 1989; Gresset et al., 2014).

1.4 Seasonal pattern of carbon isotope discrimination

As discussed in the previous section, the isotope discrimination against ^{13}C varies during photosynthesis as a function of the both stomatal conductance and carbon fixation biochemical processes, providing an integrated measurement of plant responses to temporal variations of environmental conditions. It has been well accepted that environmental stresses (*e.g.* drought) resulted of an increase in $\delta^{13}C$ values of C_3 plants (Farquhar et al., 1989; Farquhar and Sharkey, 1982). For C_4 plants, it was assumed that $\delta^{13}C$ values remained constant seasonally and were not significantly affected by the environmental factors, including water stress (Yoneyama et al., 2010). However, this premise was contested based on the results from growth-chamber studies (Buchmann et al., 1996; Saliendra et al., 1996). These studies showed that $\delta^{13}C$ values of C_4 plants can be affected by environmental factors, in particular the water stress probably due to increasing losses of CO_2 (φ). Cernusak et al. (2013) consider that $\delta^{13}C$ variations in C_4 plants in response to environmental variations are significant, though smaller than in C_3 plants.

Smedley et al. (1991) measured the seasonal pattern of isotope discrimination of 42 species, including both C_3 and C_4, in grassland communities of arid Western North America. These ecosystems are often characterized by a seasonal increase in ambient temperature and evaporative demand, leading to a decline in soil moisture. The authors monitored changes in grassland species gas exchange in response to local environmental conditions. Their results show that there is a statistically significant

average decrease of 1‰ of $\Delta^{13}C$ values during the growing season. They also report a reduction in the number of species active throughout the sampling campaigns. Their results also show an increase in perennial species with respect to annual species, with significantly larger isotope discrimination than perennial species. In addition, physiological processes controlling gas exchange changed significantly throughout the growing season. The seasonal decrease in discrimination indicated that the c_i/c_a ratio diminishes as the drought period developed and that stomatal limitation of photosynthesis increased as the soil water availability decreased.

Yoneyama et al. (2010) evaluated the seasonal variation of $\delta^{13}C$ values of C_3 and C_4 plants during wet and dry seasons in Thailand and the Philippines. Their results showed strong seasonal $\delta^{13}C$ variations for C_4 plants, with values ranging from -14.5 ± 0.68‰ during dry season (February and March) to -12.7 ± 0.56‰ during rainy season (July and August) in Thailand. The authors associated the more negative values of $\delta^{13}C$ during the dry season to an increase in the leakage of CO_2 from the bundle-sheath cells to the mesophyll (φ). As previously mentioned in this chapter, φ is an important factor to determine if the relationship between $\Delta^{13}C$ and c_i/c_a ratio are positively or negatively correlated (Cernusak et al., 2013; Farquhar et al., 1989; Gresset et al., 2014). Surprisingly, no significant differences between dry and rainy season $\delta^{13}C$ values were found for C_3 plants by Yoneyama et al. (2010).

1.5 Combined use of isotope and micrometeorological techniques to study isotope exchange in ecosystems

Several micrometeorological approaches have been combined with in-situ isotope measurements to study isotope exchange in plant canopies. The most difficult challenge to be overcome for in-situ isotope measurement techniques is to capture the

short-time (< 1h) responses of isotope fluxes to environmental factors with high accuracy (Griffis, 2013). Recent advancements in spectroscopy (optical) techniques has allowed near-continuous isotope measurements with good accuracy, opening new opportunities for ecosystem scale studies (Bowling et al., 2003; Lee et al., 2009; Xiao et al., 2012).

The eddy covariance (EC) method is the most popular micrometeorological technique used to measure the CO_2 and energy fluxes at the ecosystem scale thought hundreds of sites around the world (Baldocchi et al., 2001). The EC method has recently also been used to study isotope exchange at the ecosystem level (Sturm et al., 2012; Wehr et al., 2013; Wehr and Saleska, 2015). Griffis et al. (2008) were the first ones to use the EC and the tunable diode laser spectroscopy (TDL) technique to quantify CO_2 isotope fluxes above a soybean canopy. Although their results showed a good agreement between the isotope fluxes measured using the EC method with the ones provided by the flux gradient method, the EC application for isotope measurements is limited by the trace gas analyser precision (Good et al., 2012; Sturm et al., 2012; Wehr et al., 2013). Additionally, the high cost of fast response sensors also limits the widespread use of the EC technique to quantify stable isotope exchange in ecosystems.

More recently, the flux-gradient approach and tunable diode laser spectroscopy measurements have been applied as an alternative to estimate isotope exchange over and within plant canopies by the isotope flux ratio (IFR) method (Griffis et al., 2005b; Santos et al., 2012). The IFR method use the K-theory principle (Taylor, 1922), where the mean turbulent fluxes are related to the mean concentration gradient of CO_2 isotopologues to calculate the ratio between fluxes of heavier and lighter isotopologues (Griffis et al., 2004). Although the IFR method has some advantages over EC, because

it does not require bulky and high-cost sensors, it also has been shown to be highly sensitive to the concentration measurements. Griffis et al. (2005) and Santos et al. (2012) found large uncertainties in IFR flux ratio estimates when mean CO_2 concentration gradient was smaller than 3.2 ppm.

Analytical Lagrangian analysis can also be used to study scalar isotope exchange in plant canopies (Haverd et al., 2011; Santos et al., 2012; Styles et al., 2002). Raupach, (1989) introduced an analytical Lagrangian analysis, based on localized near-field theory (LNF), for relating mean scalar concentration to source distributions in plant canopies, providing a solution to the forward problem, which consists to find the concentration field from source/sink distributions. In LNF theory, plumes of marked fluid particles carrying mass and energy are released from different source (*S*) points in the canopy (Figure 1.2). The path of plumes of marked particles released from a given *S* is divided into near-field and far-field regions. In the near-field, dispersion is non-diffusive and dominated by the persistence, so that the plumes of marked particles increase linearly with time, while far-field is dominated by the diffusion in such way that the plumes increase by the square root of time (Raupach, 2001, 1989a, 1989b).

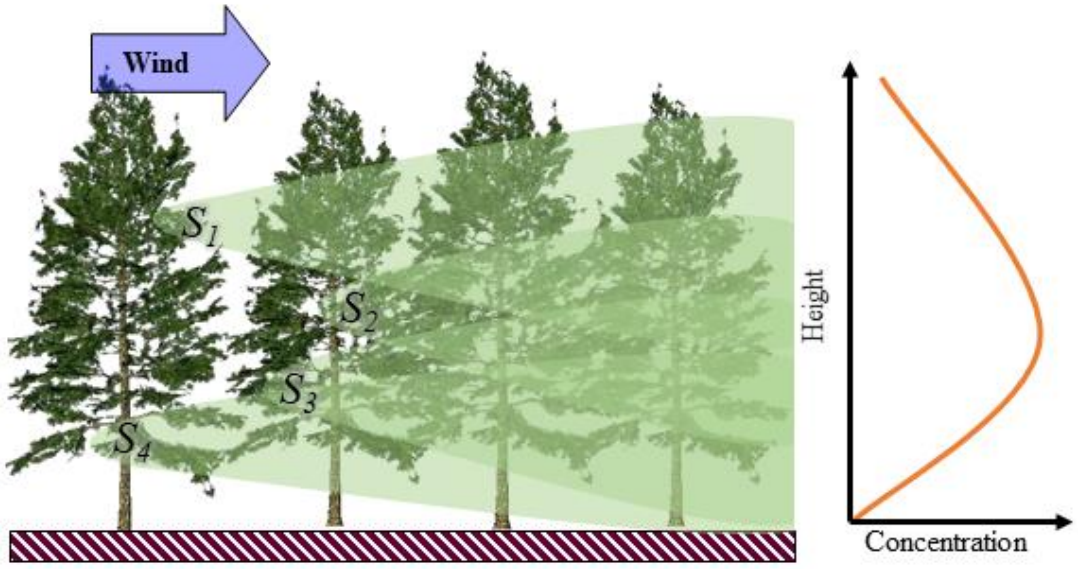

Figure 1.2. Diagram showing the released plumes of marked particles released from different source points in the canopy.

The LNF theory considers that the concentration in an arbitrary layer *i* is the superposition of source/sink layers (*j*) contributions from near-field and far-field regions. The LNF basic formulation can also be used in a discrete form to solve the inverse problem, which is required for most of practical applications (Harper et al., 2000; Raupach, 1989a; Siqueira et al., 2000; Ueyama et al., 2014). To solve the inverse problem, the canopy is divided into *m* layers, with unknown source/sink distributions (Figure 1.3), and measurements of vertical concentration gradient ($C_i - C_R$) are used for inferring individual source/sink strengths. Then, the flux for individual layers is calculated by multiplying the source/sink strength with the layer thickness, so that $F_j = S_j \Delta z_j$ (Figure 1.3). Finally, the total flux is calculated by adding the individual fluxes for all layers.

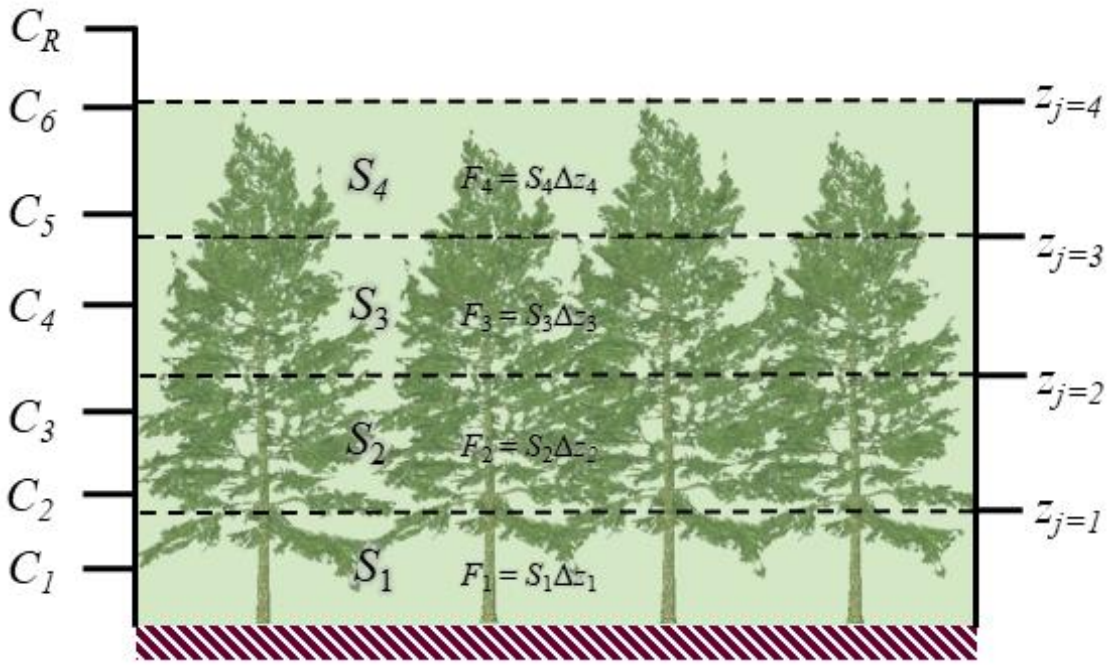

Figure 1.3. Diagram showing the canopy separation used by the multi-layer Lagrangian analysis (LNF) to solve the inverse problem for m = 4 layers. The C_i represents the concentration measurements and z_j are the top of source layers of thickness Δz_j.

This inverse Lagrangian formulation described above can also be combined with laser-based isotope measurements to calculate the fluxes of heavier (F_j^H) and lighter (F_j^L) isotopologues separately for each source/sink layer (F_j^H/F_j^L). Lately, the ratio F_j^H/F_j^L is converted to delta notation by Eq. 1.1. Further details on this methodology are shown in Chapter 2.

1.6 Applying stable isotopes for partitioning the net ecosystem CO_2 exchange into photosynthesis and non-foliar respiration.

EC measurements of net ecosystem CO_2 exchange (NEE) have advanced our knowledge of processes governing the carbon exchange in different terrestrial ecosystems around the world (Baldocchi et al., 2001). However, gross ecosystem production (GEP) and total ecosystem respiration (R_{eco}) drivers still remain poorly understood because the EC technique does not measure GEP and R_{eco} separately.

Currently, there are different approaches for partitioning EC NEE measurements with non-isotopic based methods. For example, the method proposed by Reichstein et al. (2005) relies on the assumption that daytime R_{eco} shows the same response to air or soil temperatures than night-time R_{eco}. Another NEE partitioning approach proposed by Lasslop et al. (2010) assumes that GEP follows the same light-response curves as individual leaves. However, these kind of approaches have been criticized due to its many fundamental limitations, as briefly revised in Fassbinder et al. (2012).

Another alternative non-isotopic flux partitioning method is the flux variance similarity (FVS) method (Scanlon and Kustas, 2010; Scanlon and Sahu, 2008). The FVS method is based on the flux variance similarity relationships and correlation analyses of high-frequency EC measurements. The FVS method requires a computationally complex algebraic solution to solve the partitioning problem, which has severely limited its use. Recently, Skaggs et al. (2018) developed Fluxpart, which provides a simplified algebraic solution to the FVS partitioning implemented in a free and open source Python 3 module. However, the FVS approach showed high sensibility to the water use efficiency parameter and requires further tests over a range of environmental conditions.

The isotopic flux partitioning (IFP) arises as an alternative for partitioning the NEE into its gross components (Bowling et al., 2001; Yakir and Wang, 1996). In summary, the IFP approach separates the NEE into net photosynthesis (F_A) and non-foliar respiration (F_R), based on mass balance principles by assuming that each flux component are related to a unique isotopic signature as follows:

$$\delta_{\mathrm{N}}\mathrm{NEE} = \delta_{\mathrm{R}}F_{\mathrm{R}} + (\delta_a - \Delta_{\mathrm{canopy}})F_{\mathrm{A}} \quad (1.3)$$

where δ_{N} is the isotopic composition of NEE over a homogeneous vegetated surface, δ_{R} is the isotope composition of non-foliar respired CO_2 and the isotopic composition

of CO_2 assimilated via photosynthesis (δ_P) is usually found by the difference between the isotope composition of ambient air (δ_a, approximately -8.5‰) and the photosynthetic discrimination of whole canopy (Δ_{canopy}).

The IFP approach account for non-foliar respiration (F_R) instead of total ecosystem respiration (R_{eco}). In addition, a fundamental assumption of IFP is that δ_R value must be distinct from δ_P, This difference is called isotopic disequilibrium ($D_{eq} = \delta_P - \delta_R$). If D_{eq} approaches zero, there is no unique information enough to partition NEE and the partitioning become impracticable.

1.7 Outline and objectives

In addition to this first chapter, providing a review on the combined use of stable isotopes and micrometeorological techniques in ecological and atmospheric studies, this thesis includes three additional chapters.

In chapter 2, near-continuous measurements of stable isotopes of CO_2 collected in three different ecosystems were used to quantify isotope exchange at canopy level. The main objective of this study was to evaluate the use of the localized near-field theory (LNF) to study $^{13}CO_2$ and $C^{18}OO$ isotope exchange in different plant canopies by comparing its estimates with values provided by the IFR method. This study shows the first attempt to combine LNF theory with several months of near-continuous measurements of stable CO_2 isotopes in different plant canopies.

Chapter 3 aims to the use of LNF theory as an independent method for isotopic and non-isotopic flux partitioning. More specifically, the objectives of this study were: 1) to examine the LNF theory as an independent method to estimate separately the net-photosynthesis and non-foliar respiration in a corn canopy; and (2) to evaluate whether direct half-hourly estimates of δ_P and δ_R determined with LNF could be used to partition NEE measured by EC system using mass balance principle (IFP approach).

Short-term δ_P and δ_R estimative from LNF may encounter some complications in the application of the IFP approach, providing additional information about daytime soil respiration and canopy physiology, respectively.

Finally, chapter 4 provides a brief overview of the main results and conclusions of the studies presented in chapters 2 and 3 as well as directions for future researches.

CHAPTER 2 – EVALUATING A LAGRANGIAN INVERSE MODEL FOR INFERRING ISOTOPE CO_2 EXCHANGE IN PLANT CANOPIES

Santos, Marshall; Santos, Eduardo; Wagner-Riddle, Claudia; Brown, Shannon; Stropes, Kyle; Staebler, Ralf; Nippert, Jesse, 2019. Evaluating a Lagrangian inverse model for inferring isotope CO_2 exchange in plant canopies. ***Agricultural and Forest Meteorology***, v. 276–277, 107651.

Abstract

Multi-layer Lagrangian models could be an alternative to study stable isotope exchange within and just above plant canopies. The main objective of this study was to evaluate the use of an analytical Lagrangian analysis (localized near-field theory, LNF), to study $^{13}CO_2$ and $C^{18}OO$ isotope exchange in different plant canopies by comparing the LNF estimates with those provided by the eddy covariance (EC) technique and the isotope flux ratio method (IFR). Mixing ratios of stable isotopes of CO_2 were measured within and above a temperate deciduous forest, tallgrass prairie and corn field using a multi-port sampling system and the tunable diode laser spectroscopy technique. Wind velocity data and the net CO_2 ecosystem exchange (NEE) were measured above the plant canopies using an EC system. The wind velocity data and CO_2 stable isotope mixing ratios were combined with the LNF theory to infer NEE and source/sinks of isotopes inside canopies. The LNF NEE estimates were likely affected by the flux decoupling in the forest canopy, resulting in a low correlation (R^2 ranging from 0.03 to 0.35) between LNF and EC NEE estimates. On the other hand, LNF NEE estimates for corn and grassland canopies showed better correlation with EC NEE estimates (R^2 ranging from 0.58 to 0.85), suggesting better coupling between in and above canopy air flows. Although, both LNF and IFR estimates showed large variability, our results show that the LNF approach reduced the uncertainties of the

isotope compositions of NEE when compared to the IFR approach. These results suggest that LNF is a useful tool to study isotope exchange within plant canopies.

2.1 Introduction

Stable isotopes of carbon dioxide and water vapour are useful tools to investigate biophysical processes in ecosystems (Griffis, 2013; Werner et al., 2012). High temporal resolution and accurate isotope measurements suitable for ecosystem scale studies have become available with recent advancements in laser spectroscopy techniques. These advancements allowed the development of field-deployable trace gas analysers capable of providing accurate and near-continuous isotope measurements under field conditions (Griffis, 2013). Recently, atmospheric concentrations of CO_2 and H_2O isotopologues started to be monitored continuously at different ecosystems across the United States (National Ecological Observatory Network, 2018). These concentration measurements can bring new insights into the biophysical mechanisms governing the isotope exchange in ecosystems as they provide a transient imprint of isotope sources and sinks in the biosphere (Raupach, 2001).

Micrometeorological approaches, such as the eddy covariance technique (Griffis et al., 2011; Sturm et al., 2012; Wehr et al., 2013; Wehr and Saleska, 2015) and the flux gradient approach (Griffis et al., 2005b, 2004; Santos et al., 2012; Yakir and Sternberg, 2000) have been used to study isotope exchange in ecosystems. The eddy covariance (EC) approach is a well-stablished micrometeorological method widely used to measure CO_2 and energy fluxes in several sites around the world (Baldocchi, 2003; Xiao et al., 2012). Griffis et al. (2008) applied the EC technique to measure CO_2 isotope exchange above a soybean canopy. They found a relatively good agreement between the isofluxes measured using the EC method with the ones

provided by the flux gradient method. However, the high cost of fast response sensors required for EC measurements constrains the widespread use of the EC technique to quantify stable isotope exchange in ecosystems.

The isotope flux ratio (IFR) method has been used as an alternative to measure isotope exchange in ecosystems (Griffis et al., 2005b, 2004; Santos et al., 2012). The IFR method is based on the gradient-diffusion theory (K-theory), which relates the mean turbulent vertical flux to mean concentration gradients measured above plant canopies (Denmead and Bradley, 1987; Griffis et al., 2004). When compared to the EC approach, a major advantage of the IFR method is that this approach does not require fast response gas analysers. In addition, flux gradient approaches allow multiple sites to be measured near-simultaneously with a single trace gas analyser combined with a multiport sampling system (Brown and Wagner-Riddle, 2017). However, the accuracy of the IFR estimates is quite sensitive to errors in measurements of concentration gradients. Small gradients of concentration often lead to large uncertainties in estimates of the isotope exchange due to the small signal to noise ratio of concentration gradients (Griffis, 2013; Griffis et al., 2005a). One alternative to increase the signal to noise ratio of concentration gradient measurements is to take concentration measurements inside plant canopies where vertical gradients of concentration are often strong (Buchmann et al., 1996). However, flux-gradient methods are prone to errors within the canopies due the proximity of source/sinks of scalars as well as to the presence of turbulent eddies with length scales larger than the distance over which vertical gradients of concentration are measured (Corrsin, 1975; Denmead and Bradley, 1987; Raupach, 1987).

Multi-layer Eulerian and Lagrangian models have been applied to study the dispersion of scalars within plant canopies (Katul et al., 1997; Katul and Albertson,

1999; Raupach, 1989b, 1989a; Siqueira et al., 2000; Warland and Thurtell, 2000). The Lagrangian dispersion models infer the average scalar concentration field by tracking the position of small fluid particles (Raupach, 2001). This leads to a better description of the turbulent motions responsible for the dispersion of scalars within plant canopies in comparison to the flux-gradient theory (Raupach, 1987; Warland and Thurtell, 2000). Lagrangian dispersion models can be used to solve the so-called forward problem, i.e. to determine a scalar concentration field from scalar source/sink distributions (S). But for most practical applications these models are used to solve the inverse problem, in which S is inferred based on turbulent statistics and mean scalar concentration gradients measured above and inside plant canopies (Raupach, 1989b, 1989a).

The localized near-field (LNF) theory, proposed by Raupach (1989a), is a multi-layer Lagrangian canopy model that has been used for inferring scalar source/sink distributions and fluxes of heat, water vapour, CO_2 and other traces gases within different plant canopies (Harper et al., 2000; Katul et al., 1997; Katul and Albertson, 1999; Leuning et al., 2000; Raupach et al., 1992; Siqueira et al., 2000; Ueyama et al., 2014). Currently, studies applying multi-layer Lagrangian models to quantify isotope exchange in plant canopies are scarce (Haverd et al., 2011; Santos et al., 2012; Styles et al., 2002). Styles et al. (2002) applied a canopy scale model, based on the LNF theory, combined with a sun and shade photosynthesis and energy balance model, to infer scalar source/sink distributions, including for $^{13}CO_2$, in a Siberian mixed-coniferous forest. Their results showed great deviation between modelled and measured $\delta^{13}C$ profiles, which was attributed to instrument precision limitations, and insufficient isotope sampling rate that did not capture rapid isotope concentration changes mainly at sunrise and sunset. Haverd et al. (2011) used the LNF theory

combined with source/sink distributions of deuterium (HDO) composition of water vapour, estimated using an isotopically enabled soil vegetation atmospheric transfer model, for partitioning the evapotranspiration into soil evaporation and transpiration in a forest canopy. Both of these studies were limited to sampling campaigns in forest canopies over a few weeks. A more complete evaluation of the potential in combining the LNF theory to study isotope exchange could be obtained using larger datasets for canopies with different heights and structures.

In the present study, we used several months of near-continuous measurements of stable isotopes of CO_2 collected in three different ecosystems to quantify canopy level isotope exchange. The main objective of this study was to evaluate the performance of the LNF theory to estimate isotope exchange in plant canopies by comparing its estimates with values provided by the IFR method.

2.2 Material and methods

2.2.1 The localized near-field theory

The concentration field near plant canopies can be regarded as the result of contributions of different instantaneous sources inside the canopy. The LNF theory is a semi-Lagrangian dispersion analysis that divides the concentration field into near-field (C_n) and far-field (C_f) regions (Raupach, 1989b, 1989a). In the near-field region, the fluid particle dispersion is governed by the persistence of the Lagrangian velocity relative to the scalar source, while in the far-field region random motions of fluid particles dominate the scalar transport (Taylor, 1922). The LNF theory centres on the evaluation of a transition probability function, which is divided into far-field and near-field terms, and provides statistical means of determining the marked-fluid particle position distributions (Raupach, 2001).

The discrete form of the LNF theory assumes that for a horizontally homogeneous plant canopy and steady turbulent conditions, the scalar source densities and concentrations are only a function of height (z). In addition, the scalar concentration at a given level inside the canopy is assumed to be the result of near-field and far-field contributions from m horizontally homogenous source/sink layers with thickness Δz_j located inside the canopy. The mean scalar concentration (c_i) can be related to the source/sink strength through a dispersion matrix (Raupach, 2001), as follows:

$$C_i - C_R = \sum_{j=1}^{m} \mathbf{D}_{ij} S_j \Delta z_j \tag{2.1}$$

where i and j are indices corresponding to concentration (C) and source (S) layers, respectively, C_R is the scalar concentration at a reference level (z_R), and $\mathbf{D}_{ij}$ is the dispersion matrix. The dispersion matrix ($\mathbf{D}_{ij}$) is essentially a discrete form of a particle distribution transition probability function and provides a prediction of the position of the fluid particles within and above the canopy over time. For the calculation of $\mathbf{D}_{ij}$ terms, $\mathbf{D}_{ij}$ is divided into far field ($\mathbf{D}_{ij}^{(F)}$) and near field ($\mathbf{D}_{ij}^{(N)}$) parts:

$$\mathbf{D}_{ij} = \mathbf{D}_{ij}^{(F)} + \mathbf{D}_{ij}^{(N)} \tag{2.2}$$

The elements of $\mathbf{D}_{ij}^{(F)}$ are given by:

$$\mathbf{D}_{ij}^{(F)} = \int_{\max(z_i, Z_j)}^{z_R} \frac{dz'}{\sigma_w^2(z') T_L(z')} \tag{2.3}$$

where z_i is the concentration measurement heights, Z_j is the height in the center of the source layer, σ_w is the standard deviation of the wind vertical velocity and T_L is the Lagrangian time scale.

The near-field part of $\mathbf{D}_{ij}$ is given by

$$\mathbf{D}_{ij}^{(N)} = \frac{1}{\sigma_{wj}}\left[k_N\left(\frac{z_i - Z_j}{\sigma_{wj}T_{Lj}}\right) + k_N\left(\frac{z_i + Z_j}{\sigma_{wj}T_{Lj}}\right) - k_N\left(\frac{z_r - Z_j}{\sigma_{wj}T_{Lj}}\right) - k_N\left(\frac{z_r + Z_j}{\sigma_{wj}T_{Lj}}\right)\right] \tag{2.4}$$

for z_i not in (z_{j-1}, z_j)

$$\mathbf{D}_{ij}^{(N)} = \frac{T_{Lj}}{\Delta z_j}\left[I_N\left(\frac{z_i - z_{j-1}}{\sigma_{wj}T_{Lj}}\right) + I_N\left(\frac{z_j - z_i}{\sigma_{wj}T_{Lj}}\right)\right] + \frac{1}{\sigma_{wj}}\left[k_N\left(\frac{z_i + Z_j}{\sigma_{wj}T_{Lj}}\right) - k_N\left(\frac{z_r - Z_j}{\sigma_{wj}T_{Lj}}\right) - k_N\left(\frac{z_r + Z_j}{\sigma_{wj}T_{Lj}}\right)\right] \tag{2.5}$$

for z_i in (z_{j-1}, z_j)

where k_N (ζ) is the "near-field kernel" which represents the near-field contribution for a unit plane source at z_0, and I_N (ζ) is defined as the integral of k_N (ζ) from 0 to ζ. The adimensional variable ζ represents the height interval z - z_0 (Raupach, 1989c). Further details about the calculation of the far-field and near-field parts of $\mathbf{D}_{ij}$ can be found in Raupach (2001).

In this study, profiles of T_L and σ_w were estimated using parameterization of turbulence statistics proposed by Leuning (2000). The generated turbulent statistics profiles (σ_w and T_L) were corrected for atmospheric stability conditions as suggested by Leuning (2000).

To infer source strength using scalar concentration measurements, the dispersion matrix ($\mathbf{D}_{ij}$) is computed by dividing the canopy into m source layers (S_j). Measurement errors in concentration profiles can introduce uncertainties in the LNF

results. Raupach (2001) recommended the use of redundant concentration data to minimize these uncertainties, by ensuring that m is smaller than n.

The scalar source strength is obtained from Eq. 2.1, by solving a system of m linear equations (Raupach, 1989b):

$$\sum_{k=1}^{m} \mathrm{A}_{jk} S_k = \mathrm{B}_j \text{ with } \begin{cases} \mathrm{A}_{jk} = \sum_{i=1}^{n} \mathbf{D}_{ij} \Delta z_j \, \mathbf{D}_{ik} \Delta z_k \\ \mathrm{B}_j = \sum_{i=1}^{n} (C_i - C_R)_{(\mathrm{means})} \mathbf{D}_{ij} \Delta z_j \end{cases} \tag{2.6}$$

The scalar flux for each source layer (F_j) is given by:

$$F_j = \sum_{j=1}^{m} S_j \Delta z_j \tag{2.7}$$

The net flux (F_N) is obtained by adding F_j values for all source layers. The estimated F_N for lighter and heavier isotopes were converted to delta notation (δ_N, ‰) as follows:

$$\delta_N = \frac{R_\mathrm{N}}{R_\mathrm{VPDB}} - 1 \tag{2.8}$$

where R_N is the ratio of the heavier to lighter isotopologues fluxes (F_N^H/F_N^L) defined as F_N^H/F_N^L for $^{13}CO_2$ and $^{12}CO_2$ fluxes, or $0.5F_N^{18}/F_N^{16}$ for $C^{18}O^{16}O$ and $C^{16}O_2$ fluxes, and R_VPDB represents the standard molar ratio ($^{13}C/^{12}C$ or C^{18}/C^{16}) of the Vienna Pee Dee Belemnite.

2.2.2 The isotope flux ratio method

The isotope flux ratio (IFR) method proposed by Griffis et al. (2004) is based on the flux-gradient theory, which assumes that: (1) the turbulent transfer in the inertial sublayer above plant canopies is analogous to molecular diffusion, and (2) the

turbulent flux is proportional to the product of the mean vertical concentration gradient and the eddy diffusivity (Corrsin, 1975). The IFR method allows calculating the ratio between fluxes of heavier and lighter isotopologues, as follows:

$$\frac{F_N^H}{F_N^L} = \frac{-(K\overline{\rho_a}/M_a)\mathrm{d}[\bar{\mathrm{H}}]/\mathrm{d}z}{-(K\overline{\rho_a}/M_a)\mathrm{d}[\bar{\mathrm{L}}]/\mathrm{d}z} \tag{2.9}$$

where K is the eddy diffusivity, which is assumed to be the same for heavy and light isotopologues, $\overline{\rho_a}$ is the mean density of dry air, M_a is the molar mass of dry air, and $\mathrm{d}[\bar{\mathrm{L}}]/\mathrm{d}z$ and $\mathrm{d}[\bar{\mathrm{H}}]/\mathrm{d}z$ are the time-averaged vertical gradients of the heavy and light isotopologues. After some simplifications, Eq. 2.9 can be rewritten in a discrete form as follows:

$$\frac{F_N^H}{F_N^L} = \frac{[\bar{\mathrm{H}}]_{z_2} - [\bar{\mathrm{H}}]_{z_1}}{[\bar{\mathrm{L}}]_{z_2} - [\bar{\mathrm{L}}]_{z_1}} \tag{2.10}$$

where $[\bar{\mathrm{H}}]$ and $[\bar{\mathrm{L}}]$ are the half-hourly mean mixing ratios of isotopologues at two heights (z_1 and z_2) above the canopy.

Lastly, the ratio of isotopologues fluxes (F_N^H/F_N^L) were converted to delta notation using Eq. 2.8. Thus, the isotope composition of F_N (δ_N) provided by the IFR method was directly compared with the LNF estimates.

2.2.3 Experimental sites

Field experiments were carried out at three sites: 1) the Borden Forest Research Station (BFRS); 2) the Konza Prairie Biological Station (KPBS); and 3) the Elora Research Station (ERS). The site locations, vegetation types and measurement periods are summarized in Table 2.1. Overall, air temperatures decreased from early August (day of year, DOY = 220) to early November (DOY = 310), as expected at these locations. The mean air temperatures during the experimental periods for the BFRS,

KPBS and ERS sites were 18.7 ºC, 13.5ºC and 16.9ºC, respectively. Further experimental details about the sites is given by Santos et al. (2012, 2011) and Stropes (2017).

Table 2.1. Location, vegetation type and measurement periods at the three experimental sites: Borden Forest Research Station (BFRS), Konza Prairie Biological Station (KPBS) and Elora Research Station (ERS).

Site	Location	Vegetation	Measurement period
BFRS	Borden, ON, Canada (44º 19'N, 79º 56'W)	mixed deciduous forest	August to September, 2009
KPBS	Manhattan, KS, USA (39° 59'N, 96°34'W)	native tallgrass prairie	September to November, 2015
ERS	Elora, ON, Canada (43º 39'N, 80º25'W)	corn (*Zea mays* L.)	August to October, 2008

2.2.4 Isotope measurements

The mixing ratios of the CO_2 isotopologues ($^{12}C^{16}O_2$, $^{13}CO_2$ and $C^{18}OO$ for the forest; $^{12}C^{16}O_2$ and $^{13}CO_2$ for grassland and corn) were measured at a frequency of 10 Hz using tunable diode laser trace gas analysers (TGA100A or TGA200, Campbell Sci., Logan, UT, USA). Table 2.2 provides information of isotope measurements for each site. The ambient air was sampled using eight air intakes, set up within and above the canopies. Each air intake consisted of a 1 m-long stainless tube (0.43 cm I.D.) with a rain diverter. Inline-stainless filters (SS-4F-K4-7, 7 μm sintered element filter, Swagelok, OH, USA) were positioned downstream from each air intake. To prevent water vapour condensation inside the filters and sampling lines, the filter holder was heated using a 0.5W heater connected to a 12V DC power supply, and a critical flow orifice located downstream of the filter was used to reduce the air pressure in the sampling line. The sampling lines were directed to a custom-made manifold (Campbell Scientific, Logan, UT) that controlled the flow of ambient air from the air inlets and calibration gases through the TGA. The air was drawn continuously through all air

intakes at a flow rate of approximately 600 mL min^{-1} using a vacuum pumps. A sub-sample of the total flow was directed to the TGA with a flow rate of approximately 200 mL min^{-1}. The manifold also kept the TGA sample cells at constant operating pressures (TGA100A at 1.8 kPa and TGA200 at 3 kPa). Each air intake was measured for 15 s at BFRS and ERS sites and for 30 s at KPBS. The longer intake sampling time at KPBS took into account the longer residence time of the air within the TGA200 sampling cell.

Table 2.2. Isotope measurement instrumentation, measured isotopologues, canopy and air intake heights at the three experimental sites. Refer to Table 2.1 for the meaning of the site acronyms.

Site	Gas analyzer	Measured isotopologues	Canopy height (m)	Air intake heights (m)
BFRS	TGA100A	$^{12}C^{16}O_2$, $^{13}CO_2$ and $C^{18}OO$	22.0	0.45, 1.45, 5.51, 9.65, 16.69, 20.77, 25.81 and 36.81
KPBS	TGA200	$^{12}C^{16}O_2$ and $^{13}CO_2$	1.3	0.18, 0.31, 0.45, 0.56, 0.73, 1.29, 2.00 and 3.00
ERS	TGA100A	$^{12}C^{16}O_2$ and $^{13}CO_2$	2.4	0.16, 0.63, 1.03, 1.47, 1.86, 2.25, 2.75 and 3.15

2.2.5 Flux measurements

At all sites, the NEE was measured continuously above the canopies by EC systems. A sonic anemometer (CSAT3, Campbell Sci.) and open-path CO_2/H_2O infrared gas analyzer (LI-7500, LI-COR, Lincoln, NE, USA) were used to measure the three wind components and CO_2 mixing ratios, respectively. The EC system was installed at 33.4 m for the forest, 2.5 m for the grassland and 2.84 m for the corn canopy. All sensor signals were recorded at 20 Hz using dataloggers (CR3000 and CR23X, Campbell Sci.).

2.3 Results and discussion

2.3.1 CO_2 mixing ratio and isotope composition of the air

The CO_2 mixing ratios were usually higher near the ground than near the canopy top and during the night-time periods at all sites (Figure 2.1d to f) when compared to daytime values. The grassland site showed a smaller spatial variability in [CO_2] in comparison to the corn and forest canopies (Figure 2.1b and e).

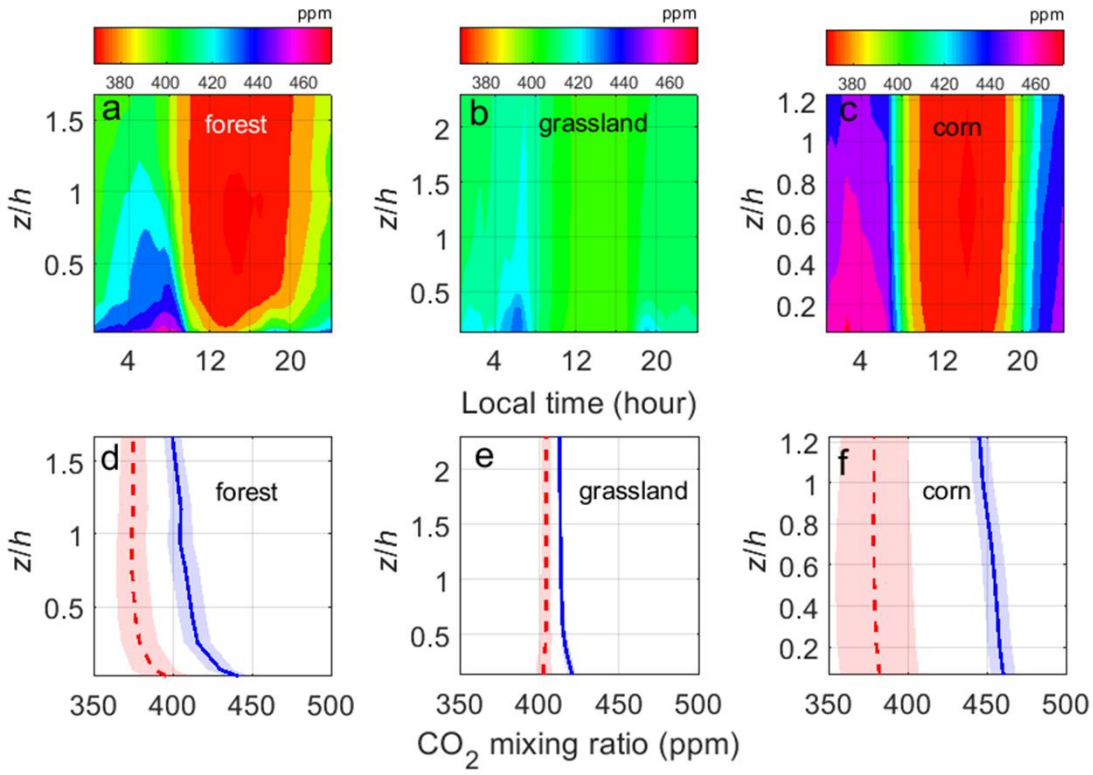

Figure 2.1. a, b and c) diel ensemble CO_2 mixing ratio for forest, grassland and corn ecosystems, and d, e and f) mean vertical profiles of CO_2 mixing ratio during daytime (10:00 – 15:00 h, red dashed lines) and night-time (22:00 – 3:00 h, blue solid lines). The shaded areas in the bottom panels represent the standard deviation (σ) of CO_2 mixing ratio. *z/h* denote the ratio of air intake to the canopy heights.

The smaller [CO_2] gradients at the grassland site can be explained by the fact the measurements at this site were taken near the end of the growing season (Table 2.1), when [CO_2] gradients and fluxes were often smaller than the ones expected for

the peak of the growing season. The average (±SD) NEE over the measurement period ranged from -8.5 (± 11.1) µmol m^{-2} s^{-1}, -1.1 (± 8.4) µmol m^{-2} s^{-1} and -0.4 (± 7.3) µmol m^{-2} s^{-1} for the corn, forest and grassland ecosystems, respectively. The forest and corn sites showed a distinct [CO_2] diel pattern, with the highest [CO_2] values being observed just before sunrise (4 – 6:00 h) and low [CO_2] during mid-day (Figure 2.1a and c). The high [CO_2] in the early morning is a result of continuous build-up of respiratory CO_2 throughout the night when turbulent mixing is low (Buchmann et al., 1996). The diel [CO_2] variation is in agreement with previous studies and is a result of the changes in atmospheric boundary layer and turbulent mixing, as well as photosynthetic uptake and ecosystem respiration (Buchmann et al., 1996; Buchmann and Ehleringer, 1998; Hsieh et al., 2003).

The $^{13}CO_2$ (and $C^{18}OO$ for the forest) compositions of atmospheric air (δ_a^{13} and δ_a^{18}, respectively) were less negative during daytime than night-time (Figure 2.2). These diel patterns of δ_a^{13} and δ_a^{18} are driven primarily by the isotope enrichment of the atmospheric air during daytime due to photosynthetic fractionation and changes in the atmospheric boundary layer (Farquhar et al., 1989). The opposite trend was observed during night-time, when ecosystem respiration releases CO_2 to the atmosphere depleted in heavy isotopologues ($^{13}CO_2$ and $C^{18}OO$) and atmospheric mixing is low (Flanagan et al., 1996; Yakir and Sternberg, 2000).

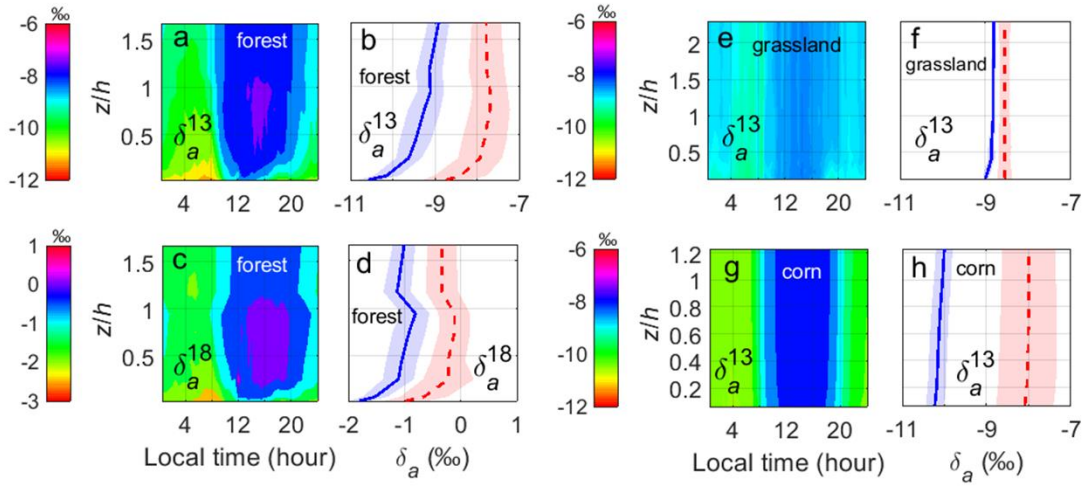

Figure 2.2. a, c e and g) ensemble averages of CO_2 isotope compositions of the ambient air ($\delta_a{}^{13}$ and $\delta_a{}^{18}$) measured within and above forest, grassland and corn canopies; and b, d, f and h) averaged daytime (10:00 – 15:00 h, red dashed lines) and night-time (22:00 – 3:00 h, blue solid lines) vertical profiles of $\delta_a{}^{13}$ and $\delta_a{}^{18}$ (for forest) for the same canopies. The shaded areas represent the standard deviation (σ) of $\delta_a{}^{13}$ or $\delta_a{}^{18}$.

There was also a clear distinction between δ_a^{13} (and δ_a^{18} for forest) daytime and night-time profiles (Figure 2.2b, d, f and h). For grassland (Figure 2.2e and f) and corn (Figure 2.2g and h) canopies, the δ_a^{13} gradients were smaller than the ones measured at the forest site, which could be in part explained by the lower discrimination against $^{13}CO_2$ by C_4 species (corn and grassland) in comparison to the forest vegetation. In addition, in taller forest canopies the large air volume and lower air mixing within the canopy contribute to large gradients of scalar concentration (Figure 2.2b and d). Conversely, in short canopies such as grassland and corn, the air volume within the canopy is smaller which could promote better turbulent mixing in these short canopies.

2.3.2 LNF estimates of CO_2 source strength distributions and CO_2 fluxes

To investigate the performance of the LNF theory in estimating net scalar fluxes, the NEE computed by LNF was compared with the NEE measured using the

EC technique. We also investigated the effect of different friction velocity (u_*) values on the relationship between LNF and EC estimates (Table 2.3).

Table 2.3. Statistical coefficients of the relationship between net ecosystem CO_2 exchange (NEE) obtained using the eddy covariance method and the LNF theory for different friction velocity screening thresholds.

Ecosystem	u_* (m s^{-1})	n	R^2	Slope	Intercept	d_r
Forest	> 0.1	617	0.03	0.47*	12.8*	0.93
	> 0.2	465	0.09	0.56*	12.5*	0.94
	> 0.3	345	0.18	0.60*	12.1*	0.95
	> 0.4	240	0.35	0.81*	13.6*	0.96
Grassland	> 0.1	564	0.84	0.80*	-0.16*	0.99
	> 0.2	412	0.89	0.84*	-0.22*	0.99
	> 0.3	299	0.91	0.85*	-0.27*	0.99
	> 0.4	179	0.88	0.81*	-0.22*	0.99
Corn	> 0.1	1190	0.45	0.58*	2.04*	0.79
	> 0.2	865	0.48	0.67*	3.11*	0.80
	> 0.3	545	0.57	0.73*	3.84*	0.82
	> 0.4	267	0.72	0.83*	5.21*	0.83

*significant by a t-test at a 5% probability level.

In general, the correlation and agreement, expressed respectively by the R^2 and refined index of agreement (d_r) (Willmott et al., 2012), for LNF and EC NEE relationships, improved as the u_* values increased (Table 2.3). However, for the grassland site, a slightly better correlation between EC and LNF NEE estimates were found for u_* >0.3 m s^{-1} (R^2 = 0.91) than for u_* >0.4 m s^{-1} (R^2 = 0.88), where very good agreements (d_r = 0.99) were found for both cases. Considering only the NEE data for u_* >0.4 m s^{-1}, the grassland canopy showed the best correlation (R^2 = 0.88) and agreement (d_r = 0.99) between EC and LNF NEE estimates, followed by corn (R^2 = 0.72 and d_r = 0.83) and forest canopies (R^2 = 0.35 and d_r = 0.96). Although stricter u_* values tended to improve correlation and agreement between the methods, they also resulted in a drastic decrease in the number of NEE available data points (Table 2.3).

To evaluate the dependence of LNF on atmospheric stability, we separated the observed and modelled NEE in classes based on the atmospheric stability conditions (APPENDIX A). The atmospheric stability condition was determined by the ratio

between the canopy height and the Obukhov length (h/L), and classified as: unstable ($-0.01 < h/L$), neutral ($-0.01 \leq h/L < 0.01$) and stable ($h/L \geq 0.01$). Considering only the NEE data for $u_* > 0.3$ m s^{-1}, the forest showed a very poor correlation between measured and modelled NEE under unstable conditions ($R^2 = 0.20$), and a reasonable correlation under neutral ($R^2 = 0.45$) and stable conditions ($R^2 = 0.50$). For the grassland, higher correlation between measured and modelled NEE was found when the atmosphere was unstable ($R^2 = 0.90$), following by stable ($R^2 = 0.73$) and near neutral ($R^2 = 0.67$) conditions. For the corn canopy, a very poor correlation between measured and modelled NEE was found when the atmosphere was stable ($R^2 = 0.30$), however, higher correlation was observed under unstable ($R^2 = 0.50$) and near neutral ($R^2 = 0.63$) conditions.

The poor performance of the LNF theory to estimate NEE above the forest canopy in our study is in agreement with the results reported by Siqueira et al. (2000), who applied the LNF theory to study CO_2 exchange at the Duke Forest in North Carolina. They also evaluated the impact of atmospheric stability conditions on LNF CO_2 fluxes. They found that LNF performed best for near neutral stability conditions ($R^2 = 0.25$), followed by the unstable atmospheric condition ($R^2 = 0.23$) and stable atmospheric conditions ($R^2 \approx 0$).

Leuning et al. (2000) found that the LNF performance to estimate daytime NEE in a rice canopy was better when $u_* > 0.1$ m s^{-1} and under a near neutral stability condition. They also observed that NEE was overestimated by the LNF theory at night, which they attributed to the lack of atmospheric stability corrections to their σ_w and T_L profiles. Santos et al. (2011) applied an analytical Lagrangian dispersion analysis, proposed by Warland and Thurtell (2000), to infer CO_2 and energy fluxes for a corn canopy. They also applied the atmospheric stability corrections on σ_w and T_L profiles

and found the best correlation between measured and modelled NEE for unstable atmospheric conditions and the poorest correlation under stable conditions.

For this study, we hypothesized that the poor performance of the LNF theory above the forest canopy, when compared to EC NEE measurements, could be related to some degree to the decoupling between within and above-canopy air flows (Haverd et al., 2009). Similar to other canopy multilayer models, the LNF assumes that the turbulent transport occurs under steady state conditions, so changes in mass or energy storage within the canopy volume affect the LNF performance. We calculated the change in CO_2 storage flux (hereafter CO_2 storage), which was used as an indicator of the degree of flow decoupling between with and above-canopy air flows. The CO_2 storage was calculated following Aubinet et al. (2001) and Papale et al. (2006), as follows:

$$\mathrm{CO_2\ storage} = \frac{P}{\mathbf{R}\,T_{air}} \int_0^{z_h} \frac{\partial[\mathrm{CO_2}](z)}{\partial t}\,\partial z \qquad (2.11)$$

where P is the atmospheric pressure (Pa), $\mathbf{R}$ is the molar gas constant (J mol^{-1} K^{-1}), T_{air} is the air temperature (K), [CO_2] is the CO_2 mixing ratio (μmol mol^{-1}), measured at a given height z (m) along a vertical profile with height z_h, and t is time (s). Half-hourly profiles of CO_2 mixing ratio were used in this study to estimate CO_2 storage.

The ensemble-averaged CO_2 storage values calculated from [CO_2] profiles for the different canopies are shown in Figure 2.3a. The forest canopy showed the largest depletion rate of stored CO_2 in comparison to the other canopies.

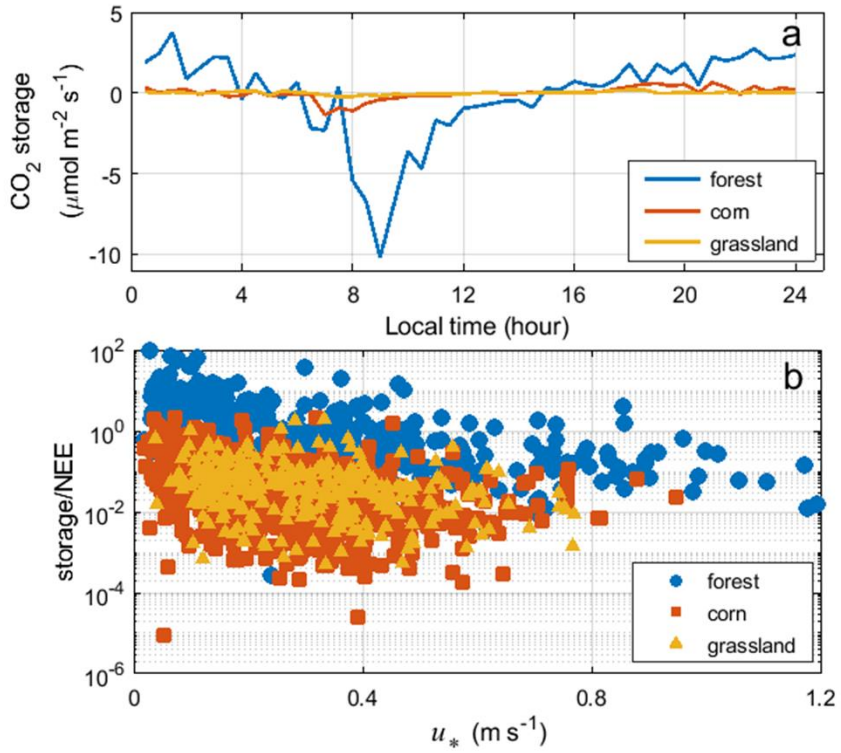

Figure 2.3. a) ensemble-averaged CO_2 storage flux estimated for forest, corn and grassland canopies; and b) relationship between the friction velocity ($u*$) and the ratio between CO_2 storage and the net CO_2 ecosystem exchange (storage/NEE) for corn, grassland and forest canopies.

The forest depletion rate peak was observed at about 9:00 h and by 15:00 h the canopy air was usually completely well mixed with the air aloft and CO_2 storage approached zero. This diel pattern is in agreement with the results reported by Iwata et al. (2005) who estimated the CO_2 storage in an Amazonian rainforest. The corn canopy showed a much lower depletion rate peak due to the smaller canopy air volume in comparison to the forest. The corn depletion rate peak occurred at about 7:00 h and about 11:00 h the canopy was already well mixed with the atmospheric flow. The grassland canopy showed a negligible change in CO_2 storage throughout the day.

To evaluate the magnitude of the storage term with respect to NEE, we calculated the ratio between CO_2 storage and absolute values of NEE measured by the EC system, following Iwata et al. (2005). The storage/NEE values for the forest canopy

were larger than for grassland or corn even under vigorous above canopy turbulence (u_*>0.4 m s^{-1}) (Figure 2.3b). These results suggest that atmospheric layers above and within the forest canopy may be fully or partly decoupled leading to large changes in CO_2 storage within the canopy (Haverd et al., 2009; Van Gorsel et al., 2011). This could explain the low correlation between EC and LNF estimates for the forest canopy and a better performance of LNF for the corn and grassland canopies. These results are supported by Göckede et al. (2007)'s findings who used a wavelet tool to characterize several typical states of coupling and decoupling between within-canopy airspace flow and above-canopy flow. They concluded that the flow decoupling is likely to occur in tall canopies with moderate density, and also suggested that improvements in turbulence statistics considering the decoupling effects could minimize errors in Lagrangian stochastic model estimates.

The ensemble-averaged profiles of CO_2 source strengths (S_c) and CO_2 fluxes (F_c) modelled using the LNF are shown in Figure 2.4. We only show S_c estimates for the grassland and corn canopies since the LNF performance to estimate NEE for the forest, and consequently F_c and S_c, was affected by the flow decoupling as discussed previously. We observed a distinct diel variation of S_c for both corn and grassland canopies (Figure 2.4a and c), with lower S_c values during daytime than during night-time periods.

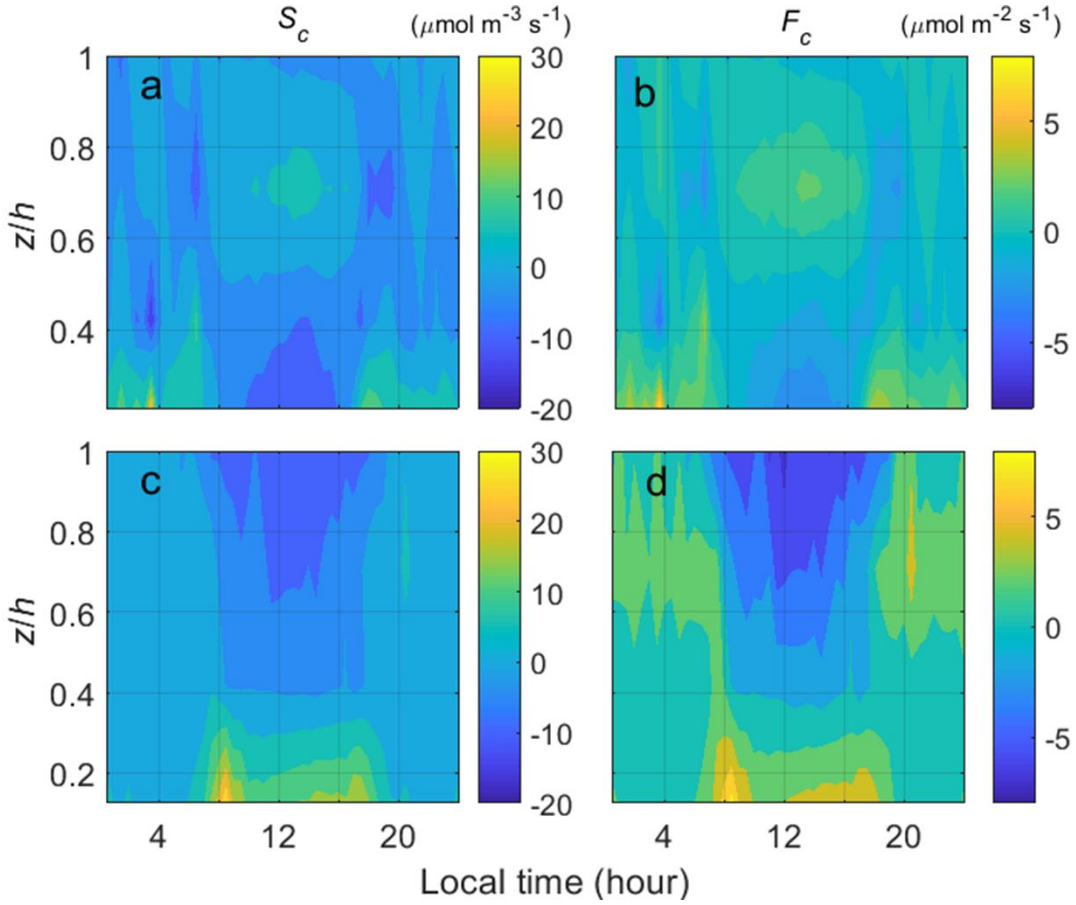

Figure 2.4. a and c) spatial and temporal variations of ensemble averaged CO_2 source strength (S_c, µmol m^{-3} s^{-1}), and b and d) CO_2 fluxes (F_c, µmol m^{-2} s^{-1}) estimated using the LNF theory for grassland (a and b) and corn (c and d) canopies.

Corn canopy showed a large CO_2 sink (on average of 13.0 µmol m^{-3} s^{-1}) in the upper layers (z/h > 0.6) and a large CO_2 source (on average of -11.0 µmol m^{-3} s^{-1}) in the bottom layers(z/h < 0.4) during the daytime (Figure 2.4c). At night, the corn canopy had a more homogeneous S_c profile, with an average S_c of 2.7 µmol m^{-3} s^{-1} throughout the canopy. The CO_2 flux values also showed a diel trend for both ecosystems (Figure 2.4b and d). For the corn canopy (Figure 2.4d), a maximum assimilation of -7.0 µmol m^{-2} s^{-1} was observed at midday for top canopy layer (z/h > 0.8). The bottom layers, on the other hand, showed a predominance of respiratory fluxes. A maximum release of 8.9 µmol m^{-2} s^{-1} was observed between 6:30 and 8:30 h at z/h < 0.4 due to a build-up of respiratory fluxes overnight, which extended over all canopy layers during the

referred period. For the grassland (Figure 2.4b), most assimilation occurred at z/h < 0.6 with a maximum value of -4.2 μmol m^{-2} s^{-1} at 14:00 h and a maximum release of 7.5 μmol m^{-2} s-1 observed at bottom layers around 4:00 h. The low assimilation observed for the grassland is related to a reduction in the photosynthetic rates due to the end of growing season. These results suggest that the LNF theory was able to capture the expected spatial and temporal patterns of CO_2 source/sink and CO_2 fluxes for corn and grassland canopies.

The S_c spatial and temporal variability in this study is consistent with the results reported by Hsieh et al. (2003) who proposed the use of a two-dimensional Lagrangian stochastic dispersion model to compute source/sink spatial-temporal variations within a forest canopy. Our results are also in agreement with CO_2 source/sink and flux profiles reported by Leuning et al. (2000) for a rice canopy. They found F_c to be always positive in the lower layers, which agrees with our F_c predictions for the corn canopy. Most studies to date have used the LNF theory to examine scalar exchange in forests, but our results indicate that the LNF theory could be a valuable tool to study scalar exchange in short canopies in which within-canopy EC measurements are not possible with the currently available EC instrumentation.

2.3.3 Comparison between IFR and LNF isotope compositions of CO_2 fluxes

To investigate the performance of the LNF theory to study isotope exchange in different plant canopies, we compared the LNF estimates of isotope compositions of NEE (δ_N) with the ones provided by the IFR approach (Eq. 2.10). Previous studies have shown that the magnitude of CO_2 concentration gradients have great impact on IFR estimate uncertainties (Griffis et al., 2005a; Santos et al., 2012). The LNF performance is also expected to be dependent on the accuracy of scalar concentration gradients. In this study, the influence of [CO_2] gradient magnitude on IFR and LNF δ_N

estimates was evaluated by calculating the moving coefficient of variation (CV) of δ_N. To do that, δ_N values were sorted based on the ascending order of magnitude of [CO_2] gradients measured by the two highest air intakes. The δ_N CV was then calculated for both methods using the moving standard deviation and moving averages of δ_N for a window size corresponding to four data points.

Figure 2.5 shows the relationship between absolute gradients of [CO_2], measured using the two intakes above the canopies, and the CV of δ_N estimated by IFR and LNF approaches. Both methods showed large uncertainties with the IFR δ_N estimates having a larger CV for a given [CO_2] gradient when compared to the LNF estimates.

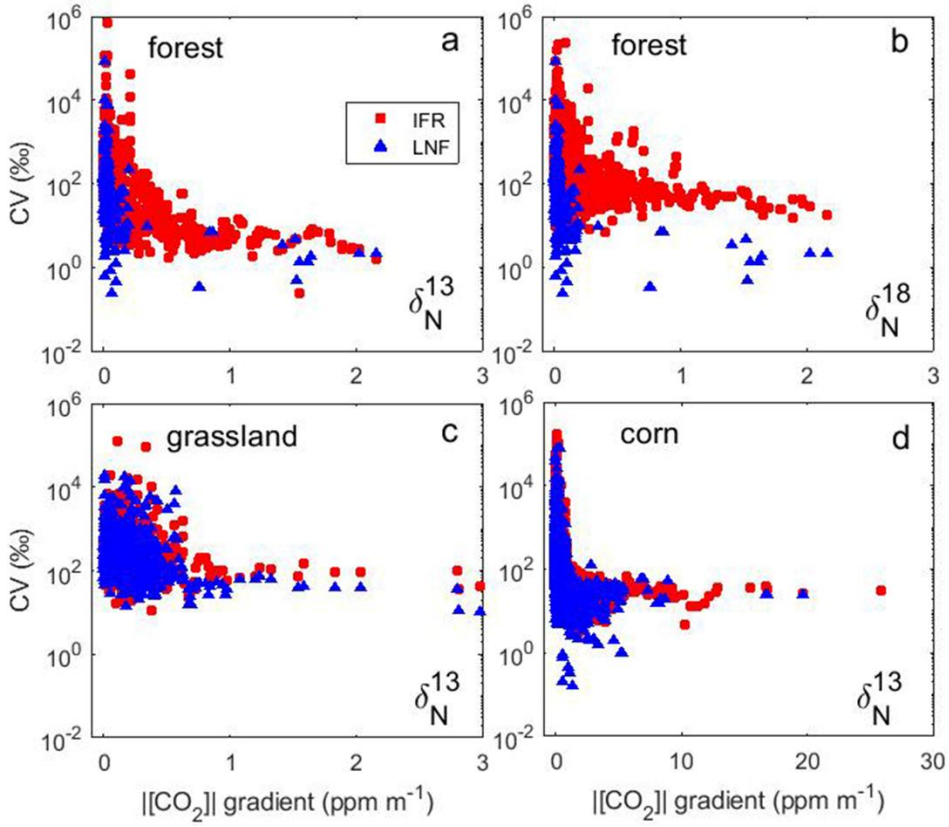

Figure 2.5. Relationship between the moving coefficient of variation (CV) of isotope signatures of net CO_2 ecosystem exchange (δ_N^{13} and δ_N^{18}) and the absolute CO_2 mixing ratio vertical gradient. δ_N^{13} and δ_N^{18} were estimated by the IFR method (red squares) and the LNF theory (blue triangles) for different plant canopies. The CV was

calculated using moving averages and standard deviations of δ_N^{13} and δ_N^{18} for a window of 4 data points.

On average, the CV values decreased to less than 100% when [CO_2] gradients exceeded 0.4 ppm m^{-1} for LNF and 0.9 ppm m^{-1} for IFR (Figure 2.5a, 2.5b and 2.5d). However, for the grassland canopy, both methods showed similar δ_N uncertainties, with CV values above 100% for basically all ranges of [CO_2] gradients for both methods (Figure 2.5c). Larger gradients of [CO_2] were usually observed for the corn canopy in comparison to the [CO_2] gradients for the other ecosystems (Figure 2.5d). These gradients above the corn canopy were likely a result of the placement of the two intakes in a region with strong [CO_2] gradients above the corn canopy (i.e. relatively closer to canopy height) as well as to larger CO_2 fluxes during the growing season when compared to grassland, where CO_2 fluxes were usually smaller near the end of the growing season (section 2.3.1).

Previous studies reported large uncertainties in IFR δ_N estimates for small isotopologues concentration gradients, frequently observed just above plant canopies, due to small signal to noise ratio of the concentration data (Griffis et al., 2005a; Santos et al., 2011; Zhang et al., 2006). Our results confirm that δ_N estimate uncertainties are highly dependent on the signal to noise ratio of isotope measurements and that the LNF theory could reduce some of the δ_N uncertainties. Based on the averages of CV, considering all sites, the CV for LNF δ_N estimates was 74% lower than the CV for IFR predictions.

We established an arbitrary screening criterion based on the CV to exclude IFR and LNF δ_N values with large uncertainties. For the CV screening, the δ_N values associated with a CV larger than 70% were excluded from our analyses. The utilization of a CV criterion of 70% was necessary due to the data availability and higher variability of δ_N values, mainly for the grassland. In addition to the CV filter, the LNF

and IFR δ_N^{13} estimates smaller than -40‰ and larger than 0‰ were excluded from our analyses. For LNF and IFR δ_N^{18} estimates for the forest, the values excluded were smaller than -40‰ and larger than 40‰.

The IFR and LNF δ_N comparisons are shown in Table 2.4. In general, the IFR and LNF δ_N estimates showed poor to moderate correlation (R^2 ranging 0.11 to 0.41) and good agreement (d_r ranging from 0.73 to 0.98). We hypothesize that uncertainties in CO_2 isotopologue concentration measurements above the canopies affected the performance of the IFR method. An alternative to increase the signal to noise ratio of the CO_2 isotopologue gradient measurements could be to increase the distance between air intake, and thus the gradients of scalar concentration. In this study, increasing the spacing between air intakes would require the use of air intakes just below the canopy.

Table 2.4. Statistical coefficients of the relationship between isotope signatures of net ecosystem CO_2 exchange (δ_N) provided by IFR method and predicted from LNF theory.

Ecosystem	δ_N	z_1/h	***n***	R^2	**Slope**	**Intercept**	d_r
		m					
Forest	$\boldsymbol{\delta_N^{13}}$	1.17	125	0.14	0.21*	-20.01*	0.93
		0.94^{+}	216	0.01	-0.02$^{\mathbf{n.s.}}$	-25.03*	0.98
	δ_N^{18}	1.17	43	0.11	0.43*	-5.80$^{n.s.}$	0.96
		0.94^{+}	185	0.12	0.08*	-7.49*	0.95
Grassland	δ_N^{13}	1.53	12	0.18	0.52$^{\mathbf{n.s.}}$	-13.99$^{n.s.}$	0.73
		0.99^{+}	36	0.68	0.78*	-4.37$^{n.s.}$	0.99
Corn	δ_N^{13}	1.15	470	0.41	0.49*	-8.40*	0.86
		0.94^{+}	594	0.57	0.55*	-7.53*	0.93

n.s., not significant by a t-test at a 5% probability level.
*significant by a t-test at 5% probability level.
$^{+}$ z_1 slightly inside the canopy.

The use of in-canopy data in IFR calculations could violate some of the K-theory assumptions due to the proximity of scalar sources and the length scale of turbulence within canopies, leading under some circumstance to counter-gradient fluxes (Corrsin, 1975). To investigate the effect of using in-canopy data on IFR

estimates, we calculated δ_N using IFR and concentration data obtained using the highest air intake and the first air intake immediately below the top of the canopies at *z/h* of 0.94, 0.99 and 0.94 for the forest, grassland and corn canopies, respectively (Table 2.4). The use of data for larger intake spacing resulted in better correlation (R^2 ranging from 0.57 to 0.68) and agreement (d_r ranging from 0.93 to 0.99) for the relationship between δ_N values estimated using IFR and LNF for the grassland and corn canopies when concentration data for larger intake separation were used in the IFR calculations (Table 2.4). However, for the forest canopy the use of in-canopy data did not improve the relationships between IFR and LNF δ_N estimates, which could be an indication of K-theory failure for that canopy. Using model simulations, Raupach (1987) demonstrated that counter gradient fluxes resulting from near-field effects can be expected to occur just below a strong scalar source within the canopy. It is possible that due to the forest canopy structure near-field effects were stronger than just below the canopy when compared to the grassland and corn canopies.

Our results show that both IFR and LNF methods can capture seasonal variation in δ_N^{13} (Figure 2.6). The seasonal averages of δ_N^{13} provided by IFR and LNF for the corn canopy were -20.6 and -18.5 ‰, respectively.

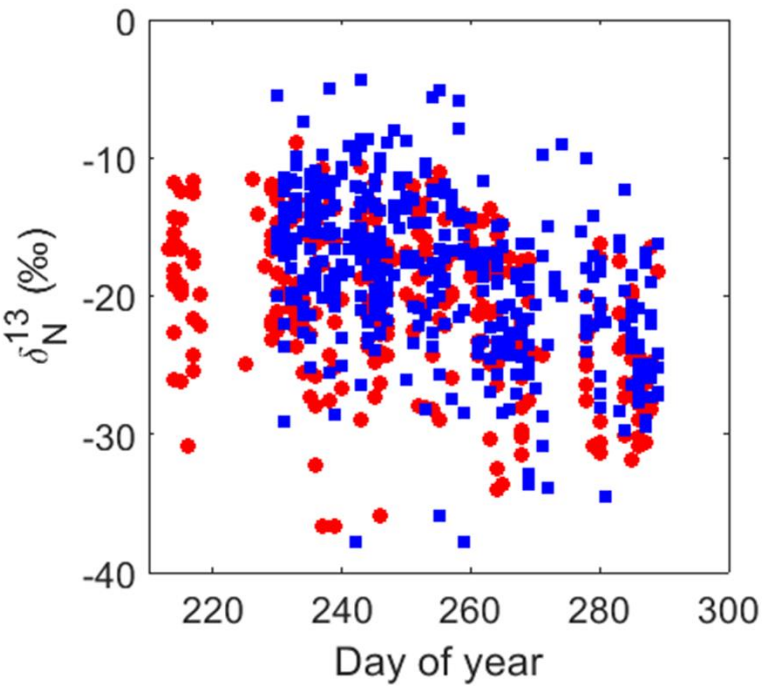

Figure 2.6. Seasonal variation in the isotope composition of net ecosystem $^{13}CO_2$ exchange ($\delta_N{}^{13}$) estimated using the IFR (red circles) and LNF theory (blue squares) for the corn canopy.

The temporal variation of δ_N^{13} showed a downward trend toward the end of the growing season. This seasonal variation in δ_N^{13} was likely due to a larger contribution of C_3 residue in the soil organic matter to the ecosystem respiration in comparison to flux contributions from corn plants that were reaching senescence. A similar trend was observed in previous studies carried out in corn/soybean rotations (Griffis et al., 2008, 2005a).

Figure 2.7 shows the half-hourly averaged vertical distribution of the isotope composition of CO_2 flux (δ_F) estimated by LNF for different canopies. Unfortunately, we were unable to plot the δ_F vertical distribution for the grassland canopy due to the low data availability after data screening procedures (Section 2.3.3).

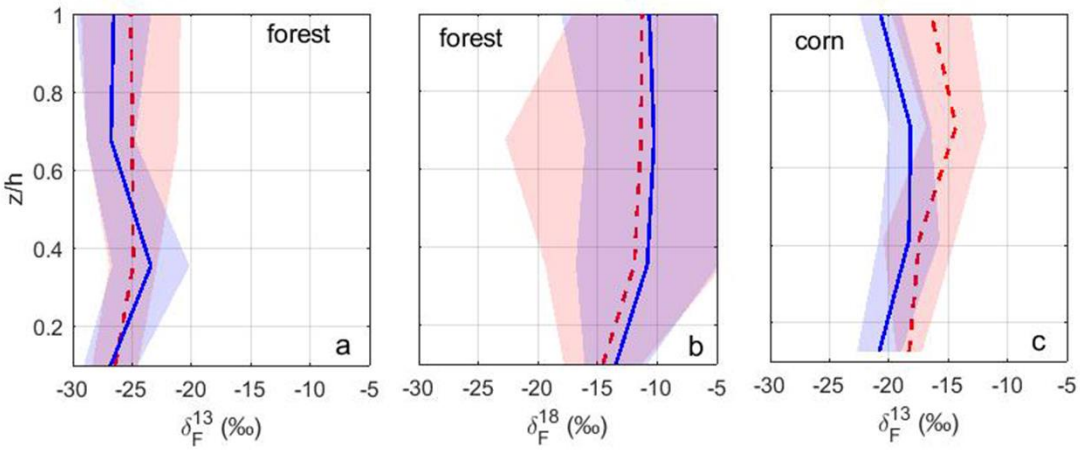

Figure 2.7. Half-hourly averaged vertical distribution of isotope composition of CO_2 flux ($\delta_F{}^{13}$ and $\delta_F{}^{18}$) estimated using the LNF theory for different plant canopies during daytime (red dashed lines) and nighttime (blue solid lines) periods. The shaded areas represent the standard deviation (σ) of $\delta_F{}^{13}$ or $\delta_F{}^{18}$.

Larger variability in δ_F were found for the forest canopy (Figure 2.7 a and b) in comparison to the δ_F variability observed for the corn canopy (Figure 2.7c). For the corn canopy, where the mean standard deviation (σ) was lower than for the forest, the average LNF δ_F^{13} (±σ) during the daytime was -17.8 (±2.0) ‰ for the source layer below z/h<0.4 and -15.4 (±2.9) ‰ for other source layers. At night a similar pattern was observed, i.e. more depleted LNF δ_F^{13} for the source layers near the ground with a lower value of -20.8 (±1.8) ‰ than for higher source layers of -19.0 (±1.9) ‰. The range of δ_F^{13} and δ_F^{18} values provided by the LNF in these vertical distributions are in agreement with those found in previous studies with C_3 and C_4 ecosystems (Griffis et al., 2008, 2005a, Santos et al., 2014, 2012). The large variability in δ_F^{18} could be a result of the high temporal dynamics of the $C^{18}OO$ isopologue at the forest ecosystem, which agrees with the data provided by Santos et al. (2014) for that ecosystem.

2.3.4 Estimating the ^{13}C isoforcing

To quantify the effect of isotope biosphere-atmosphere exchange on the δ_a^{13} budget, we calculated the ecosystem-scale ^{13}C isoforcing (I_F) following Griffis et al. (2008) and Lee et al. (2009).

$$I_F = \frac{\mathrm{NEE}}{c_a}(\delta_{\mathrm{N}}^{13} - \delta_a^{13}) \tag{2.12}$$

where, NEE is the net CO_2 ecosystem exchange (μmol m^{-2} s^{-1}), c_a is the half-hour CO_2 concentration (μmol m^{-3}), and δ_a^{13} is the ^{13}C composition of ambient air (‰).

We calculated I_F using two different approaches by combining EC measurements of NEE: 1) with flux ratios (δ_{N}^{13}) estimated by the IFR method and 2) δ_{N}^{13} estimated using the LNF theory. Following Sturm et al. (2012), we also calculated a hypothetical isoforcing for both IFR and LNF methods. The hypothetical isoforcing were calculated using constants of δ_{N}^{13} of -20.6 and -18.5 ‰, which correspond to the average δ_{N}^{13} estimated by IFR and LNF methods, respectively. Unfortunately, we were unable to perform the same calculation for forest and grassland canopies due to the low data availability after data screening procedures (Section 2.3.3).

The ensemble-averaged diel of δ_{N}^{13} calculated by IFR and LNF approaches for the corn canopy is shown in Figure 2.8. Large fluctuations were observed in IFR δ_{N}^{13} estimates mainly between 6:00 and 18:00 h (Figure 2.8a). This large variability in δ_{N}^{13} is a result of small concentration gradients of [CO_2] observed during daytime periods under turbulent conditions (see section 2.3.1). The LNF estimates of δ_{N}^{13} were less variable than IFR estimates (Figure 2.8b).

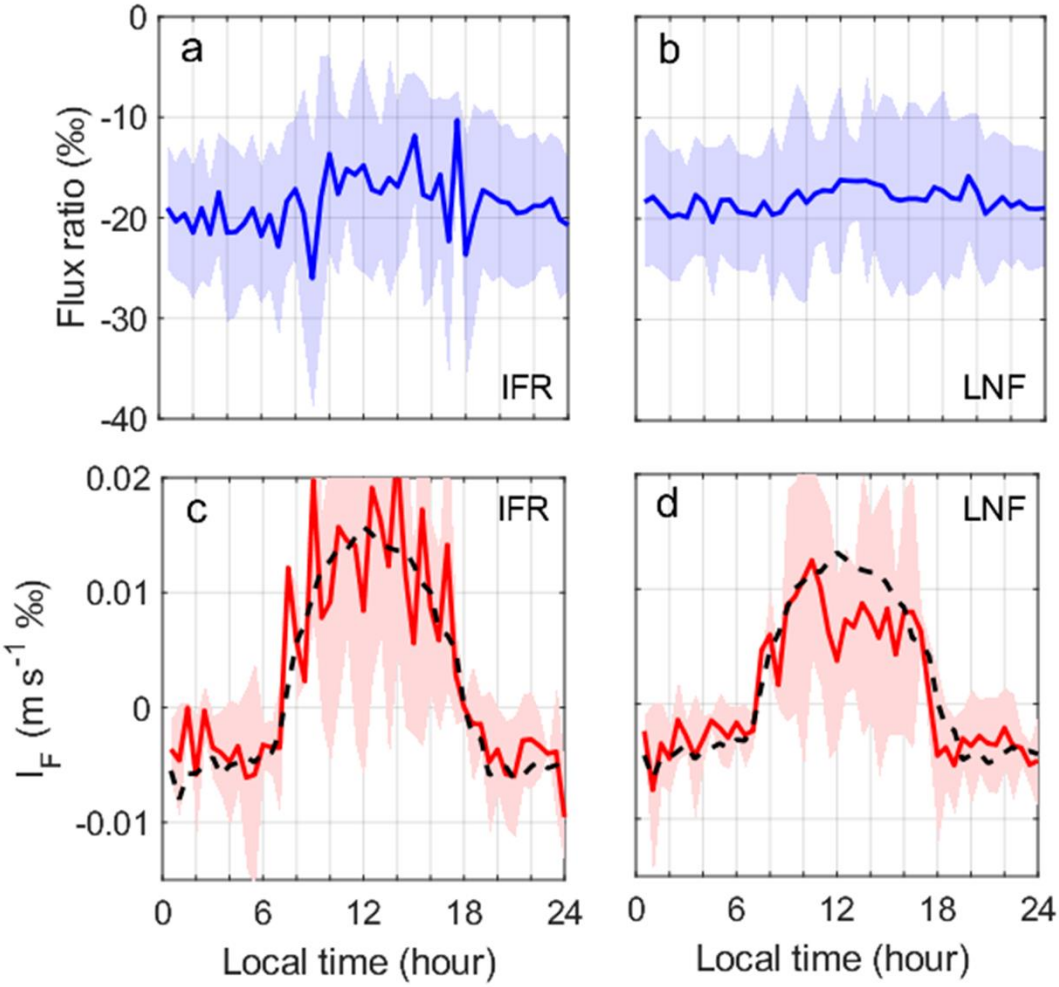

Figure 2.8. a and b) ensemble average of $^{13}CO_2$ compositions of NEE (δ_N^{13}) estimated using the IFR method and LNF theory for the corn canopy; and c and d) mean diurnal ^{13}C isoforcing (I_F) calculated combining eddy covariance NEE measurements with: δ_N^{13} provided by IFR method and δ_N^{13} predicted by the LNF theory. The dashed lines represent the calculated hypothetical isoforcing with a constant δ_N^{13} of -20.6 and -18.5 ‰ for IFR and LNF, respectively. The shaded areas represent the standard deviation (σ) of flux ratio or I_F.

The diurnal pattern of I_F was mainly driven by the NEE diel variation. The large variability in IFR I_F estimates during daytime periods were a result of the large uncertainties in IFR estimates (Figure 2.8c). The LNF I_F estimate uncertainties were lower than the IFR estimates (Figure 2.8d). Estimated LNF I_F show a small difference between the hypothetical isoforcing and LNF I_F of 0.003 (± 0.003) m s^{-1} ‰ during

daytime between 8:00 and 11:00 h. Large difference is observed between 11:30 h and 15:30 of 0.005 (±0.002) m s^{-1} ‰, which the maximum difference was found at 12:00 with a value of 0.009 m s^{-1} ‰. This may be an indication that δ_N^{13} contributed to some degree to the isoforcing's diurnal variation, as supported by the LNF δ_N^{13} values that showed a small diurnal variation with δ_N^{13} values ranging from -15.8 ‰ to -20.3 ‰ (Figure 2.8b). This suggests a small isotopic disequilibrium for the corn ecosystem. The large inherent noises of the IFR method (Figure 2.8a) limited the use of IFR I_F for constraining isotope budgets (Sturm et al., 2012)

2.4 Conclusions

In this study, we evaluated the use of the localized near-field theory (LNF) to study $^{13}CO_2$ and $C^{18}OO$ isotope exchange in different plant canopies. The LNF estimates of NEE were highly sensitive to the below and above canopy flow decoupling. The large depletion peak of CO_2 storage associated with strong flow decoupling in the forest canopy was shown to affect the NEE estimates from LNF, which showed the lowest correlation (R^2 = 0.35) with NEE measured using the EC technique. For the corn and grassland, where the depletion peak of CO_2 storage was found to be very small or negligible, the model performed better than forest with R^2 of 0.72 and 0.88, respectively. These results suggest that the LNF theory may provide better estimates for short canopies, in which there is lower CO_2 storage within canopy airspace in comparison to forest canopies. This could be a great advantage of LNF to study scalar transport within short canopies since the EC instrumentation is too bulky to be used to measure fluxes within short canopies.

The CV for LNF δ_N estimates was 74% lower than the CV for IFR predictions and, therefore the LNF theory can reduce some of the IFR δ_N uncertainties. The period of measurement near the end of growing season for the grassland contributed to a

smaller spatial variation of [CO_2] than forest and corn, thus leading to an even smaller precision of the methods in this specific case. On average, the CV values decreased to less than 100% when [CO_2] gradients exceeded 0.4 ppm m^{-1} for LNF and 0.9 ppm m^{-1} for IFR. However, for the grassland canopy, both methods showed similar δ_N uncertainties, showing high relative variability with values of CV larger than 100% for practically all [CO_2] gradient ranges. The correlation (R^2) between δ_N IFR and δ_N LNF estimates for grassland and corn canopies increased, on average, from 0.29 to 0.62 and the agreement approached one (d_r increased, on average, from 0.79 to 0.96) when IFR was calculated using one air intake of measurement slightly inside the canopy.

Our study shows the first attempt to combine LNF predictions with several months of near-continuous measurements of stable isotopes of CO_2 in different vegetation canopies. These results indicate that LNF is potentially a useful tool to provide new insights to study CO_2 exchange processes within well-mixed short canopies, where the flux measurements using traditional micrometeorological techniques are even more challenging. In addition, LNF also can be useful for inferring isotope exchange within plant canopies, which allows the separation of the isotope exchange between soil and plant components.

CHAPTER 3 - USING STABLE ISOTOPES OF CO_2 AND A MULTI-LAYER LAGRANGIAN INVERSE MODEL FOR PARTITIONING NET CO_2 ECOSYSTEM EXCHANGE IN A CORN CANOPY

Abstract

High-temporal resolution isotope measurements can be combined with multi-layer Lagrangian models to partition net ecosystem–atmosphere exchange (NEE) of carbon dioxide (CO_2) into net photosynthesis (F_A) and non-foliar respiration (F_R). In this study, we investigated the application of the localized near-field theory (LNF) as an alternative non-isotopic method for NEE partitioning in a corn canopy. In addition, we performed the NEE partitioning using the isotope flux partitioning (IFP) approach with LNF derived half-hourly direct estimates of isotope composition of NEE (δ_N), F_A (δ_P) and F_R (δ_R). Mixing ratios of stable isotopes of CO_2 were measured within and above the corn canopy using a multiport sampling system and the tunable diode laser spectroscopy (TDLAS) technique. NEE and wind velocity data were measured above the canopy using an EC system. LNF and IFP partitioned fluxes were evaluated with an independent night-time based partitioning (RP) method. We also evaluated the expected physiological responses in F_A and F_R estimated by the methods by using light and temperature response curves. Our results showed a seasonal variation in NEE (-18.4 to -11.0 μmol m^{-2} s^{-1}), δ_N (-14.0 to -20.6‰), δ_P (-15.3 to -20.7‰) and δ_R (-17.5 to -22.1‰) following closely the canopy phenology. The LNF theory showed more ability in reproducing the expected F_A seasonal variation than RP. LNF F_R showed large uncertainties under low turbulent mixing periods when the canopy was fully developed, reaching unrealistic values on the order of 50 μmol m^{-2} s^{-1}. However, good agreement (d_r = 0.65) between LNF F_R and RP F_R was observed at the end of the growing season. For isotope-derived fluxes, IFP F_A and IFP F_R predictions were high

sensitive to the D_{eq}. However, unrealistic flux estimates were considerably reduced when weak D_{eq} (< 3.2 ‰) periods were filtered out from IFP predictions. We conclude that the LNF is an advantageous alternative method for non-isotopic and isotopic flux partitioning. In addition, our results suggest that the future success of the IFP approach is highly dependent on isotope measurements techniques advances, providing estimates of D_{eq} at high temporal-resolution with more precision.

3.1 Introduction

Terrestrial ecosystems are a large sink of carbon (3.2 Gt C yr^{-1}) , which offsets more than one-quarter of the annual global fossil fuel CO_2 emissions (9.4 Gt C yr^{-1}) to the atmosphere (Le Quéré et al., 2018). The magnitude of the CO_2 sink in ecosystems is a result of two processes: the assimilation of carbon though photosynthesis and release of CO_2 to the atmosphere thought the respiration process. Since these processes are governed by different biotic and abiotic drivers, partitioning the CO_2 flux between the soil and vegetation components can help us to better understand the terrestrial ecosystems role on the global C budget.

Measurements of C isotope fluxes have been shown to be useful for partitioning net CO_2 ecosystem exchange (NEE) into net photosynthesis (F_A) and non-foliar respiration (F_R) (Bowling et al., 2001; Lai et al., 2003; Yakir and Wang, 1996). Therefore, the combination of novel high-temporal resolution isotope measurements and micrometeorological techniques has provided new insights into environmental factors governing F_A and F_R at the ecosystem scale (Fassbinder et al., 2012; Griffis et al., 2005a; Wehr et al., 2016; Wehr and Saleska, 2015; Zobitz et al., 2008). It is also important for improving our comprehension of the C cycling in terrestrial ecosystems, and its sensitivity to climate variation and land use change.

The eddy covariance (EC) is a well-established micrometeorological method to measure the exchanges of carbon dioxide around the world (Baldocchi et al., 2001). Although some recent studies have been using sub-canopy EC measurements to partition CO_2 fluxes in forest canopies (Paul-Limoges et al., 2017; Sulman et al., 2016). Below-canopy EC measurements are usually problematic due to low wind speed and intermittent turbulence in the sub-canopy airspace. In addition, bulky EC instrumentations cannot be deployed within short plant canopies. Alternatively, NEE is often partitioned using two different approaches. The first approach is the nigh-time based flux partitioning method, in which F_R values, derived from night-time values of NEE, are extrapolated to the daytime by using temperature response functions (Lloyd and Taylor, 1994; Reichstein et al., 2005a). The second method is the daytime based flux partitioning method, where light-response curves are fitted to daytime NEE measurements to estimate F_A (Lasslop et al., 2010), which offers an alternative to the use of potentially problematic night-time NEE values (Aubinet et al., 2012).

Although both night-time and daytime based methods for flux partitioning have been gaining popularity over the last decades (Lasslop et al., 2010; Reichstein et al., 2005a; Stoy et al., 2006; Wang et al., 2015), concerns have been raised due to their several fundamental limitations, as briefly revised by Fassbinder et al. (2012). For example, for night-time based methods these limitations may include the lack of skill in capturing physiological controls on short-term (< 24 h) variations of NEE due the use of seasonal temperature data (Lloyd and Taylor, 1994; Reichstein et al., 2005a). For the daytime-based method, a major downside is the inhibition of leaf respiration by light, known as the Kok effect, that lead to large discrepancies between daytime and night-time ecosystem respiration (Wehr et al., 2016).

The isotope flux partitioning (IFP) method provides an alternative for partitioning NEE into F_A and F_R, based on differences of isotope composition of plant and soil organic matter. Photosynthesis preferentially fixes $^{12}CO_2$ leading to a reduction in ^{13}C abundance in plant biomass. Therefore, during the day the ambient air near plant canopies is enriched in $^{13}CO_2$, which is later diluted by the depleted isotope composition of respiration (Farquhar et al., 1989). The isotope composition of soil and plant CO_2 fluxes can be inferred by using atmospheric concentration of CO_2 isotopologues. These information help us to independently partition the net CO_2 fluxes into its elementary flux components (F_A and F_R) (Flanagan et al., 1996). However, the feasibility of the IFP method is dependent on the existence of a temporal isotopic disequilibrium (D_{eq}) between carbon isotope composition of F_A (δ_P) and F_R (δ_R) (Bowling et al., 2001). Otherwise, the errors in F_A and F_R estimates become large as the D_{eq} approaches zero (Wehr et al., 2013; Zobitz et al., 2008).

Several studies have attempted to develop an isotope partitioning approach of general use (Bowling et al., 2001; Ogée et al., 2003; Wehr and Saleska, 2015; Zhang et al., 2006; Zobitz et al., 2007). However the lack of precision of field-scale isotope measurements and fundamental limitations in the theoretical framework to use those measurements have limited its utilization (Wehr and Saleska, 2015). For example, the first attempt to propose an isotope-derived flux partitioning method based on the mass balance principle was made by Yakir and Wang (1996). They introduced the IFP approach, by using CO_2/H_2O infrared gas analyser and flask samples of H_2O and CO_2 above croplands for determination of concentration and isotopic gradients, respectively. Their IFP approach has some limitations for short-term flux partitioning applications due to the use of integrated isotope ratios of soil and plants components. This integration was based on analysis of water and organic matter from leaves, stems

and soil samples collected in a single day during peak activity. Some improvements in this methodology were made by Bowling et al. (2001) who combined EC and flask-measurements of carbon isotopes ratios of CO_2 (EC/flask method) on a continuous-flow mass spectrometer to measure the isoflux of NEE (δ_NNEE) over a deciduous forest. However, their δ_N measurements were temporally coarse.

Recent developments in laser spectroscopy techniques enabled near-continuous measurements of CO_2 and H_2O isotopologues in the air under field conditions (Griffis, 2013). These high-frequency measurements can be combined with micrometeorological techniques to study isotope exchange at ecosystems and, therefore to implement the IFP approach (Griffis et al., 2008, 2004; Griffis, 2013). Several studies have applied the IFP method proposed by Bowling et al. (2001) with near-continuous isotope measurements (Griffis et al., 2005b; Zobitz et al., 2008, 2007). These studies usually determined δ_N by using the flux-gradient method with tunable diode laser (TDL) absorption spectroscopy measurements (also known as IFR method, see section 2.2.2). However, IFR δ_N estimates are quite sensitive to errors in measurements of concentration gradients (Griffis et al., 2005a; Santos et al., 2012). In addition, the gradient diffusion theory, the basis for the IFR method, is sensible to near-field effects and cannot be applied near the top or within plant canopies (Corrsin, 1975; Denmead and Bradley, 1987). More recently, Wehr and Saleska (2015) proposed an improved isotopic method for partitioning NEE by using EC measurements of δ_N and quantum cascade laser spectrometer (QCLS) measurements of CO_2 isotopologues. They modified the original IFP to include photorespiration, foliar daytime 'dark' respiration, and other refinements. They results showed that their improved IFP approach could reduce uncertainties of standard IFP for quantifying environmental controls on NEE. However, this method requires a numerical solution

of several equations and a complex interaction of many input parameters that can introduce biases to the flux partitioning.

The localized near-field (LNF) theory, proposed by Raupach (1989a), is a multi-layer Lagrangian canopy model which has been used for inferring scalar source/sink distributions within plant canopies (Katul and Albertson, 1999; Leuning et al., 2000; Siqueira and Katul, 2010). In addition, a few studies used the LNF to study isotope exchange in forest canopies (Haverd et al., 2011; Styles et al., 2002). The LNF theory allows the separation of scalar source/sink distributions and isotope exchange between soil and plant components, as previously demonstrated in Chapter 2. Hence, the use of the LNF approach provides a non-isotopic alternative to partitioning CO_2 fluxes within plant canopies as well as a new method for estimating δ_N, δ_P and δ_R to be used in the IFP approach.

In this study, we used the LNF theory to independently estimate F_A, F_R and its respective isotope compositions (δ_P and δ_R) in a corn canopy. The objectives of this study were: (1) to evaluate the performance of the LNF theory for partitioning NEE into soil and plant components and (2) to evaluate whether high temporal resolution estimates of δ_P and δ_R estimated using the LNF theory could be used to partition EC NEE using a mass balance principle.

3.2 Material and methods

3.2.1 The localized near-field theory

The LNF theory is a multi-layer semi-Lagrangian analysis that separates the concentration field within plant canopies into diffusive (far-field) and non-diffusive (near-field) regions to estimate the distribution of marked-fluid particle positions, based on turbulence statistics (Raupach, 2001). As previously described in details in

Chapter 2, the LNF theory assumes that the canopy is divided into m horizontally homogenous source/sink layers (hereafter S layers) with thickness Δz. Therefore, the scalar concentration at an arbitrary level n inside the canopy is a result of both near-field and far-field contributions from S_m. Hence, the mean vertical concentration can be related to source/sink distributions through a dispersion matrix (**D**), which provides both spatial and temporal dimensions of particle trajectory (Eq. 2.1 to 2.5). Values of S strength from each m layer can be found by solving a liner system of m equations (Eq. 2.6). Finally, the scalar flux for individual source layers (F_j) can be obtained from Eq. 2.7 and the canopy net flux (F_N) by adding F_j for all source layers.

In this study, the turbulence statistics parameterization and corrections for atmospheric stability proposed by Leuning (2000) were used to estimate **D** (Eq. 2.1 to 2.5). The corn canopy was divided into only two source layers to estimate non-foliar and foliar CO_2 fluxes. As the canopy height was 2.4 m, the thickness of sources layers were defined as 0.30 m for the bottom, assumed to have negligible contribution from plant CO_2 fluxes and 2.1 m for the top (canopy flux component) layers. The LNF scalar fluxes estimates for non-foliar respiration (F_R) and net photosynthesis (F_A) were then estimated by using Eq. 2.7.

3.2.2 Isotope flux partitioning theory

The isotopic flux partitioning (IFP) approach is based on the assumption that mass balance principles can be used to quantify CO_2 exchange between plant canopies and the atmosphere (Bowling et al., 2001; Yakir and Wang, 1996). Thus, the net CO_2 exchange above a given vegetated surface (NEE) is a result of the balance between the net photosynthesis (F_A) and non-foliar respiration (F_R) at ecosystem level, as follows:

$$\mathrm{NEE} = F_R + F_A \tag{3.1}$$

where by convention $F_R > 0$ and $F_A < 0$. Following Lai et al. (2003), changes in CO_2 storage were not accounted in our flux partitioning calculations, since it was shown to be small for the corn canopy (Section 2.3.2) even under low turbulent conditions (u_* <0.1 m s^{-1}) (Figure 2.3). Both left and right-hand side of Eq. 3.1 can be attributed to distinct isotope signatures. Therefore, by re-writing Eq. 3.1 and expressing the isotopes signatures in delta notation (Eq. 2.8), the isotopic mass balance can now be expressed as:

$$\delta_{\mathrm{N}}\mathrm{NEE} = \delta_{\mathrm{R}}F_{\mathrm{R}} + \delta_{\mathrm{P}}F_A \tag{3.2}$$

where δ_{N} represents the isotope composition of NEE, δ_{R} is the isotope composition of non-foliar respiration and δ_{P} is the isotope composition of CO_2 assimilated during photosynthesis. Since NEE can be directly measured by the EC method (EC NEE) and the isotope signatures can be directly estimated by LNF, we can obtain F_R and F_A by rearranging (3.1) and (3.2) as follows (Lai et al., 2003):

$$F_{\mathrm{A}} = \frac{\delta_{\mathrm{N}} - \delta_{\mathrm{R}}}{\delta_{\mathrm{P}} - \delta_{\mathrm{R}}}\mathrm{NEE} \tag{3.3a}$$

$$F_{\mathrm{R}} = \frac{\delta_{\mathrm{P}} - \delta_{\mathrm{N}}}{\delta_{\mathrm{P}} - \delta_{\mathrm{R}}}\mathrm{NEE} \tag{3.3b}$$

In the IFP approach developed from Bowling et al. (2001), foliar respiration (F_L) is removed from total ecosystem respiration (R_{eco}) and incorporated into F_A (i.e., $F_R = R_{\mathrm{eco}} - F_L$). Therefore, F_A account for both gross ecosystem production (GEP) and F_L (i.e., $F_A = GEP + F_L$), so that F_R in Eq. 3.1 is assumed to express only non-foliar (heterotrophs, stems and roots) respiration (Lloyd et al., 1996; Zobitz et al., 2007).

3.2.3 Daytime isotope flux partitioning

In this study, half-hourly LNF estimated fluxes ratios of F_N, F_R and F_A for lighter and heavier isotopes were converted to delta notation (Eq. 2.8) to obtain the δ_N, δ_R, δ_P values, respectively. The isotope flux partitioning approach was performed based on mass balance principles (Section 3.2.2) for half-hourly periods. Daytime data were determined by a threshold of incoming solar radiation (R_g) larger than 20 W m^{-2} (daylight hours), according to Reichstein et al. (2005b). The linear system of equations (Eq. 3.1 to 3.2) was solved by using half-hourly values of NEE, δ_N, δ_P, and δ_R to estimate 30 min values of F_A and F_R. For night-time periods, as there is no photosynthetic fractionation, the use of IFP approach is not applicable (Zobitz et al., 2008).

3.2.4 Field experiment

Field experiment was carried out at the Elora Research Station (ERS) in a cornfield (*Zea Mays*) of approximately 30 ha. Measurements span from anthesis to after senescence. Additional details regarding location and measurement periods were summarized in Table 2.1. Further experimental information about the ERS site is given by Santos et al. (2011).

3.2.5 Isotope and flux measurements

The mixing ratios of the CO_2 isotopologues ($^{12}C^{16}O_2$, $^{13}CO_2$) were continuously measured at a frequency of 10 Hz using a tunable diode laser trace gas analyser (TGA100A, Campbell Sci., Logan, UT, USA). The ambient air was sampled using eight air intakes installed within and above the canopy, as described in Table 2.2. Further details about isotope measurements can be found in Section 2.2.4.

Half-hourly values of NEE were continuously measured using an EC system set up at 2.84 m above the ground. The three wind components and CO_2 and H_2O mole fractions were measured using a sonic anemometer (CSAT3, Campbell Sci.) and open-path CO_2/H_2O infrared gas analyzer (LI-7500, LI-COR, Lincoln, NE, USA), respectively. Sensor signals from EC were recorded at a frequency of 20 Hz with a datalogger (CR23X, Campbell Sci.).

3.2.6 The night-time based flux partitioning approach.

Values of NEE were gap-filled and partitioned into F_A and R_{eco} using a night-time based partitioning method (Reichstein et al., 2005a; Stoy et al., 2006) incorporated in the REddyProc 0.7-1 R package online tool (Wutzler et al., 2018). For simplicity, this method will be referred as RP hereafter, and will serve as a reference to evaluate LNF and IFP flux partitioning. Although, the RP approach has some limitations (Section 3.1), it has been widely used by the flux community (Reichstein et al., 2005a; Stoy et al., 2006; Sulman et al., 2016; Wutzler et al., 2018). The coefficient of determination (R^2) and Willmott et al. (2012)'s refined index of agreement (d_r) were used to evaluate the correlation and agreement between flux partitioning methods, respectively.

Since the RP method provides an estimative of R_{eco}, and both LNF and IFP methods estimate F_R, we simply assumed that RP non-foliar respiration is half of estimated R_{eco}. This conversion factor is based on the observations of Gao et al. (2017) and Wang et al. (2015) who combined EC systems with soil chambers measurements to evaluated R_{eco} and its components in a spring and summer corn cropland in China, respectively. Their results showed that F_R account on average between 49 to 54 % of R_{eco}.

3.3 Results and discussion

3.3.1 Seasonal and diurnal variation of NEE and isotope flux ratios

Figure 3.1 shows the seasonal (left-hand panels) and diurnal (right-hand panels) variation of net ecosystem CO_2 exchange measured by the EC system (EC NEE, Figure 3.1a and b) and the isotope composition of: NEE ($\delta_{N,}$ Figure 3.1c and d), net photosynthesis (δ_P) and non-foliar respiration (δ_R) (Figure 3.1e and f) estimated by LNF theory. Following the same criteria used in the Chapter 2, the LNF flux ratios predictions were filtered using a CV > 50%. In addition, implausible flux ratios values smaller than -40‰ and larger than 0‰ were also excluded from our analyses.

The corn ecosystem is shown to be highly productive with maximum half-hourly CO_2 uptake reaching -40 μmol m^{-2} s^{-1} (Figure 3.1a). The maximum night-time R_{eco} reached values close to 20 μmol m^{-2} s^{-1}, suggesting an expected upper limit of daytime photosynthesis of about -60 μmol m^{-2} s^{-1}. CO_2 uptake rates decreased significantly as the growing season progressed from day of year (DOY) 230 to 260, remaining relatively constancy after this period (Figure 3.1a). The midday (11 – 13 h) average of NEE (±SD) during the first half of the studied period (i.e., from DOY 230 to 259), indicated that the corn canopy acted as a strong sink of CO_2 (-18.4 ± 3.6 μmol m^{-2} s^{-1}). After this period (i.e., from DOY 260 to 289), the CO_2 uptake rates were reduced, yielding to a midday NEE average (±SD) = -11.0 ± 2.3 μmol m^{-2} s^{-1} (Figure 3.1b). The ensemble diurnal variation of NEE (Figure 3.1b) showed an expected pattern with strong CO_2 uptake reaching a mean midday value of -13.5 ± 2.7 μmol m^{-2} s^{-1} and a mean midnight (23 - 1 h) CO_2 release of 5.7 ± 0.7 μmol m^{-2} s^{-1} over the growing season period.

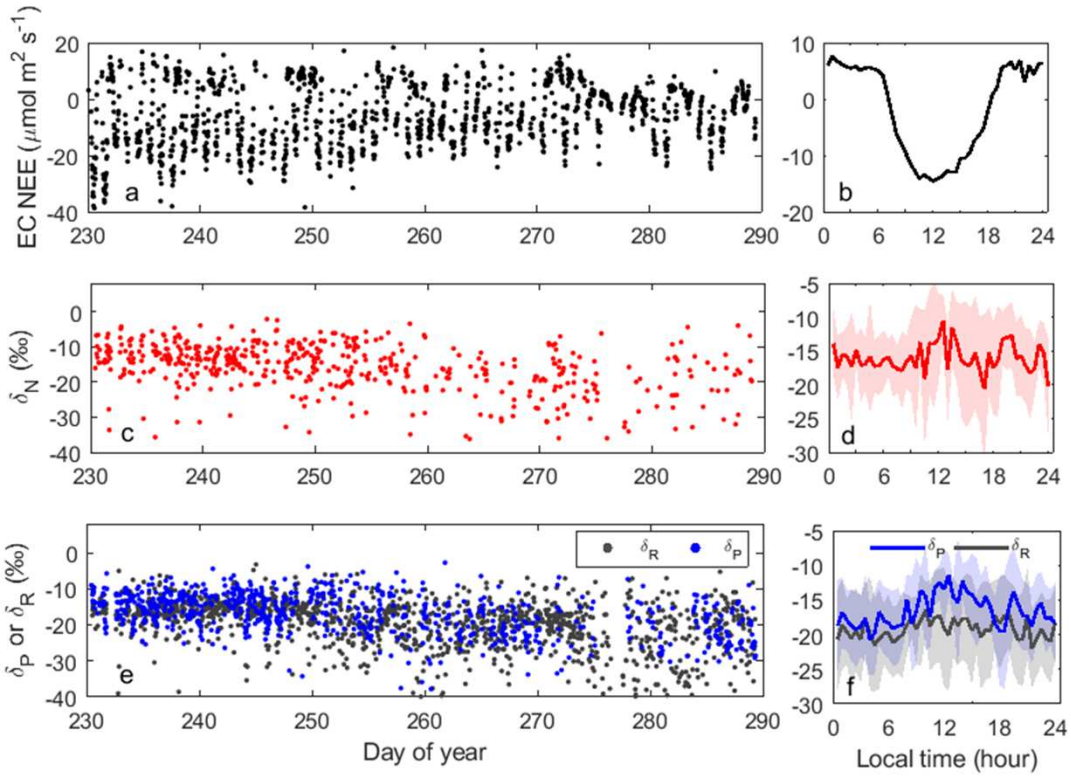

Figure 3.1. Half-hourly values (left panels) and ensemble average (right panels) of: a and b) measured net CO_2 ecosystem exchange (NEE), estimated isotope composition of c and d) NEE (δ_N), e and f) non-foliar respiration (δ_R) and net photosynthesis (δ_P) during growing season.

In this study, we quantified the isotope composition of NEE, net photosynthesis and non-foliar respiration using the LNF theory in order to evaluate if these information could be helpful to constraint the partitioning of NEE measured by EC system (Figure 3.1a and b) into its gross flux components (F_A and F_R). The seasonal variation of δ_N, δ_P and δ_R values (Figure 3.1c and e) estimated by the LNF theory showed a similar pattern becoming more negative after DOY 260 with the reduction of photosynthetic rates with the end of the growing season. The δ_N varied, on average, from -14.0 ± 5.5 ‰ in the fist-half of measured period (DOY < 260) to -20.6 ± 6.3 ‰ after the referred period (Figure 3.1c). Values of δ_P and δ_R ranged, on average, from -15.3 ± 4.7 ‰ and -17.5 ± 4.6 ‰ before DOY 260 to -20.7± 4.7 ‰ and -22.1 ± 6.4 ‰ after DOY 260, respectively (Figure 3.1e). δ_P showed a large diurnal variation (Figure

3.1f) with an averaged absolute difference between midday and midnight hours of 5.0 ‰. δ_N and δ_R presented smaller diurnal variation (Figure 3.1d and f) than δ_P, with a difference of 2.0 and 1.9 ‰, respectively.

The estimated δ_R from the LNF theory reported in this study are in agreement with the soil incubation results for this same site reported by Ramnarine et al. (2011). Their δ_R values ranging from -17.0 to -22.6 ‰. Fassbinder et al. (2012) found a 15-day averaged δ_R of -17.0 ‰ measured using soil chambers for corn grown under controlled environmental conditions. The decrease in isotope flux ratios (Figure 3.1c and e) after DOY 260 may indicate a larger contribution of C_3 residue to NEE than from corn plants that, at the referred period, were already reaching the senescence (Griffis et al., 2008, 2005a). The large diurnal variation in δ_P (Figure 3.1f) indicate that LNF estimates were able to capture the expected sensitive stomatal responses to hourly-diurnal environmental perturbations (Buchmann et al., 1996; Lai et al., 2003).

3.3.2 LNF flux partitioning

RP F_A estimates showed larger uncertainties than LNF F_A, reaching unrealistic absolute values on the order of 100 μmol m^{-2} s^{-1}. However, a good agreement (d_r = 0.67) between RP F_A and LNF F_A was observed during the peak of the growing season (i.e., between DOY 230 and DOY 250). In addition, LNF predictions were able to capture the expected seasonal pattern indicated by the NEE measurements, showing a relatively large reduction of photosynthetic rates after DOY 260 (Figure 3.2a). The maximum half-hourly CO_2 uptake predicted by LNF reached -55.8 μmol m^{-2} s^{-1} at DOY 230.

The R_{eco} predicted by the RP method was weighted by a F_R/R_{eco} ratio of 0.5 to correspond to non-foliar respiration (Figure 3.2b), as previously mentioned in the section 3.2.6. Large uncertainties were observed in LNF F_R estimates during the peak

of the growing season, reaching values up to 54.2 μmol m^{-2} s^{-1} at DOY 247. After DOY 260, good agreement was observed between the two methods (d_r = 0.65). The half-hourly values of RP F_R ranged from 9.7 μmol m^{-2} s^{-1} on DOY 264 to 0.4 μmol m^{-2} s^{-1} at DOY 281.

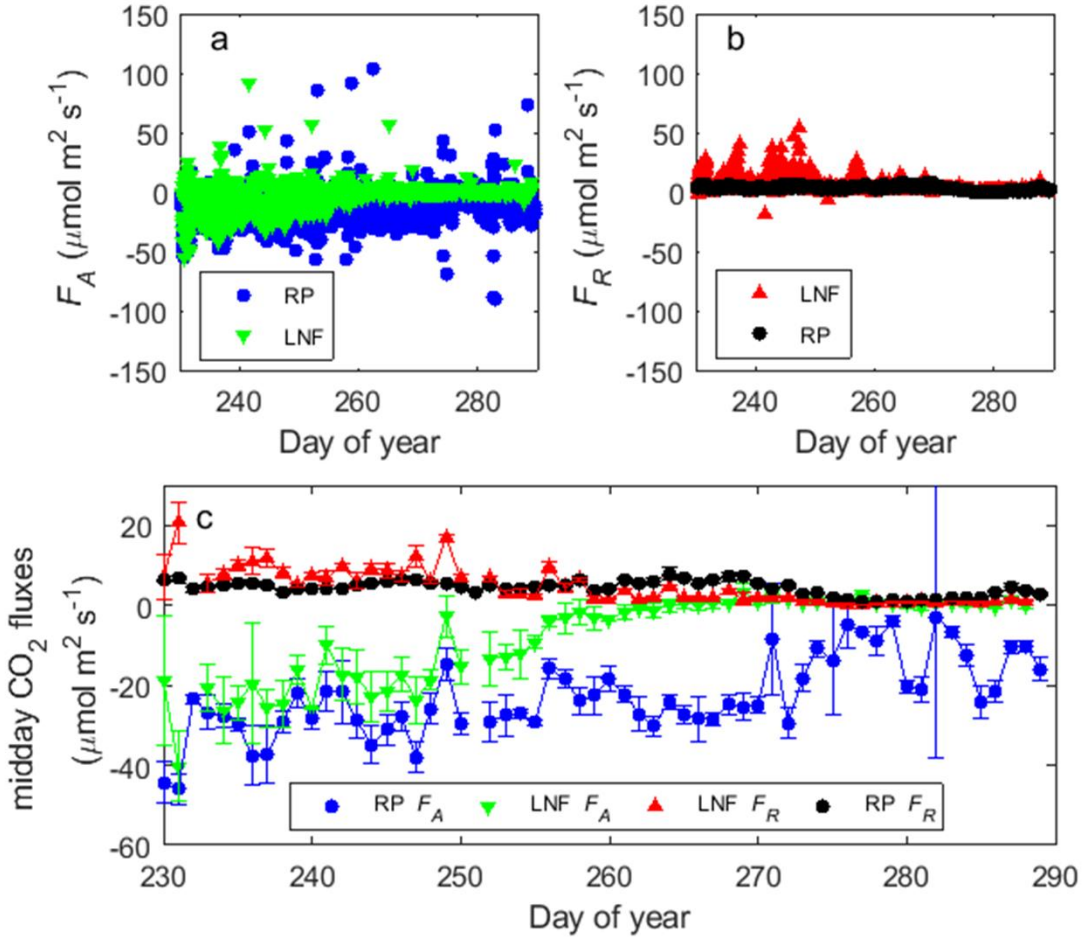

Figure 3.2. Time series by half-hourly values of (a) photosynthetic (F_A) and (b) respiratory (F_R) fluxes partitioned by the traditional night-time based method (RP) and localized near-field (LNF) theory and (c) respective midday (11 – 13 h) averaged seasonal variation of CO_2 fluxes with the standard deviation (σ) represented by the vertical bars.

The large noises observed for RP F_A estimates (Figure 3.2a) were related to the hours when atmospheric stability was in transition (i.e., early morning and late afternoon). Therefore, these uncertainties were drastically reduced during midday hours (Figure 3.2c) when the turbulent mixing was often strong, with u_* > 0.4 m s^{-1}.

The low ability of the RP method to represent F_A seasonal trend (Figure 3.2a and c), are likely due to the lack of skill of the RP method to capture short-term (< day) physiological controls of NEE. This model limitation is due to the use of 15-day periods of night-time data to fit temperature response curves (Wutzler et al., 2018). The greater ability of LNF in reproducing the expected seasonal pattern of F_A indicates that LNF is able to capture environmental and physiological short-term variations drivers of NEE components. It may suggest a great advantage of use LNF instead the traditional night-time based method for flux partitioning.

Regarding uncertainties in F_R estimated by the LNF theory (Figure 3.2b), as showed in Chapter 2, the LNF theory assumes the steady state conditions so changes in CO_2 storage can affect its estimates. Although the changes in CO_2 storage were smaller for the corn canopy (section 2.3.2), there is still a certain degree of decoupling between the below and above canopy air flows (Figure 2.3a). This apparently did not disturb LNF F_A estimates (Figure 3.2a and c). However, it may have a greater effect on LNF F_R predictions, since the flow decoupling is expected to be higher in the lowest layers of canopy airspace due to the lower turbulent mixing combined with possible stable thermal stratification in this region (Iwata et al., 2005; Yang et al., 2007). Therefore, as the storage flux is not accounted in our IFP approach (see Section 3.2.2), we presumed that CO_2 accumulation in the lower canopy airspace has caused the large overestimations in LNF F_R during the period when the canopy was fully developed (Figure 3.2b). This hypothesis is reinforced by the drastic reduction of the uncertainties during the midday hours (Figure 2.3c), when the turbulent mixing is usually strong, and by the good agreement between RP F_R and LNF F_R observed after DOY 260, when the corn is already reaching the senescence and therefore changes in CO_2 storage become even smaller.

3.3.3 Isotope flux partitioning

Once the LNF theory was introduced as an alternative non-isotopic method for flux partitioning, now we are going to evaluate whether short-term δ_P and δ_R values predicted by LNF can help to constraint on the partitioning of NEE measurements into its gross flux components (F_A and F_R) by using the IFP approach (section 3.2.2). Hereafter, these isotope-derived F_A and F_R fluxes will be referred to as IFP F_A and IFP F_R, respectively.

A fundamental assumption of the IFP approach is the existence of isotopic disequilibrium (D_{eq}) between δ_P and δ_R sufficiently large to distinguish F_A and F_R ($D_{eq} = \delta_P - \delta_R$). Otherwise, the ecosystem reaches an "isotopic equilibrium" and therefore F_A and F_R cannot be discerned because under these circumstances the equations (3.1) and (3.2) converge into a single equation (Bowling et al., 2001; Lai et al., 2003). At half-hourly time step, D_{eq} is expected to be mainly driven by diel variations in photosynthetic fractionation (Ogée et al., 2004). Our results suggest the existence of a stronger diurnal variation in δ_P (5.0 ‰) than δ_R (1.9 ‰), it may indicate a large isotopic disequilibrium at this ecosystem (Figure 3.1f).

The seasonal diel-averaged pattern of D_{eq} predicted by LNF indicate a seasonal variation (Figure 3.3a). Although the large variability, D_{eq} was predominantly positive during the late summer until DOY 260, with a mean of 2.3 ± 6.3 ‰. After this period, as the corn plants reached senescence with the end of the growing season, D_{eq} became predominantly negative with a mean of -0.9 ± 6.4‰. Similarly, Zobitz et al. (2008) also reported positive D_{eq} during the late summer in a subalpine forest at Niwot Ridge AmeriFlux site. For our specific case, we attributed this depletion in D_{eq} to the reductions of photosynthetic fractionation after DOY 260, where the more depleted δ_R turn into the major contribution for δ_N. However, other factors such the variations in

soil water content, light and temperature over the season may also have contributed to changes in D_{eq} sign (Zobitz et al., 2008).

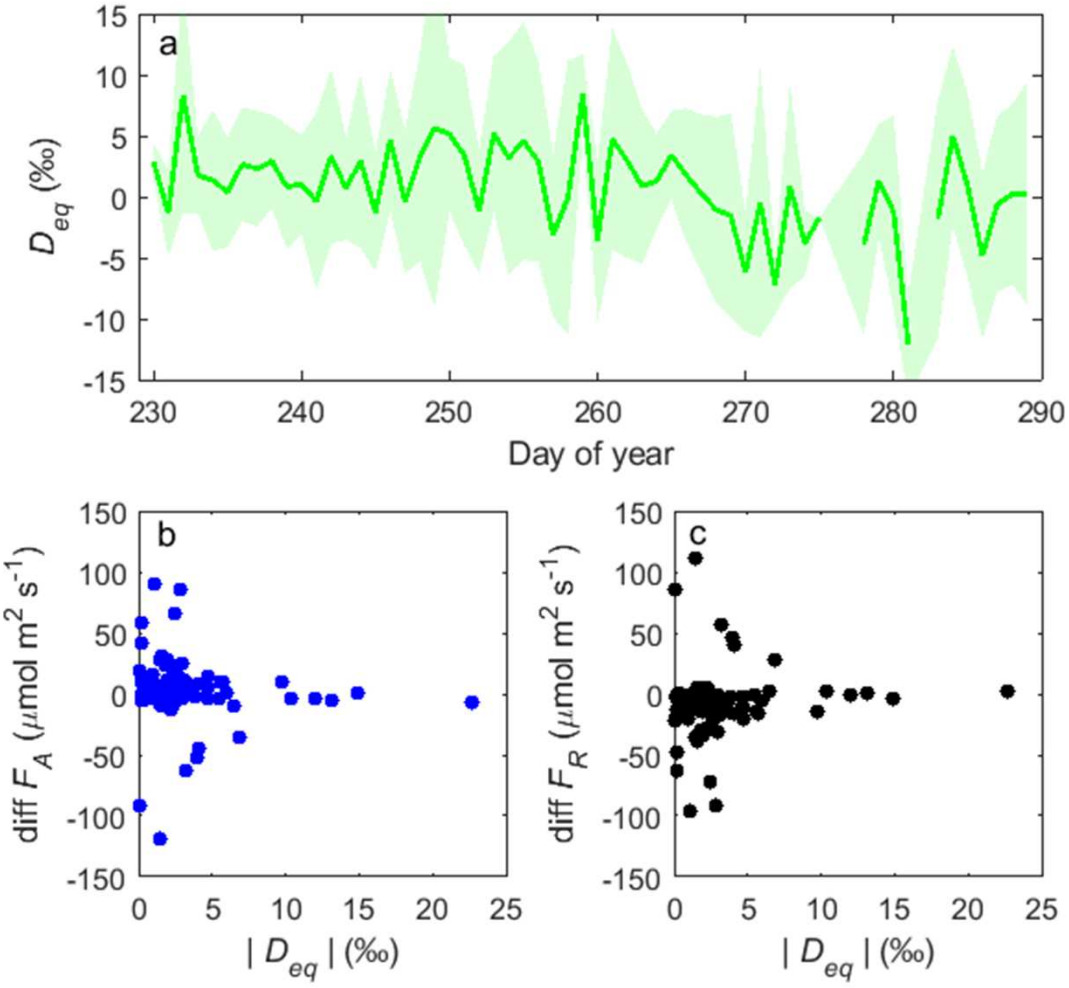

Figure 3.3. a) Daily-averaged seasonal variation of isotopic disequilibrium ($D_{eq} = \delta_P - \delta_R$) and the difference between night-time based (RP) and IFP partitioning methods versus the absolute isotopic disequilibrium ($|D_{eq}|$) for b) net photosynthesis (diff F_A = RP F_A – IFP F_A) and c) non-foliar respiration (diff F_R = RP F_R – IFP F_R).

To evaluate the effect of D_{eq} on IFP predictions, we plotted the relationship between absolute values of D_{eq} and the difference between RP and IFP estimated fluxes (Figure 3.3). Since RP is a non-isotopic partitioning method, it is not expected to be affected by the D_{eq}, though it could eventually show large random errors when small D_{eq} values coincide with small NEE magnitude. Therefore, we expect large diff F_A and diff F_R when D_{eq} has major effect on IFP estimates. Large uncertainties in both

IFP F_A and IFP F_R estimates were observed when D_{eq} was smaller than 3.2 ‰, which these values were mainly detected from early morning and late afternoon periods. Negative values of D_{eq}, associated with end of the growing season (i.e., after DOY 260), also yielded to large errors in our partitioning approach. Previous studies have also reported large errors in isotopic flux partitioning when D_{eq} is small than 4.0 ‰ (Ogée et al., 2004, 2003). In addition, some unrealistic values are observed in the half-hourly D_{eq} estimates (for example, $| D_{eq} | > 10$ ‰ in Figure 3.3b and c), which may be attributed to a limited precision of the LNF method that eventually yielded to these large errors. However, the quantification of the random and systematic errors of LNF method is beyond the scope of this study, but this issue should be addressed in future studies.

Once the IFP estimates was shown to be high sensitive to the low D_{eq} values, we restrained the isotope flux partitioning to the periods with strong isotopic disequilibrium (i.e., $D_{eq} > 3.2$ ‰, that occurred mostly during midday hours) to evaluate if it would result in a reduction of the uncertainties from IFP predictions. These gross partitioned photosynthetic and respiratory fluxes filtered by $D_{eq} > 3.2$ ‰ are shown in the Figure 3.4, referred as $\text{IFP}_\text{f}\, F_A$ and $\text{IFP}_\text{f}\, F_R$, respectively.

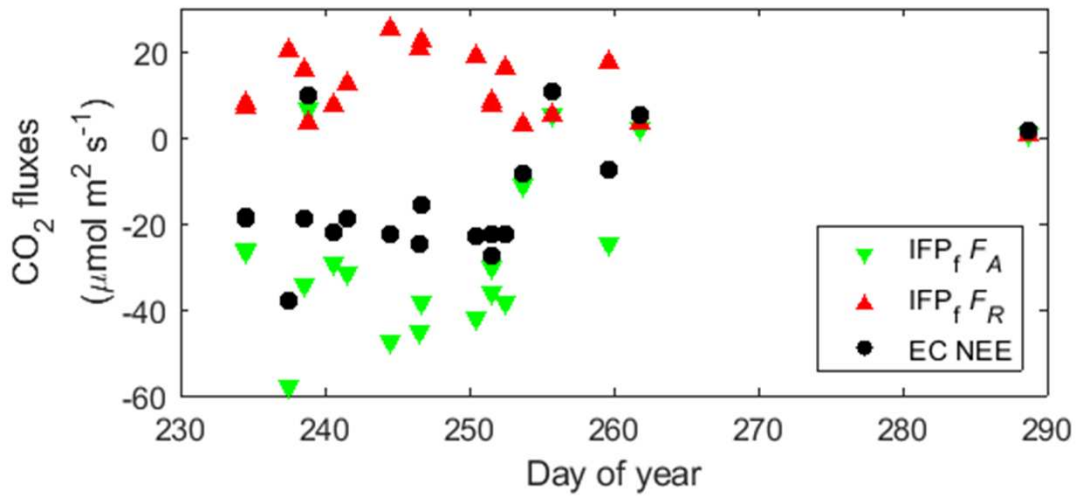

Figure 3.4. Isotopic flux partitioning of EC measurements of NEE (EC NEE) into net photosynthesis (F_A) and non-foliar respiration (F_R) filtered by a D_{eq} > 3.2 ‰ (IFP_f F_A and IFP_f F_R, respectively).

The IFP method was highly sensitive to the magnitude of D_{eq} values. There was a considerable reduction in the flux partitioning uncertainties when IFP predictions was filtered by a D_{eq} value of > 3.2 ‰ (IFP_f) (Figure 3.4). It also resulted in more realistic gross flux predictions (IFP_f F_A and IFP_f F_R), based on net CO_2 flux measurements (EC NEE). This may indicate that applying the IFP method using directly estimated half-hourly δ_R and δ_P from LNF can offer new insights on the processes governing the isotope exchange. In addition, given the high sensitivity of IFP to the isotopic disequilibrium, advances in the techniques to measure δ_R and δ_P with even more accuracy and precision are required for the future success of IFP approach.

3.3.4 Light and temperature response

We evaluated the expected physiological responses in F_A and F_R estimated by the methods by using light and temperature response curves (Figure 3.5). These data were bin-averaged in order to highlight the underlying physiological responses to light

and temperature, attenuating the effects of intermittent turbulence (Greco and Baldocchi, 1996; Zobitz et al., 2008).

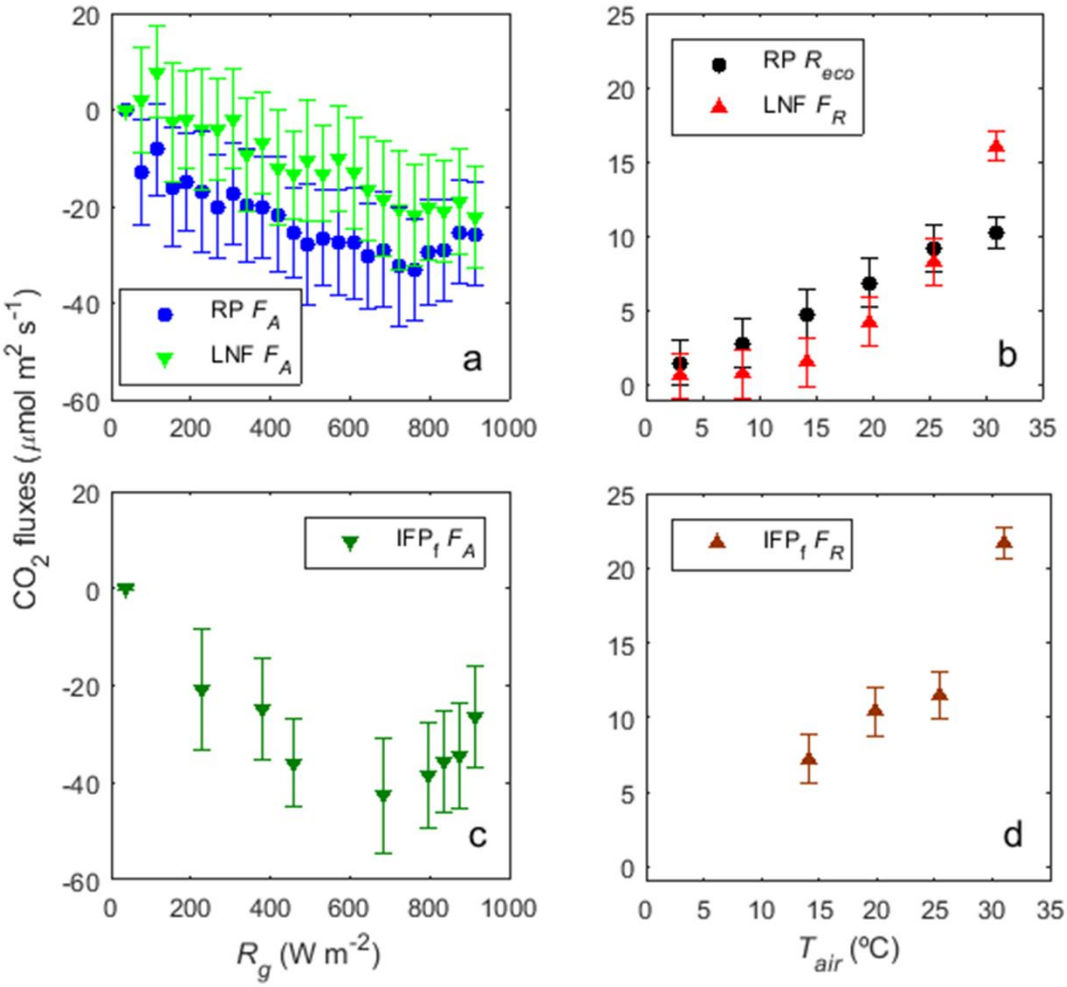

Figure 3.5. Relationship between average values of (a) canopy CO_2 fluxes (F_A) with incoming solar radiation (R_g), and (b) respiratory CO_2 fluxes (F_R and R_{eco}) with air temperature (T_{air}) using LNF, RP and IFP flux estimates. The bin-averaged F_A was restricted to the peak of the growing season (from DOY 230 to 260) and during periods when R_g was larger than 60 W m^{-2}. R_g was binned in 38.0 W m^{-2} increments and T_{air} was binned in 5.6 ºC increments.

Values of F_A estimated using different methods showed similar light responses, showing a trend towards saturation at R_g > 700 W m^{-2} (Figure 3.5a and c). For the relationship of RP R_{eco}, LNF F_R and IFP F_R to air temperature (Figure 3.5b and d), the estimates shown that both R_{eco} and F_R were correlated with T_{air}. A similar pattern is

observed between the methods, except for LNF F_R air temperature relationship that showed large values when T_{air} was larger than 20ºC (Figure 3.5b). We hypothesise that when the canopy was fully developed, changes in CO_2 storage may have an effect on LNF F_R estimates (Figure 3.2b and Figure 2.3a). We have also observed that when LNF temperature response curve was restricted to the end of the growing season (i.e., DOY > 260), it showed similar trend to RP R_{eco} air temperature curve for all ranges of T_{air} (data not shown).

Regarding isotopic-derived fluxes (Figure 3.5c and d), sensitivities of F_A to light (Figure 3.5a) and of F_R to air temperature (Figure 3.5b) were observed. For the photosynthetic fluxes, the trend observed for the light-response relationship are in agreement with the pattern observed from other studies using different canopy conductance models (Bowling et al., 2001; Wehr et al., 2016; Zobitz et al., 2007). Similar patterns were also reported by Greco and Baldocchi (1996) at the canopy scale, that observed a linear response of NEE to light over a subalpine forest. For respiratory fluxes, as indicated by the Figure 3.5b, R_{eco} is expected to respond to T_{air} variations, though it is also driven by other environmental variables, such as water content, C substrate quality and quantity, and nutrient availability (Davidson and Janssens, 2006; Reichstein et al., 2005b, 2002). This relationship between R_{eco} and T_{air} has been also observed in other corn canopies (Gao et al., 2017). However, F_R is still a poorly understood flux in the global C budget and its responses to air temperature remains unclear (Reichstein et al., 2005b). Some isotopic partitioning studies have reported failure in reproduce its expected relationship (Bowling et al., 2001; Knohl and Buchmann, 2005; Zobitz et al., 2008, 2007). However, our isotope-derived F_R estimates shows a strong temperature sensitivity (Figure 3.5d), in accordance with the results reported by Greco and Baldocchi (1996) and Knohl and Buchmann (2005).

3.3.5 Comparisons of flux partitioning methods

The gross fluxes derived from LNF and IFP methods were compared to night-time based (RP) estimates (Figure 3.6 and Figure 3.7). The inter-comparison between the partitioning methods, showed in this study, uses the RP method as a reference because it is currently the most widely used partitioning method (Reichstein et al., 2005a; Stoy et al., 2006; Sulman et al., 2016; Wutzler et al., 2018; Zobitz et al., 2008) as well as due to the lack of a method of general use for this purpose. However, although RP is taken as a reference it is prone to random and systematic errors just as the tested methods (LNF and IPF) and therefore do not represent the 'real' flux. All flux partitioning methods were performed using the same criteria for low turbulent periods ($u_* > 0.1$ m s^{-1}).

For the non-isotopically partitioned fluxes, relatively poor correlation (R^2 of 0.23 for F_A and R^2 of 0.18 for F_R) and good agreement (d_r of 0.77 for F_A and d_r of 0.74 for F_R) between RP and LNF methods were observed for both photosynthetic (Figure 3.6a) and respiratory (Figure 3.7a) fluxes. When these methods were evaluated at midday (Figure 3.6b and Figure 3.7b), it was observed a substantial increase in R^2 to the detriment of agreement, with drastic decrease of d_r. The high precision and small agreement may suggest a large contribution of the systematic component to the total error (Willmott, 1981).

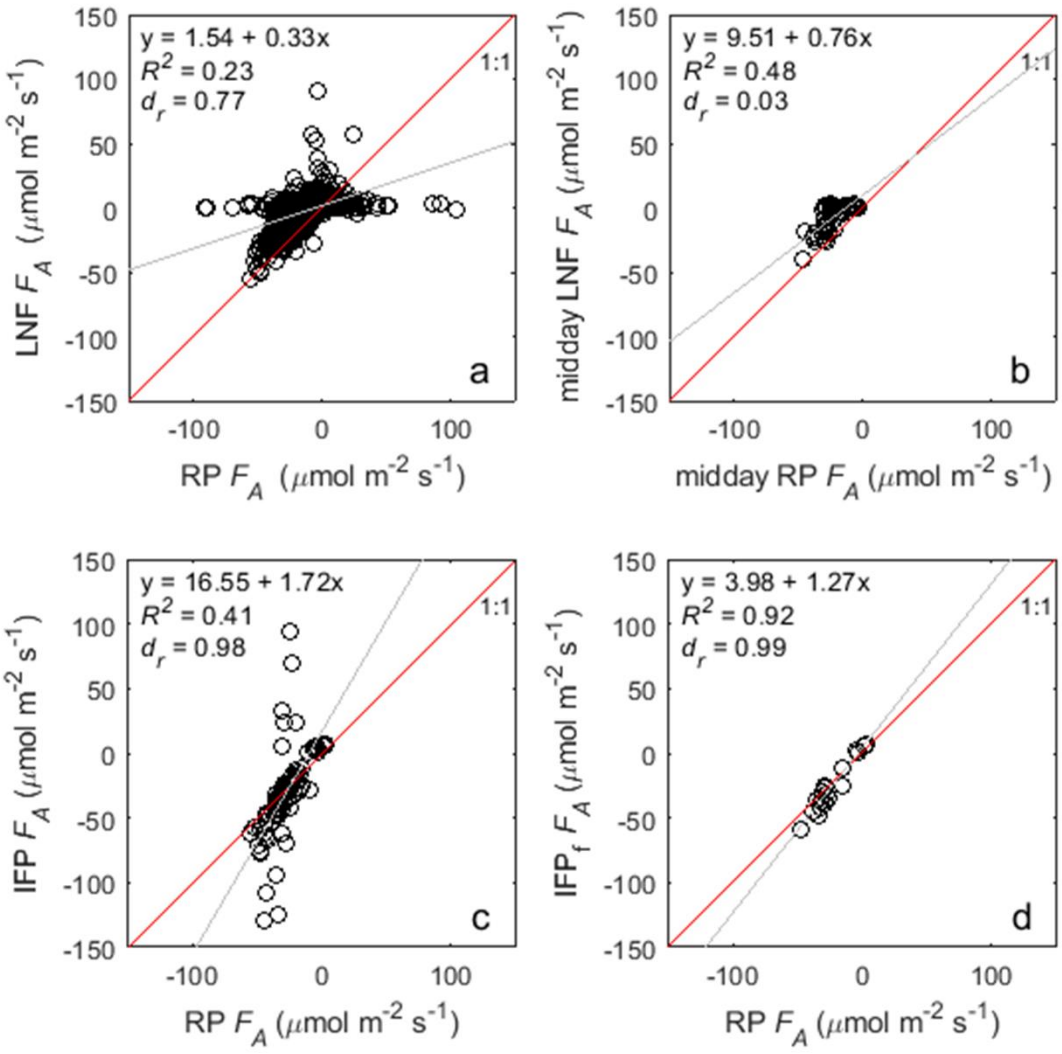

Figure 3.6. Comparison of photosynthetic CO_2 fluxes partitioned by the night-time based method (RP) and different partitioning approaches: a) Lagrangian near-field theory (LNF), b) LNF theory during midday hours (midday LNF F_A), c) isotope flux partitioning (IFP) and d) IFP filtered by the isotopic disequilibrium (IFP$_f$).

For the isotopic-derived fluxes, before applying the D_{eq} filter (Figure 3.6c and Figure 3.7c), although the very good agreement (d_r > 0.90), a reasonable correlation (R^2 = 0.41) was observed for F_A and a very poor correlation (R^2 = 0.01) for respiratory fluxes. When IFP method was performed under strong D_{eq} (> 3.2‰) (Figure 3.6d and Figure 3.7d), a substantial improvement in correlation and agreement are observed between RP and IFP methods, mainly for F_A that showed a very good R^2 of 0.92 (Figure 3.6d).

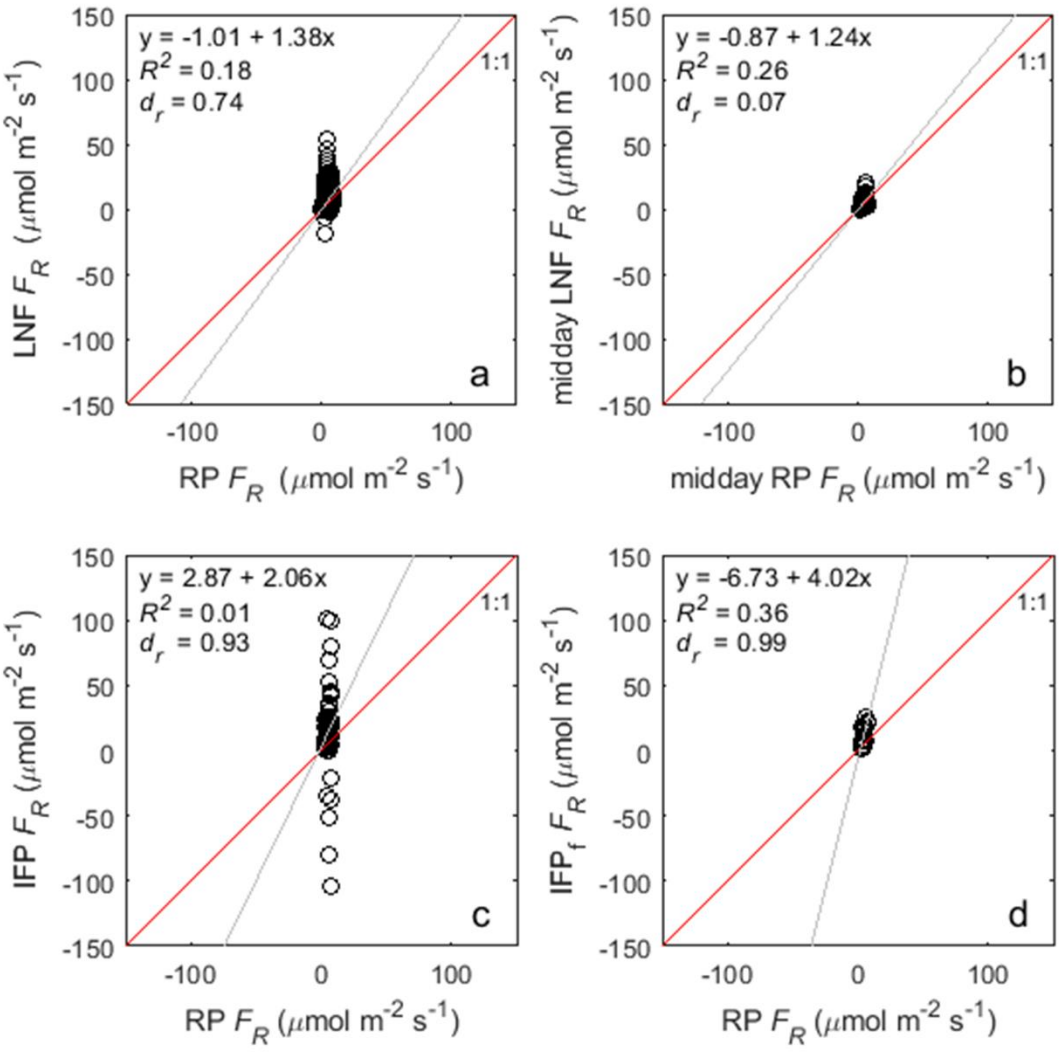

Figure 3.7. Comparison of respiratory CO_2 fluxes partitioned by the night-time based method (RP) and different partitioning approaches: a) Lagrangian near-field theory (LNF), b) LNF theory during midday hours (midday LNF F_R), c) isotope flux partitioning (IFP) and d) IFP filtered by the isotopic disequilibrium (IFP$_f$).

Therefore, the use of LNF analysis to determine δ_R and δ_P values may help us to overcome at least two potential limitations of the IFP formulation proposed by Bowling et al. (2001). First, because the δ_R value for IFP is traditionally determined by using the Keeling plot (Lai et al., 2003; Zobitz et al., 2008) or isotope flux ratio (Griffis et al., 2005a; Zhang et al., 2006) approaches during night-time or non-growing season periods (i.e., in the absence of photosynthetic activity). In practice, the determination of δ_R using these methods usually account for both foliar and non-foliar

respiration. However, in the IFP formulation, δ_R should reflect only non-foliar respiratory fluxes (F_R) (Lloyd et al., 1996; Zobitz et al., 2007), as in principle is assumed for our LNF estimates. Additionally, δ_R may show a diurnal variation (Ekblad et al., 2005; Högberg et al., 2001) due to an apparent fractionation of soil respiration (Bowling et al., 2008). Therefore, the extrapolation of the night-time δ_R estimates to the following day may not be appropriate.

Second, because the δ_P value is usually determined by the difference between the isotope signature of ambient air (δ_a) and canopy discrimination (Δ_{canopy}) (Lai et al., 2003; Lloyd et al., 1996; Wehr and Saleska, 2015; Zobitz et al., 2008). However, although δ_a can be measured, the determination of Δ_{canopy} critically depends on the use of stomatal conductance models scaled from leaf to canopy level (Lai et al., 2003). The estimation of canopy scale stomatal conductance is usually done using the Penman-Monteith equation, however this approach is afflicted by uncertainties due to the lack of energy balance closure (Monteith and Unsworth, 2013; Zhang et al., 2006) and the use of many species-specific parameters to scaling of leaf-level quantities to the canopy (Ball et al., 1987; Collatz et al., 1992). The leaf to canopy level scaling has been shown to be one of the main limitation of IFP method, because it often introduce biases to the δ_P estimative (Lai et al., 2003; Zobitz et al., 2008, 2007).

3.4 Conclusions

In this study, we evaluated the use of the localized near-field theory (LNF) as an alternative non-isotopic method for NEE partitioning. In addition, the NEE partitioning was performed using the isotope flux partitioning (IFP) approach using LNF derived half-hourly direct estimates of δ_P and δ_R. Comparisons of night-time based partitioning method (RP) and LNF showed good agreement (d_r = 0.67) for net-photosynthesis (F_A) estimates at the peak of the growing season. After this period, as

the end of the growing season approached, RP F_A estimates did not reproduced the expected seasonal pattern, resulting in large differences between RP F_A and LNF F_A estimates. In addition, RP F_A predictions showed larger variability than LNF F_A. For non-foliar respiration (F_R) estimates, the CO_2 accumulation in lower canopy airspace yielded to large overestimates of LNF F_R during the peak of the growing season. However, the use of midday time periods was shown to minimize these unrealistic estimates. The use of midday periods also drastically reduced the noises associated with low turbulent mixing in RP F_A estimates and a few outliers in LNF F_A estimates. The greater ability of LNF in reproduce the expected seasonal pattern of net photosynthesis may indicate a great advantage of use LNF instead the traditional night-time based method for flux partitioning.

For isotope-derived gross fluxes (IFP F_A and IFP F_R), our isotope partitioning approach showed high sensitivity to the isotopic disequilibrium (D_{eq}). Large uncertainties were observed for both IFP F_A and IFP F_R predictions when D_{eq} was smaller than 3.2‰. However, when IFP estimates was filtered by $D_{eq} > 3.2$‰ (IFP_f), it reduced drastically the noises related to weak D_{eq}. The comparison of independent RP and IFP_f methods showed very good correlation ($R^2 = 0.92$) and agreement ($d_r = 0.99$) for F_A. A reasonable correlation ($R^2 = 0.36$) and very good agreement ($d_r = 0.99$) were observed for respiratory fluxes.

A major advantage of using LNF as an alternative to non-isotopic and isotopic flux partitioning is that in addition to estimates of F_A and F_R separately, δ_R and δ_P are directly estimated in a half-hourly time-step. These directly and independent half-hourly flux ratios derived from LNF may overcome limitations of using stomatal conductance models scaled to the canopy level, which is usually applied to the traditional IFP approaches developed so far. In addition, the LNF theory also provides

an independent way to determine daytime δ_R, which is traditionally extrapolated from night-time periods. Finally, although the high variability in D_{eq} estimates observed here, our results suggest that the future success of the isotope partitioning approach is highly dependent on advancements on isotope measurements techniques, providing estimates of D_{eq} at high temporal-resolution with more precision.

CHAPTER 4 – GENERAL CONCLUSIONS AND FUTURE DIRECTIONS

4.1 Summary of conclusions

The study of isotope CO_2 exchange over ecosystem is important to elucidate the biosphere-atmosphere exchange processes. Recent developments in optical isotope techniques have allowed to fast and precise isotope measurements, which is often combined with micrometeorological techniques to study isotope fluxes in vegetation canopies. However, the quantification of CO_2 exchange in plant canopies is still challenging due to the several limitations related to the precision of the micrometeorological approaches to estimate the isotope fluxes. In this thesis, we investigated the use of the Lagrangian near-field theory (LNF) to study CO_2 isotope exchange in different plant canopies. The evaluation of LNF theory included: (1) the comparison with the traditional isotope flux ratio (IFR) approach within different plant canopies and (2) its feasibility as an independent non-isotopic method for partitioning the net ecosystem CO_2 exchange (NEE) into plant and soil CO_2 flux components in a corn canopy. In addition, the LNF theory was also investigated as an independent method to provide direct estimates of the isotope composition of canopy (δ_P) and soil (δ_R) flux components to partition NEE using the isotope flux ratio (IFP) approach.

The general objective of this study was to evaluate the LNF theory as an alternative method to study isotopic CO_2 exchange and for partitioning net CO_2 fluxes in vegetation canopies. The following conclusions can be drawn from this study.

1. The performance of LNF theory at estimating NEE and δ_N was evaluated based on comparisons with EC measurements and IFR method, respectively. Overall, the results showed that the LNF theory is suitable for estimate net CO_2 exchange and isotope CO_2 exchange in plant canopies.

2. Changes in CO_2 storage were used to investigate the degree of decoupling between below and above-canopy airflows. The LNF estimates of NEE were highly sensitive to the changes in CO_2 storage. Hence, better LNF performance was found for grassland and corn than for the forest, which showed large change in CO_2 storage in the canopy airspace. This may indicate a great advantage of use LNF to study scalar transport within short canopies, given that the EC instrumentation is too bulky to be deployed within short canopies.
3. The influence of [CO_2] gradient magnitude on IFR and LNF δ_N estimates was evaluated by calculating the moving coefficient of variation (CV) of δ_N. The results showed that the magnitude of [CO_2] gradients had great impact on both IFR and LNF δ_N estimates. However, the LNF theory was shown to reduce, on average, 74% the uncertainties of IFR method.
4. The effect of using in-canopy [CO_2] data on IFR estimates was investigated by calculating δ_N using the highest air intake and the first air intake immediately below the top of the canopies. Although this approach violates assumptions of the K-theory, this resulted in better correlation (coefficient of determination ranging from 0.57 to 0.68) and agreement (coefficient of agreement ranging from 0.93 to 0.99) for the relationship between LNF δ_N and IFR δ_N values only for short canopies. It may be attributed to the stronger near-field effects in the forest than grassland and corn canopies, suggesting a K-theory failure in the forest canopy.
5. The LNF theory was also evaluated on estimating net photosynthesis (F_A) and non-foliar respiration (F_R) though comparisons with an independent night-time based flux partitioning (RP) method. The LNF captured the expected photosynthetic seasonal pattern better than RP. This limitation in the RP

method is likely due to the use of long-term seasonal nigh-time data to fit the temperature response function. This may indicate that the use of LNF instead the traditional RP method is more advantageous at estimating photosynthetic fluxes.

6. The IFP method was evaluated by using half-hourly estimates of δ_P and δ_R from LNF to constraint the partitioning of NEE measurements into F_A and F_R. The results showed that IFP method was highly sensitive to the D_{eq}, and large uncertainties were found for $D_{eq} < 3.2$ ‰. However, an expressive reduction in the uncertainties and more realistic flux estimates were observed when weak D_{eq} (< 3.2 ‰) periods was filtered out from IFP predictions. Therefore, the high sensitivity of the IFP predictions on the D_{eq} suggests that advances in isotope measurements, providing more precisely short-term determinations of D_{eq}, is crucial to the future success of IFP approach.
7. The use of δ_P and δ_R values provided by LNF on the IFP approach allows overcome some of the limitations of the IFP approach, such as the dependence of scaled stomatal conductance values from leaf to the canopy level and night-time data extrapolation to determine δ_P and δ_R, respectively. However, further studies are still needed to quantify the random and systematic errors associated with LNF predictions.

This study showed the first attempt to combine LNF analysis with several months of near-continuous measurements of stable isotope of CO_2 over different plant canopies. Additionally, here the LNF theory was introduced as an independent way to separately estimate canopy photosynthesis and soil respiration as well as to provide its respective short-term isotope compositions estimates to the isotope flux partitioning (IFP) approach. Overall, these results showed that the LNF is potentially a useful tool

to study CO_2 exchange processes within well-mixed short canopies, where the flux measurements using traditional micrometeorological techniques are even more challenging. In addition, the use of LNF as an independent way to directly estimate canopy photosynthesis and soil respiration as well as its respective isotope compositions can open new perspectives to study process governing below canopy and photosynthetic fluxes in ecosystems.

4.2 Future research directions

From the main findings drawn from this study, we can provide the following suggestions for enhancing the applicability of LNF theory as an independent method to study isotope CO_2 exchange in plant canopies:

1. The results from this study indicated that the performance of the LNF theory is greatly affected by the changes in CO_2 storage. Future studies should examine the possibility of correcting LNF estimates for changes in storage.
2. This study also showed that the variability in both LNF and IFR flux ratio estimates is drastically reduced under large [CO_2] gradients. Placing the air intakes relatively close to the canopy height and taking the observations during the peak of the growing season would allow to stronger [CO_2] gradients and therefore, under such conditions, less variability is expected in flux ratio predictions. In addition, improvements in the methods to measure concentration gradients within plant canopies could improve LNF theory estimates.
3. We evaluated F_R predictions from LNF and IFP only using the night-time based (RP) method. Future studies should include direct chamber-based soil CO_2 flux measurements to a better and more confident evaluation of LNF and IFP performance on estimating F_R.

REFERENCES

Aubinet, M., Chermanne, B., Vandenhaute, M., Longdoz, B., Yernaux, M., Laitat, E., 2001. Long term carbon dioxide exchange above a mixed forest in the Belgian Ardennes. Agric. For. Meteorol. 108, 293–315. https://doi.org/10.1016/S0168-1923(01)00244-1

Aubinet, M., Feigenwinter, C., Heinesch, B., Laffineur, Q., Papale, D., Reichstein, M., Rinne, J., Gorsel, E. Van, 2012. Nighttime flux correction, in: Eddy Covariance: A Practical Guide to Measurement and Data Analysis. pp. 133–157. https://doi.org/10.1007/978-94-007-2351-1

Baldocchi, D., Falge, E., Gu, L., Olson, R., Hollinger, D., Running, S., Anthoni, P., Bernhofer, C., Davis, K., Evans, R., others, 2001. FLUXNET: A new tool to study the temporal and spatial variability of ecosystem-scale carbon dioxide, water vapor, and energy flux densities. Bull. Am. Meteorol. Soc. 82, 2415–2434. https://doi.org/10.1175/1520-0477(2001)082<2415:FANTTS>2.3.CO;2

Baldocchi, D.D., 2003. Assessing the eddy covariance technique for evaluating carbon dioxide exchange rates of ecosystems: past, present and future. Glob. Chang. Biol. 479–492. https://doi.org/10.1046/j.1365-2486.2003.00629.x

Ball, J.T., Woodrow, I.E., Berry, J.A., 1987. A Model Predicting Stomatal Conductance and its Contribution to the Control of Photosynthesis under Different Environmental Conditions, in: Progress in Photosynthesis Research. Springer Netherlands, Dordrecht, pp. 221–224. https://doi.org/10.1007/978-94-017-0519-6_48

Bowling, D.R., Pataki, D.E., Randerson, J.T., 2008. Carbon isotopes in terrestrial ecosystem pools and CO_2 fluxes. New Phytol. 178, 24–40. https://doi.org/10.1111/j.1469-8137.2007.02342.x

Bowling, D.R., Sargent, S.D., Tanner, B.D., Ehleringer, J.R., 2003. Tunable diode laser absorption spectroscopy for stable isotope studies of ecosystem – atmosphere CO_2 exchange. Agric. For. Meteorol. 118, 1–19. https://doi.org/10.1016/S0168-1923(03)00074-1

Bowling, D.R., Tans, P.P., Monson, R.K., 2001. Partitioning net ecosystem carbon exchange with isotopic fuxes of CO2. Glob. Chang. Biol. 7, 127–145. https://doi.org/10.1046/j.1365-2486.2001.00400.x

Brown, S.E., Wagner-Riddle, C., 2017. Assessment of random errors in multi-plot nitrous oxide flux gradient measurements. Agric. For. Meteorol. 242, 10–20. https://doi.org/10.1016/j.agrformet.2017.04.005

Buchmann, N., Ehleringer, J.R., 1998. CO_2 concentration profiles, and carbon and oxygen isotopes in C_3 and C_4 crop canopies. Agric. For. Meteorol. 89, 45–58. https://doi.org/10.1016/S0168-1923(97)00059-2

Buchmann, N., Kao, W.Y., Ehleringer, J.R., 1996. Carbon dioxide concentrations within forest canopies - Variation with time, stand structure, and vegetation type. Glob. Chang. Biol. 2, 421–432. https://doi.org/10.1111/j.1365-2486.1996.tb00092.x

Cerling, T.E., Harris, J.M., MacFadden, B.J., Leakey, M.G., Quade, J., Eisenmann, V., Ehleringer, J.R., 1997. Global vegetation change through the Miocene/Pliocene boundary. Nature 389, 153–158. https://doi.org/10.1038/38229

Cernusak, L.A., Ubierna, N., Winter, K., Holtum, J.A.M., Marshall, J.D., Farquhar, G.D., 2013. Environmental and physiological determinants of carbon isotope discrimination in terrestrial plants. New Phytol. 200, 950–965. https://doi.org/10.1111/nph.12423

Collatz, G., Ribas-Carbo, M., Berry, J., 1992. Coupled photosynthesis-stomatal conductance model for leaves of C_2 plants. Funct. Plant Biol. 19, 519. https://doi.org/10.1071/PP9920519

Corrsin, S., 1975. Limitations of gradient transport models in random walks and in turbulence. Adv. Geophys. 18, 25–60. https://doi.org/10.1016/S0065-2687(08)60451-3

Davidson, E.A., Janssens, I.A., 2006. Temperature sensitivity of soil carbon decomposition and feedbacks to climate change. Nature 440, 165. https://doi.org/10.1038/nature04514

Dawson, T.E., Brooks, P.D., 2001. Fundamentals of stable isotope chemistry and measurement. Springer, Dordrecht, pp. 1–18. https://doi.org/10.1007/978-94-015-9841-5_1

Deleens, E., Ferhi, A., Queiroz, O., 1983. Carbon isotope fractionation by plants using the C4 pathway. Physiol. Veg.

Denmead, O.T., Bradley, E.F., 1987. On scalar transport in plant canopies. Irrig. Sci. 8, 131–149. https://doi.org/10.1007/BF00259477

Ehleringer, J.R., Cerling, T.E., Helliker, B.R., 1997. C_4 photosynthesis, atmospheric CO_2 , and climate. Oecologia 112, 285–299. https://doi.org/10.1007/s004420050311

Ehleringer, J.R., Phillips, S.L., Comstock, J.P., 1992. Seasonal variation in the carbon isotopic composition of desert plants. Funct. Ecol. 6, 396. https://doi.org/10.2307/2389277

Ekblad, A., Bostrom, B., Holm, A., Comstedt, D., 2005. Forest soil respiration rate and $\delta^{13}C$ is regulated by recent above ground weather conditions. Oecologia 143, 136–142. https://doi.org/10.1007/s00442-004-1776-z

Estep, M.F., Tabita, F.R., Parker, P.L., Van Baalen, C., 1978. Carbon isotope fractionation by ribulose-1,5-bisophosphate carboxylase from various organisms. Plant Physiol. 61, 680–7. https://doi.org/10.1104/pp.61.4.680

Farquhar, G.D., Cernusak, L.A., 2005. On the isotopic composition of leaf water in the non-steady state. Funct. Plant Biol. 32, 293–303. https://doi.org/10.1071/FP04232

Farquhar, G.D., Ehleringer, J.R., Hubick, K.T., 1989. Carbon isotope discrimination and photosynthesis. Plant Physiol. Plant Mol. Biol. 40, 503–537. https://doi.org/10.1146/annurev.pp.40.060189.002443

Farquhar, G.D., Sharkey, T.D., 1982. Stomatal conductance and photosynthesis. Annu. Rev. Plant Physiol. 33, 317–345. https://doi.org/10.1146/annurev.pp.33.060182.001533

Fassbinder, J.J., Griffis, T.J., Baker, J.M., 2012. Evaluation of carbon isotope flux partitioning theory under simplified and controlled environmental conditions. Agric. For. Meteorol. 153, 154–164. https://doi.org/10.1016/J.AGRFORMET.2011.09.020

Flanagan, L.B., Brooks, J.R., Varney, G.T., Berry, S.C., Ehleringer, J.R., 1996. Carbon isotope discrimination during photosynthesis and the isotope ratio of respired CO_2 in boreal forest ecosystems. Global Biogeochem. Cycles 10, 629–640. https://doi.org/doi.org/10.1029/96GB02345

Fry, B., 2006. Stable isotope ecology. Springer New York, New York, NY. https://doi.org/10.1007/0-387-33745-8

Gao, X., Mei, X., Gu, F., Hao, W., Li, H., Gong, D., 2017. Ecosystem respiration and its components in a rainfed spring maize cropland in the Loess. Sci. Rep. 1–14. https://doi.org/10.1038/s41598-017-17866-1

Göckede, M., Thomas, C., Markkanen, T., Mauder, M., Ruppert, J., Foken, T., 2007. Sensitivity of Lagrangian Stochastic footprints to turbulence statistics. Tellus, Ser. B Chem. Phys. Meteorol. 59, 577–586. https://doi.org/10.1111/j.1600-0889.2007.00275.x

Good, S.P., Soderberg, K., Wang, L., Caylor, K.K., 2012. Uncertainties in the assessment of the isotopic composition of surface fluxes: A direct comparison of techniques using laser-based water vapor isotope analyzers. J. Geophys. Res. Atmos. 117, 1–22. https://doi.org/10.1029/2011JD017168

Graven, H., Allison, C.E., Etheridge, D.M., Hammer, S., Keeling, R.F., Levin, I., Meijer, H.A.J., Rubino, M., Tans, P.P., Trudinger, C.M., Vaughn, B.H., White, J.W.C., 2017. Compiled records of carbon isotopes in atmospheric CO_2 for historical simulations in CMIP6. Geosci. Model Dev. 10, 4405–4417. https://doi.org/10.5194/gmd-10-4405-2017

Greco, S., Baldocchi, D.D., 1996. Seasonal variations of CO_2 and water vapour exchange rates over a temperate deciduous forest. Glob. Chang. Biol. 2, 183–197. https://doi.org/10.1111/j.1365-2486.1996.tb00071.x

Gresset, S., Westermeier, P., Rademacher, S., Ouzunova, M., Presterl, T., Westhoff, P., Schon, C.-C., 2014. Stable Carbon Isotope Discrimination Is under Genetic Control in the C_4 Species Maize with Several Genomic Regions Influencing Trait Expression. Plant Physiol. 164, 131–143. https://doi.org/10.1104/pp.113.224816

Griffis, T., Sargent, S., Baker, J., Lee, X., Tanner, B., Greene, J., Swiatek, E., Billmark, K., 2008. Direct measurement of biosphere-atmosphere isotopic CO_2 exchange using the eddy covariance technique. J. Geophys. Res. Atmos. 113, D08304. https://doi.org/10.1029/2007JD009297

Griffis, T.J., 2013. Tracing the flow of carbon dioxide and water vapor between the biosphere and atmosphere: A review of optical isotope techniques and their application. Agric. For. Meteorol. 174–175, 85–109.

https://doi.org/10.1016/j.agrformet.2013.02.009

Griffis, T.J., Baker, J.M., Sargent, S.D., Tanner, B.D., Zhang, J., 2004. Measuring field-scale isotopic CO_2 fluxes with tunable diode laser absorption spectroscopy and micrometeorological techniques. Agric. For. Meteorol. 124, 15–29. https://doi.org/10.1016/j.agrformet.2004.01.009

Griffis, T.J., Baker, J.M., Zhang, J., 2005a. Seasonal dynamics and partitioning of isotopic CO_2 exchange in a C_3/C_4 managed ecosystem. Agric. For. Meteorol. 132, 1–19. https://doi.org/10.1016/j.agrformet.2005.06.005

Griffis, T.J., Lee, X., Baker, J.M., Billmark, K., Schultz, N., Erickson, M., Zhang, X., Fassbinder, J., Xiao, W., Hu, N., 2011. Oxygen isotope composition of evapotranspiration and its relation to C_4 photosynthetic discrimination. J. Geophys. Res. Biogeosciences 116, 1–21. https://doi.org/10.1029/2010JG001514

Griffis, T.J., Lee, X., Baker, J.M., Sargent, S.D., King, J.Y., 2005b. Feasibility of quantifying ecosystem-atmosphere $C^{18}O^{16}O$ exchange using laser spectroscopy and the flux-gradient method. Agric. For. Meteorol. 135, 44–60. https://doi.org/10.1016/j.agrformet.2005.10.002

Harper, L., Denmead, O., Sharpe, R., 2000. Identifying sources and sinks of scalars in a corn canopy with inverse Lagrangian dispersion analysis: II. Ammonia. Agric. For. Meteorol. 104, 75–83. https://doi.org/10.1016/S0168-1923(00)00149-0

Haverd, V., Cuntz, M., Griffith, D., Keitel, C., Tadros, C., Twining, J., 2011. Measured deuterium in water vapour concentration does not improve the constraint on the partitioning of evapotranspiration in a tall forest canopy, as estimated using a soil vegetation atmosphere transfer model. Agric. For. Meteorol. 151, 645–654. https://doi.org/10.1016/j.agrformet.2011.02.005

Haverd, V., Leuning, R., Griffith, D., van Gorsel, E., Cuntz, M., 2009. The turbulent Lagrangian time scale in forest canopies constrained by fluxes, concentrations and source distributions. Boundary-Layer Meteorol. 130, 209–228. https://doi.org/10.1007/s10546-008-9344-4

Högberg, P., Nordgren, A., Buchmann, N., Taylor, A.F.S., Ekblad, A., Högberg, M.N., Nyberg, G., Ottosson-Löfvenius, M., Read, D.J., 2001. Large-scale forest girdling shows that current photosynthesis drives soil respiration. Nature 411, 789–792. https://doi.org/10.1038/35081058

Hsieh, C.-I., Siqueira, M., Katul, G., Chu, C.-R., 2003. Predicting scalar source-sink and flux distributions within a forest canopy using a 2-D Lagrangian stochastic dispersion model. Boundary-Layer Meteorol. 109, 113–138. https://doi.org/10.1023/A:1025461906331

Iwata, H., Malhi, Y., Von Randow, C., 2005. Gap-filling measurements of carbon dioxide storage in tropical rainforest canopy airspace. Agric. For. Meteorol. 132, 305–314. https://doi.org/10.1016/j.agrformet.2005.08.005

Katul, G., Albertson, J., 1999. Modeling CO_2 sources, sinks and fluxes within a forest canopy. J. Geophys. Res. Atmos. 104, 6081–6091. https://doi.org/10.1029/1998JD200114

Katul, G., Oren, R., Ellsworth, D., Hsieh, C., Phillips, N., 1997. A Lagrangian dispersion model for predicting sources, sinks, and fluxes in a uniform loblolly pine (Pinus taeda L.) stand. J. Geophys. Res. 102, 9309–9321. https://doi.org/10.1029/96JD03785

Knohl, A., Buchmann, N., 2005. Partitioning the net CO_2 flux of a deciduous forest into respiration and assimilation using stable carbon isotopes. Global Biogeochem. Cycles 19. https://doi.org/10.1029/2004GB002301

Lai, C., Schauer, A.J., Owensby, C., Ham, J.M., Ehleringer, J.R., 2003. Isotopic air sampling in a tallgrass prairie to partition net ecosystem CO_2 exchange 108. https://doi.org/10.1029/2002JD003369

Lasslop, G., Reichstein, M., Papale, D., Richardson, A.D., Arneth, A., Barr, A., Stoy, P., Wohlfahrt, G., 2010. Separation of net ecosystem exchange into assimilation and respiration using a light response curve approach: critical issues and global evaluation. Glob. Chang. Biol. 16, 187–208. https://doi.org/10.1111/j.1365-2486.2009.02041.x

Le Quéré, C., Andrew, R.M., Friedlingstein, P., Sitch, S., Hauck, J., Pongratz, J., Pickers, P.A., Korsbakken, J.I., Peters, G.P., Canadell, J.G., Arneth, A., Arora, V.K., Barbero, L., Bastos, A., Bopp, L., Chevallier, F., Chini, L.P., Ciais, P., Doney, S.C., Gkritzalis, T., Goll, D.S., Harris, I., Haverd, V., Hoffman, F.M., Hoppema, M., Houghton, R.A., Hurtt, G., Ilyina, T., Jain, A.K., Johannessen, T., Jones, C.D., Kato, E., Keeling, R.F., Goldewijk, K.K., Landschützer, P., Lefèvre, N., Lienert, S., Liu, Z., Lombardozzi, D., Metzl, N., Munro, D.R., Nabel, J.E.M.S., Nakaoka, S., Neill, C., Olsen, A., Ono, T., Patra, P., Peregon, A., Peters, W., Peylin, P., Pfeil, B., Pierrot, D., Poulter, B., Rehder, G., Resplandy, L., Robertson, E., Rocher, M., Rödenbeck, C., Schuster, U., Schwinger, J., Séférian, R., Skjelvan, I., Steinhoff, T., Sutton, A., Tans, P.P., Tian, H., Tilbrook, B., Tubiello, F.N., van der Laan-Luijkx, I.T., van der Werf, G.R., Viovy, N., Walker, A.P., Wiltshire, A.J., Wright, R., Zaehle, S., Zheng, B., 2018. Global carbon budget 2018. Earth Syst. Sci. Data 10, 2141–2194. https://doi.org/10.5194/essd-10-2141-2018

Lee, X., Griffis, T.J., Baker, J.M., Billmark, K.A., Kim, K., Welp, L.R., 2009. Canopy-scale kinetic fractionation of atmospheric carbon dioxide and water vapor isotopes. Global Biogeochem. Cycles 23, 1–15. https://doi.org/10.1029/2008GB003331

Leuning, R., 2000. Estimation of scalar source/sink distributions in plant canopies using Lagrangian dispersion analysis: Corrections for atmospheric stability and comparison with a multilayer canopy model. Boundary-Layer Meteorol. 96, 293–314. https://doi.org/10.1023/A:1002449700617

Leuning, R., Denmead, O.T., Miyata, A., Kim, J., 2000. Source/sink distributions of heat, water vapour, carbon dioxide and methane in a rice canopy estimated using Lagrangian dispersion analysis. Agric. For. Meteorol. 104, 233–249. https://doi.org/10.1016/S0168-1923(00)00158-1

Lloyd, J., Kruijt, B., Hollinger, D., Grace, J., Francey, R., Wong, S., Kelliher, F., Miranda, A., Farquhar, G., Gash, J., Vygodskaya, N., Wright, I., Miranda, H., Schulze, E., 1996. Vegetation effects on the isotopic composition of Atmospheric CO_2 at local and regional Scales: Theoretical Aspects and a

Comparison Between rain forest in Amazonia and a boreal forest in Siberia. Funct. Plant Biol. 23, 371. https://doi.org/10.1071/PP9960371

Lloyd, J., Taylor, J.A., 1994. On the Temperature Dependence of Soil Respiration. Funct. Ecol. 8, 315. https://doi.org/10.2307/2389824

Marshall, J.D., Waring, R.H., 1984. Conifers and broadleaf species: stomatal sensitivity differs in western Oregon. Can. J. For. Res. 14, 905–908. https://doi.org/10.1139/x84-161

Marshall, J.D., Zhang, J., 1994. Carbon isotope discrimination and water-use efficiency in native plants of the North-Central Rockies. Ecology 75, 1887–1895. https://doi.org/10.2307/1941593

Monneveux, P., Rekika, D., Acevedo, E., Merah, O., 2006. Effect of drought on leaf gas exchange, carbon isotope discrimination, transpiration efficiency and productivity in field grown durum wheat genotypes. Plant Sci. 170, 867–872. https://doi.org/10.1016/J.PLANTSCI.2005.12.008

Monteith, J.L., Unsworth, M., 2013. Principles of environmental physics: plants, animals, and the atmosphere, 4th ed. Academic Press. https://doi.org/10.1016/B978-0-12-386910-4.00001-9

O'leary, M.H., 1988. Carbon isotopes in photosynthesis. Bioscience 35, 328–336. https://doi.org/10.2307/1310735

Ogée, J., Peylin, P., Ciais, P., Bariac, T., Brunet, Y., Berbigier, P., Roche, C., Richard, P., Bardoux, G., Bonnefond, J.-M., 2003. Partitioning net ecosystem carbon exchange into net assimilation and respiration using $^{13}CO_2$ measurements: A cost-effective sampling strategy. Global Biogeochem. Cycles 17, 1070. https://doi.org/10.1029/2002GB001995

Ogée, J., Peylin, P., Cuntz, M., Bariac, T., Brunet, Y., Berbigier, P., Richard, P., Ciais, P., 2004. Partitioning net ecosystem carbon exchange into net assimilation and respiration with canopy-scale isotopic measurements : An error propagation analysis with $^{13}CO_2$ and $CO^{18}O$ data. Global Biogeochem. Cycles 18, GB2019. https://doi.org/10.1029/2003GB002166

Papale, D., Reichstein, M., Aubinet, M., Canfora, E., Bernhofer, C., Kutsch, W., Longdoz, B., Rambal, S., Valentini, R., Vesala, T., Yakir, D., 2006. Towards a standardized processing of net ecosystem exchange measured with eddy covariance technique: Algorithms and uncertainty estimation. Biogeosciences 3, 571–583. https://doi.org/10.5194/bg-3-571-2006

Paul-Limoges, E., Wolf, S., Eugster, W., Hörtnagl, L., Buchmann, N., 2017. Below-canopy contributions to ecosystem CO_2 fluxes in a temperate mixed forest in Switzerland 247, 582–596. https://doi.org/10.1016/j.agrformet.2017.08.011

Peterson, B.J., Fry, B., 1987. Stable Isotopes in Ecosystem Studies. Annu. Rev. Ecol. Syst. 18, 293–320. https://doi.org/10.1146/annurev.es.18.110187.001453

Ponton, S., Flanagan, L.B., Alstad, K.P., Johnson, B.G., Morgenstern, K., Kljun, N., Black, T.A., Barr, A.G., 2006. Comparison of ecosystem water-use efficiency among Douglas-fir forest, aspen forest and grassland using eddy covariance and carbon isotope techniques. Glob. Chang. Biol. 12, 294–310.

https://doi.org/10.1111/j.1365-2486.2005.01103.x

Ramnarine, R., Voroney, R.P., Wagner-Riddle, C., Dunfield, K.E., 2011. Carbonate removal by acid fumigation for measuring the $\delta^{13}C$ of soil organic carbon. Can. J. Soil Sci. 91, 247–250. https://doi.org/10.4141/cjss10066

Raupach, M.R., 2001. Inferring biogeochemical sources and sinks from atmospheric concentrations: General considerations and applications in vegetation canopies, in: Global Biogeochemical Cycles in the Climate System. pp. 41–59. https://doi.org/http://dx.doi.org/10.1016/B978-012631260-7/50006-6

Raupach, M.R., 1989a. A practical Lagrangian method for relating scalar concentrations to source distributions in vegetation canopies. Q. J. R. Meteorol. Soc. 115, 609–632. https://doi.org/10.1002/qj.49711548710

Raupach, M.R., 1989b. Applying Lagrangian fluid mechanics to infer scalar source distributions from concentration profiles in plant canopies. Agric. For. Meteorol. 47, 85–108. https://doi.org/10.1016/0168-1923(89)90089-0

Raupach, M.R., 1989c. Stand overstorey processes. Phil. Trans. R. Soc. Lond. B 324, 175–190. https://doi.org/10.1098/rstb.1989.0043

Raupach, M.R., 1987. A Lagrangian analysis of scalar transfer in vegetation canopies. Q. J. R. Meteorol. Soc. 113, 107–120. https://doi.org/10.1002/qj.49711347507

Raupach, M.R., Denmead, O.T., Dunin, F.X., 1992. Challenges in linking atmospheric CO_2 concentrations to fluxes at local and regional scales. Aust. J. Bot. 40, 697–716. https://doi.org/10.1071/BT9920697

Reichstein, M., Falge, E., Baldocchi, D., Papale, D., Aubinet, M., Berbigier, P., Bernhofer, C., Buchmann, N., Gilmanov, T., Granier, A., Grunwald, T., Havrankova, K., Ilvesniemi, H., Janous, D., Knohl, A., Laurila, T., Lohila, A., Loustau, D., Matteucci, G., Meyers, T., Miglietta, F., Ourcival, J.-M., Pumpanen, J., Rambal, S., Rotenberg, E., Sanz, M., Tenhunen, J., Seufert, G., Vaccari, F., Vesala, T., Yakir, D., Valentini, R., 2005a. On the separation of net ecosystem exchange into assimilation and ecosystem respiration: review and improved algorithm. Glob. Chang. Biol. 11, 1424–1439. https://doi.org/10.1111/j.1365-2486.2005.001002.x

Reichstein, M., Subke, J.A., Angeli, A.C., Tenhunen, J.D., 2005b. Does the temperature sensitivity of decomposition of soil organic matter depend upon water content, soil horizon, or incubation time? Glob. Chang. Biol. 11, 1754–1767. https://doi.org/10.1111/j.1365-2486.2005.001010.x

Reichstein, M., Tenhunen, J.D., Roupsard, O., Ourcival, J.-M., Rambal, S., Dore, S., Valentini, R., 2002. Ecosystem respiration in two Mediterranean evergreen Holm Oak forests: drought effects and decomposition dynamics. Funct. Ecol. 16, 27–39. https://doi.org/10.1046/j.0269-8463.2001.00597.x

Saliendra, N.Z., Meinzer, F.C., Perry, M., Thom, M., 1996. Associations between partitioning of carboxylase activity and bundle sheath leakiness to CO_2 , carbon isotope discrimination, photosynthesis, and growth in sugarcane. J. Exp. Bot. 47, 907–914. https://doi.org/10.1093/jxb/47.7.907

Santos, E., Wagner-Riddle, C., Lee, X., Warland, J., Brown, S., Staebler, R., Bartlett, P., Kim, K., 2014. Temporal dynamics of oxygen isotope compositions of soil and canopy CO_2 fluxes in a temperate deciduous forest. J. Geophys. Res. Biogeosciences 996–1013. https://doi.org/10.1002/2013JG002525.Received

Santos, E., Wagner-Riddle, C., Lee, X., Warland, J., Brown, S., Staebler, R., Bartlett, P., Kim, K., 2012. Use of the isotope flux ratio approach to investigate the $C^{18}O^{16}O$ and $^{13}CO_2$ exchange near the floor of a temperate deciduous forest. Biogeosciences 9, 2385–2399. https://doi.org/10.5194/bg-9-2385-2012

Santos, E.A., Wagner-Riddle, C., Warland, J.S., Brown, S., 2011. Applying a Lagrangian dispersion analysis to infer carbon dioxide and latent heat fluxes in a corn canopy. Agric. For. Meteorol. 151, 620–632. https://doi.org/10.1016/j.agrformet.2011.01.010

Scanlon, T.M., Kustas, W.P., 2010. Partitioning carbon dioxide and water vapor fluxes using correlation analysis. Agric. For. Meteorol. 150, 89–99. https://doi.org/10.1016/J.AGRFORMET.2009.09.005

Scanlon, T.M., Sahu, P., 2008. On the correlation structure of water vapor and carbon dioxide in the atmospheric surface layer: A basis for flux partitioning. Water Resour. Res. 44. https://doi.org/10.1029/2008WR006932

Seibt, U., Rajabi, A., Griffiths, H., Berry, J.A., 2008. Carbon isotopes and water use efficiency: sense and sensitivity. Oecologia 155, 441–454. https://doi.org/10.1007/s00442-007-0932-7

Shimoda, S., Murayama, S., Mo, W., Oikawa, T., 2009. Seasonal contribution of C_3 and C_4 species to ecosystem respiration and photosynthesis estimated from isotopic measurements of atmospheric CO_2 at a grassland in Japan. Agric. For. Meteorol. 149, 603–613. https://doi.org/10.1016/j.agrformet.2008.10.007

Siqueira, M., Lai, C.T., Katul, G., 2000. Estimating scalar sources, sinks, and fluxes in a forest canopy using Lagrangian, Eulerian, and hybrid inverse models. J. Geophys. Res. Atmos. 105, 29475–29488. https://doi.org/10.1029/2000JD900543

Siqueira, M.B., Katul, G.G., 2010. An analytical model for the distribution of CO_2 sources and sinks, fluxes, and mean concentration within the roughness sub-Layer. Boundary-Layer Meteorol. 135, 31–50. https://doi.org/10.1007/s10546-009-9453-8

Skaggs, T.H., Anderson, R.G., Alfieri, J.G., Scanlon, T.M., Kustas, W.P., 2018. Fluxpart: Open source software for partitioning carbon dioxide and water vapor fluxes. Agric. For. Meteorol. 253–254, 218–224. https://doi.org/10.1016/J.AGRFORMET.2018.02.019

Smedley, M.P., Dawson, T.E., Comstock, Jonathan P; Donovan, L.A., Sherrill, D.E., Cook, C.S., Ehleringer, J.R., 1991. Seasonal carbon isotope discrimination in a grassland community. Oecologia 85, 314–320. https://doi.org/10.1007/BF00320605

Stanhill, G., 1986. Water use efficiency. Adv. Agron. 39, 53–85. https://doi.org/10.1016/S0065-2113(08)60465-4

Stewart, G., Turnbull, M., Schmidt, S., Erskine, P., 1995. ^{13}C Natural Abundance in Plant Communities Along a Rainfall Gradient: a Biological Integrator of Water Availability. Funct. Plant Biol. 22, 51. https://doi.org/10.1071/PP9950051

Stoy, P.C., Katul, G.G., Siqueira, M.B.S., Juang, J.-Y., Novick, K.A., Uebelherr, J.M., Oren, R., 2006. An evaluation of models for partitioning eddy covariance-measured net ecosystem exchange into photosynthesis and respiration. Agric. For. Meteorol. 141, 2–18. https://doi.org/10.1016/J.AGRFORMET.2006.09.001

Stropes, K.S., 2017. Investigating the exchange of CO_2 in a tall-grass prairie ecosystem using stable isotopes and micrometeorological methods. Kansas State University.

Sturm, P., Eugster, W., Knohl, A., 2012. Eddy covariance measurements of CO_2 isotopologues with a quantum cascade laser absorption spectrometer. Agric. For. Meteorol. 152, 73–82. https://doi.org/10.1016/j.agrformet.2011.09.007

Styles, J.M., Raupach, M.R., Farquhar, G.D., Kolle, O., Lawton, K.A., Brand, W.A., Werner, R.A., Jordan, A., Schulze, E.-D., Shibistova, O., Lloyd, J., 2002. Soil and canopy CO_2, $^{13}CO_2$, H_2O and sensible heat flux partitions in a forest canopy inferred from concentration measurements. Tellus, Ser. B Chem. Phys. Meteorol. 54, 655–676. https://doi.org/10.3402/tellusb.v54i5.16708

Sulman, B.N., Roman, D.T., Scanlon, T.M., Wang, L., Novick, K.A., 2016. Comparing methods for partitioning a decade of carbon dioxide and water vapor fluxes in a temperate forest. Agric. For. Meteorol. 226–227, 229–245. https://doi.org/10.1016/J.AGRFORMET.2016.06.002

Taylor, G.I., 1922. Diffusion by continuous movements. Proc. london Math. Soc. 2, 196–212. https://doi.org/10.1112/plms/s2-20.1.196

Ueyama, M., Takanashi, S., Takahashi, Y., 2014. Inferring methane fluxes at a larch forest using Lagrangian, Eulerian, and hybrid inverse models. J. Geophys. Res. G Biogeosciences 119, 2018–2031. https://doi.org/10.1002/2014JG002716

Van Gorsel, E., Harman, I.N., Finnigan, J.J., Leuning, R., 2011. Decoupling of air flow above and in plant canopies and gravity waves affect micrometeorological estimates of net scalar exchange. Agric. For. Meteorol. 151, 927–933. https://doi.org/10.1016/j.agrformet.2011.02.012

Victoria, R.L., Martinelli, L.A., Trivelin, P.C.O., Matsui, E., Forsberg, B.R., Richey, J.E., Devol, A.H., 1992. The Use of Stable Isotopes in Studies of Nutrient Cycling: Carbon Isotope Composition of Amazon Varzea Sediments. Biotropica 24, 240. https://doi.org/10.2307/2388518

Wang, Y., Hu, C., Dong, W., Li, X., Zhang, Y., Qin, S., Oenema, O., 2015. Carbon budget of a winter-wheat and summer-maize rotation cropland in the North China Plain. Agric. Ecosyst. Environ. 206, 33–45. https://doi.org/10.1016/J.AGEE.2015.03.016

Warland, J.S., Thurtell, G.W., 2000. A Lagrangian solution to the relationship between source strength and concentration profile under conditions of local advection. Boundary-Layer Meteorol. 96, 453–471. https://doi.org/10.1007/s10546-006-9098-9

Wehr, R., Munger, J.W., Mcmanus, J.B., Nelson, D.D., Zahniser, M.S., Davidson, E.A., Wofsy, S.C., Saleska, S.R., 2016. Seasonality of temperate forest photosynthesis and daytime respiration. Nature 534, 680–683. https://doi.org/10.1038/nature17966

Wehr, R., Munger, J.W., Nelson, D.D., Mcmanus, J.B., Zahniser, M.S., Wofsy, S.C., Saleska, S.R., 2013. Long-term eddy covariance measurements of the isotopic composition of the ecosystem – atmosphere exchange of CO_2 in a temperate forest. Agric. For. Meteorol. 181, 69–84. https://doi.org/10.1016/j.agrformet.2013.07.002

Wehr, R., Saleska, S.R., 2015. An improved isotopic method for partitioning net ecosystem – atmosphere CO_2 exchange. Agric. For. Meteorol. 214–215, 515–531. https://doi.org/10.1016/j.agrformet.2015.09.009

Werner, C., Schnyder, H., Cuntz, M., Keitel, C., Zeeman, M.J., Dawson, T.E., Badeck, F., Brugnoli, E., 2012. Progress and challenges in using stable isotopes to trace plant carbon and water relations across scales. Biogeosciences 9, 3083–3111. https://doi.org/10.5194/bg-9-3083-2012

Willmott, C.J., 1981. On the validation of models. Phys. Geogr. 184–194. https://doi.org/10.1080/02723646.1981.10642213

Willmott, C.J., Robeson, M., Matsuura, K., 2012. A refined index of model performance. Int. J. Climatol. 32, 2088–2094. https://doi.org/10.1002/joc.2419

Wutzler, T., Lucas-Moffat, A., Migliavacca, M., Knauer, J., Sickel, K., Šigut, L., Menzer, O., Reichstein, M., 2018. Basic and extensible post-processing of eddy covariance flux data with REddyProc. Biogeosciences 15, 5015–5030. https://doi.org/10.5194/bg-15-5015-2018

Xiao, J., Chen, J., Davis, K.J., Reichstein, M., 2012. Advances in upscaling of eddy covariance measurements of carbon and water fluxes. J. Geophys. Res. Biogeosciences 117, 0–5. https://doi.org/10.1029/2011JG001889

Yakir, D., Sternberg, S.L., 2000. The use of stable isotopes to study ecosystem gas exchange. Oecologia 297–311. https://doi.org/10.1007/s004420051016

Yakir, D., Wang, X.-F., 1996. Fluxes of CO_2 and water between terrestrial vegetation and the atmosphere estimated from isotope measurements. Nature 380, 515–517. https://doi.org/10.1038/380515a0

Yang, B., Hanson, P.J., Riggs, J.S., Pallardy, S.G., Heuer, M., Hosman, K.P., Meyers, T.P., Wullschleger, S.D., Gu, L.H., 2007. Biases of CO2 storage in eddy flux measurements in a forest pertinent to vertical configurations of a profile system and CO_2 density averaging. J. Geophys. Res. Atmos. 112, 1–15. https://doi.org/10.1029/2006JD008243

Yoneyama, T., Okada, H., Ando, S., 2010. Seasonal variations in natural ^{13} C abundances in C $_3$ and C $_4$ plants collected in Thailand and the Philippines. Soil Sci. Plant Nutr. 56, 422–426. https://doi.org/10.1111/j.1747-0765.2010.00477.x

Zhang, J., Griffis, T.J., Baker, J.M., 2006. Using continuous stable isotope measurements to partition net ecosystem CO2 exchange. Plant, Cell Environ. 29, 483–496. https://doi.org/10.1111/j.1365-3040.2005.01425.x

Zobitz, J.M., Burns, S.P., Oge, J., Reichstein, M., Bowling, D.R., 2007. Partitioning net ecosystem exchange of CO_2: A comparison of a Bayesian/isotope approach to environmental regression methods 112, 1–19. https://doi.org/10.1029/2006JG000282

Zobitz, J.M., Burns, S.P., Reichstein, M., Bowling, D.R., 2008. Partitioning net ecosystem carbon exchange and the carbon isotopic disequilibrium in a subalpine forest 14, 1785–1800. https://doi.org/10.1111/j.1365-2486.2008.01609.x

APPENDIX A

Table A 1. Statistical coefficients of the relationship between net ecosystem CO_2 exchange (NEE) obtained using the eddy covariance method and the LNF theory for different friction velocity (u_*) thresholds and atmospheric stability conditions: unstable (h/L <−0.01), neutral (−0.01≤ h/L < 0.01) and stable ($h/L \geq 0.01$) where h/L is the ratio between canopy height and the Obukhov length.

		Forest					Grassland					Corn				
Stability	u_*	NEE														
		n	R^2	Slope	Inters.	d_r	n	R^2	Slope	Inters.	d_r	n	R^2	Slope	Inters.	d_r
Unstable	> 0.1	250	0.21	1.92*	43.0*	0.91	183	0.87	0.81*	-0.35*	0.99	623	0.38	0.76*	4.97*	0.77
Neutral		25	0.43	1.05*	10.1*	0.97	136	0.61	0.72*	-0.03n.s	0.98	204	0.55	0.65*	2.10*	0.79
Stable		356	0.35	0.97*	2.80*	0.96	245	0.20	0.73*	0.45*	0.99	363	0.12	0.42*	1.77*	0.42
Unstable	> 0.2	209	0.24	1.44	31.8*	0.93	164	0.90	0.83*	-0.36*	0.99	535	0.38	0.78*	4.98*	0.78
Neutral		25	0.43	1.05*	10.1*	0.97	126	0.62	0.74*	-0.09n.s	0.99	187	0.55	0.66*	2.12*	0.79
Stable		237	0.44	1.08*	3.94*	0.96	122	0.42	0.60*	0.49*	0.98	143	0.21	0.66*	2.47*	0.54
Unstable	> 0.3	164	0.21	1.00*	2.40*	0.95	134	0.90	0.83*	-0.43*	0.99	355	0.50	0.78*	4.94*	0.81
Neutral		23	0.45	1.08*	10.7*	0.97	119	0.67	0.71*	-0.15n.s	0.99	143	0.63	0.77*	3.49*	0.80
Stable		164	0.50	1.16*	5.45*	0.96	46	0.73	0.76*	0.28n.s	0.99	47	0.30	0.85*	1.35n.s.	0.53
Unstable	> 0.4	121	0.44	1.41*	2.67*	0.95	68	0.91	0.82*	-0.33*	0.99	178	0.71	0.83*	5.48*	0.85
Neutral		20	0.60	1.28*	13.5*	0.97	99	0.58	0.67*	0.07n.s	0.99	87	0.70	0.84*	4.83*	0.80
Stable		103	0.50	1.16*	7.19*	0.95	12	0.83	0.57*	0.42*	0.99	0	-	-	-	-

* significant by a t-test at a 5% probability level.
n.s., not significant by a t-test at a 5% probability level.